JAERI-Research
96-053

ELECTRON BEAM FLUE GAS TREATMENT
—RESEARCH COOPERATION AMONG JAERI, IAEA AND INCT—

October 1996

Department of Radiation Research for Environment and Resources

日本原子力研究所
Japan Atomic Energy Research Institute

本レポートは，日本原子力研究所が不定期に公刊している研究報告書です。
入手の問合わせは，日本原子力研究所研究情報部研究情報課（〒319-11 茨城県那珂郡東海村）あて，お申し越しください。なお，このほかに財団法人原子力弘済会資料センター（〒319-11 茨城県那珂郡東海村日本原子力研究所内）で複写による実費頒布をおこなっております。

This report is issued irregularly.
Inquiries about availability of the reports should be addressed to Research Information Division, Department of Intellectual Resources, Japan Atomic Energy Research Institute, Tokai-mura, Naka-gun, Ibaraki-ken, 319-11, Japan.

編集兼発行　日本原子力研究所
印　　刷　いばらき印刷㈱

JAERI-Research 96-053

Electron Beam Flue Gas Treatment
- Research Cooperation among JAERI, IAEA and INCT -

Department of Radiation Research for Environment and Resources

Takasaki Radiation Chemistry Research Establishment
Japan Atomic Energy Research Institute
Watanuki-cho, Takasaki-shi, Gunma-ken

(Received September 18, 1996)

The research co-operation is conducted among Japan Atomic Energy Research Institute (JAERI), International Atomic Energy Agency (IAEA) and Institute of Nuclear Chemistry and Technology in Poland (INCT) on Electron Beam Flue Gas Treatment from January 1993 to March 1997. The first phase of the cooperation was carried out for 3 years from January 1993 to March 1995. This cooperation was performed through information exchange meetings (Coordination Meetings), held in Takasaki and Warsaw, and experiments and discussions by exchange scientists. Many useful results were obtained on electron beam treatment of flue gas from coal-combustion heat generation plant in Kaweczyn within the frame work of the research co-operation. This report includes the main results of the tripartite research cooperation.

Keywords: Electron Beam, Flue Gas Treatment, Coal-fired Boiler, SO_2 Removal, NO_x Removal, By-product Collection

---

This is the report of the research cooperation with International Atomic Energy Agency (IAEA) and Institute of Nuclear Chemistry and Technology in Poland (INCT) on Electron Beam Flue Gas Treatment.

JAERI-Research 96-053

電子ビーム排煙処理
－日本原子力研究所、国際原子力機関、ポーランド核化学・技術研究所との研究協力－

日本原子力研究所高崎研究所
環境・資源利用研究部

（1996年９月18日受理）

日本原子力研究所（ＪＡＥＲＩ）、国際原子力機関（ＩＡＥＡ）、ポーランド核化学・技術研究所（ＩＮＣＴ）は、1993年１月から1997年３月までの間、電子ビームによる排煙処理の研究協力を実施中である。本研究協力の第１期は、1993年１月から1995年３月にかけて、高崎とワルシャワで開催された情報交換会議（調整会議）ならびに研究者の相互交流による実験と討議を通じて行われた。本共同研究を通じて、カベンチンの石炭燃焼熱供給所からの排煙の電子ビーム処理に関し、有用な成果が得られた。本報告書は、この三者共同研究の主要な成果をまとめたものである。

本報告書は、「電子ビーム排煙処理」に関する国際原子力機関（ＩＡＥＡ）およびポーランド核化学・技術研究所（ＩＮＣＴ）との研究協力の成果をまとめたものである。

高崎研究所：〒370－12　群馬県高崎市綿貫町１２３３

Contents

目　　次

CHIEF EDITOR

Sueo Machi
Deputy Director General,
Department of Research and Isotopes,
International Atomic Energy Agency
P.O. Box 100, A-1400 Vienna, Austria
Tel. 43-1-2360

EDITORS

Okihiro Tokunaga
Director,
Department of Radiation Research for Environment and Resources,
Takasaki, Radiation Chemistry Research Establishment,
Japan Atomic Energy Research Institute
1233 Watanuki-cho, Takasaki-shi, Gunma-ken, Japan 370-12
Tel. 0273-46-9214

Vitomir Markovic
Scientific Officer,
Industrial and Chemistry Section,
Department of Research and Isotopes,
International Atomic Energy Agency
P.O. Box 100, A-1400 Vienna, Austria
Tel. 43-1-2360

Andrzej G. Chmielewski
Deputy Director General,
Institute of Nuclear Chemistry and Technology
Dorodna 16, 03-195 Warsaw, Poland
Tel. 0-4822-11-06-56

PREFACE

S. Machi

Needless to say, there is a great concern about the degradation of the environments discussed at UNCED in Rio 1993. Following agenda 21 of UNCED, the IAEA places high priority on the application of nuclear technology for environmental conservation. Currently 90 % of primary energy is supplied by burning fossil fuels which emit SO_2 and NO_x. Huge amounts of SO_2, for example, 15 million tons per year in USA, 25 million tons in China and 4.3 million tons in Poland are still emitted. As a consequence of the SO_2 and NO_x emission the environment has been seriously deteriorated.

To contribute in solving this problem, the innovative technology of removing SO_2 and NO_x through the use of electron beams, has been developed in Japan, USA, Germany and Poland in cooperation with the IAEA, using pilot scale plants. A feasibility study based on the results of pilot scale experiments, has shown the economical benefits on this new technology over conventional technologies.

In the development of technology of the flue gas cleaning by electron beams, it was in 1972 that a handful of scientists of JAERI and Ebara Corporation, headed by me, started for the first time the experiments to irradiate heavy oil burning flue gases in a small flow system using electron beams in JAERI. It was discovered that SO_2 and NO_x can be removed simultaneously. Since then in Japan extensive research and development work has been conducted in JAERI, Ebara and recently Chubu Electric Power Company, Incorporated. Three pilot plants for cleaning different types of flue gases from coal burning, traffic tunnel and municipal waste incineration had been successfully operated from 1992 to 1994. INCT in Poland, through its Government, has been successfully conducting the excellent IAEA project on "Flue Gas Cleaning by Electron Beams" since 1990.

In 1992, JAERI, through the Japanese Government, offered cooperation and support to IAEA and Poland for the above mentioned TC project. This cooperation has provided an excellent opportunity for scientists and engineers to cooperate, exchange information and share tasks to make the project more productive and effective.

Based on the feasibility studies of this technology carried out by the Agency's experts in cooperation with Poland and experimental achievements of pilot plants both in Poland and Japan, a large Model Project on "Industrial Demonstration Plants for Electron Beam Purification of Flue Gas" of the Agency was launched in 1995 in Poland. The purpose of the project is to establish this technology for removing SO_2 and NO_x from flue gases of coal burning power stations in industrial scale electron beams.

The Agency has already been requested by several Member States including China, Brazil, ROK, Ukraine, Chile, Thailand, Syria, Mexico, Bulgaria and others to transfer this technology to

them as soon as possible.

The first phase of the cooperation between IAEA, JAERI through Japanese Government and INCT through the Polish Government was terminated in March 1995 and the second phase of another 2 years has been started.

The extension of this cooperation is extremely important for the further development of this technology in supporting the IAEA Model Project on "Industrial Demonstration Plant for Electron Beam Purification of Flue Gas".

It is very timely to publish the outcome of the tripartite cooperation at the launching of the important Model Project and at the initiation of the 2nd phase of cooperation.

On behalf of the Agency and myself, I would like to express appreciation to all who contributed to this cooperation in IAEA, Japan and Poland.

I. Introduction

V. Markovic

1. Scope of the research cooperation

(1) The cooperative research and development programme started in early 1993 after detailed preparation involving INCT, JAERI and IAEA.

(2) The main objective was to study processes and technology of EB cleaning of flue gases, to intensify cooperation between INCT and JAERI and to augment the use of demonstration facility in Poland for studies of technical parameters and optimization of the process.

(3) In a broader sense the scope of the project is:
- cooperative research;
- establishment of mechanism for exchange of information;
- establishment of mechanism for regular monitoring of project's progress and for planning of future activities.

(4) In a more narrow (technical) sense the scope of the project is:
- optimization of process parameters affecting the efficiency of removal of toxic components;
- study of byproducts collection, in particular using bag filters;
- study of utilization of byproducts collected after the process;
- multi stage irradiation and effect on process efficiency;
- effect of moisture on process efficiency
- establishment of an effective monitoring system and control system;
- dose distribution and effect of distribution on process efficiency;
- as well as any other technical problem that may arise during operation of demonstration facility.

(5) From the point of view of implementation the project scope includes:
- exchange of scientists between Japan and Poland and joint research at facilities in both countries;
- provision of analytical and control equipments from Japan to Poland;
- organization of coordination meetings at regular intervals for evaluation, monitoring and planning of future activities.

2. Time schedule

	First Year (JFY 1992) 1993/1-1993/3	Second Year (JFY 1993) 1993/4-1994/3	Third Year (JFY 1994) 1994/4-1995/3
Collaborative research items	* Multi-stage irradiation, Effect of moisture * Effective method for product collection	* Multi-stage irradiation, Effect of moisture * Effective method for product collection	* Multi-stage irradiation, Effect of moisture * Effective method for product collection * Accelerator control

3. Research and administrative staffs relating to the cooperation

JAPAN

Okihiro Tokunaga
Director, Department of Radiation Research for Environment and Resources, TRCRE, JAERI

Shoji Hashimoto
Head, Environmental Conservation Technology Laboratory,
Department of Radiation Research for Environment and Resources, TRCRE, JAERI

Hideki Namba
Principal Scientist, Environmental Conservation Technology Laboratory,
Department of Radiation Research for Environment and Resources, TRCRE, JAERI

Koichi Hirota
Scientist, Environmental Conservation Technology Laboratory,
Department of Radiation Research for Environment and Resources, TRCRE, JAERI

POLAND

Andrzej G. Chmielewski
Deputy Director for Research and Development, INCT

Zbigniew Zimek
Head, Department of Radiation Chemistry and Technology, INCT

Edward Iller
Head, Laboratory of Nuclear Techniques for Environment Protection, INCT

Bogdan Tyminski
Pilot Plant Manager, INCT

Grazyna Zakrzewska – Trznadel
Chemical Engineer, INCT
Andrzej Dobrowolski
Principal Scientist, INCT
Sylwester Bulka
EB Processor Engineer, INCT
Przemyslaw Panta
Principal Scientist, INCT
Janusz Licki
Physicist, Institute of Atomic Energy, Otwock–Swierk
Mieczyslaw Sowinski
Associate Professor, Soltan Institute for Nuclear Studies, Otwock–Swierk
Eugeniusz Jankowski
Director, EPS Kaweczyn
Miroslaw Pedzieszczak
Head of Boiler Department, EPS Kaweczyn
Ryszard Popiel
Mechanical Engineer, EPS Kaweczyn
Radomir Kupczak
Electronic Engineer, Lillek Co., Warsaw

IAEA
Sueo Machi
Deputy Director General, Department of Research and Isotopes
Massoud Samiei
Head, Europe Section, Department of Technical Cooperation Programme
Vitomir Markovic
Scientific Officer, Industrial Application and Chemistry Section,
Department of Research and Isotopes

II. Basic Study

1. Factors affecting removal of NO_x and SO_2

2. Collection of by-products by ESP and bag filter

1. Factors affecting removal of NO_x and SO_2

S. Hashimoto, H. Namba and O. Tokunaga

Abstract

Various factors affecting on the removal of NO_x and SO_2 from coal-combustion gases are reviewed from a series of research carried out in Japan Atomic Energy Research Institute. The main factors are irradiation dose, gas temperature, ammonia injection, multi-stage irradiation and humidity. A strategy for the optimization of these factors in actual plant operation are also discussed in this report.

1.1 Introduction

Various trials were carried out to know the important factors affecting the removal of NO_x and SO_2 in coal-combustion gases. The results obtained by JAERI and some idea on optimization of those factors will be introduced in this paper. It should be noted that the composition of the flue gases varies depending on burning condition and coal itself. Some factors are related to each other, and are difficult to distinguish perfectly, however, the basic idea presented in this paper will be helpful to know the effect of each factor on removal of NO_x and SO_2. The results presented in this paper were obtained with model gases and actual flue gases; the compositions of the gases were far from actual flue gases in some experiments in order to clarify the factors discussed below.

1.2 Factors affecting NO_x and SO_2 removal

1.2.1 Irradiation dose and dose rate

It is very clear that NO_x and SO_2 removal greatly depend on irradiation dose because the reaction is started by active species formed from various molecules contained in the flue gas and the formation of active species is proportional to irradiation dose. As for the effect of dose rate, it was calculated that the removal efficiencies are independent of dose rate in the range from 7.5 to 750 kGy/sec [1].

1.2.2 Gas temperature

The NO_x and SO_2 removal efficiencies in the irradiated mixture containing 350 ppm of NO, 1000 ppm of SO_2, 2350 ppm of ammonia, 8 % of water, 6 % of oxygen and balance of nitrogen at different temperature are shown in Fig. 1 [2]. The irradiation dose is 15 kGy. SO_2 removal has large dependency on irradiation temperature and the SO_2 removal efficiency is less than 30 % at 100 °C. The SO_2 removal is independent of the initial NO concentrations and the reaction between SO_2 and OH radical increases decreasing temperature [3]. Under low temperature less

than 65 °C and the moisture content higher than 10 %, it is known that a part of SO_2 reacts directly with ammonia without electron beam irradiation [4]. This reaction is called "Thermal Reaction" to produce ammonium sulfate by oxidation, finally. On the other hand, high temperature does not affect NO_x removal or make it slightly higher with increase of temperature.

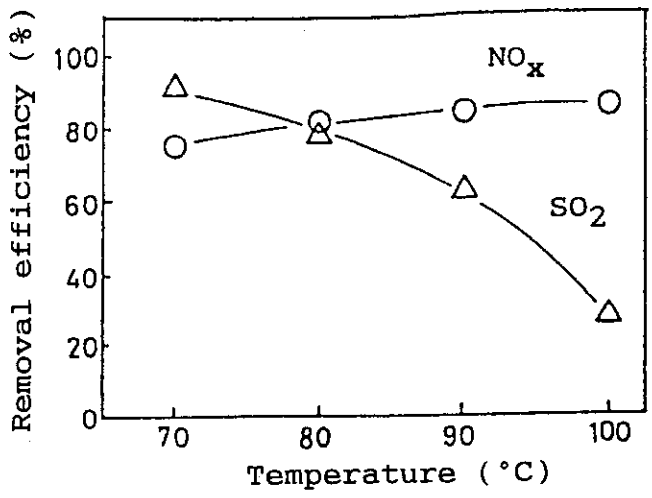

Fig. 1 Effect of temperature on removal of NO_x and SO_2

1.2.3 SO_2 concentration

Fig. 2 shows NO_x and SO_2 removal efficiencies for various inlet SO_2 concentration [5]. This result was obtained by the pilot plant test which was carried out in the premises of the Shin-Nagoya Thermal Power Station, Nagoya. Inlet NO_x concentration was fixed in the rage from

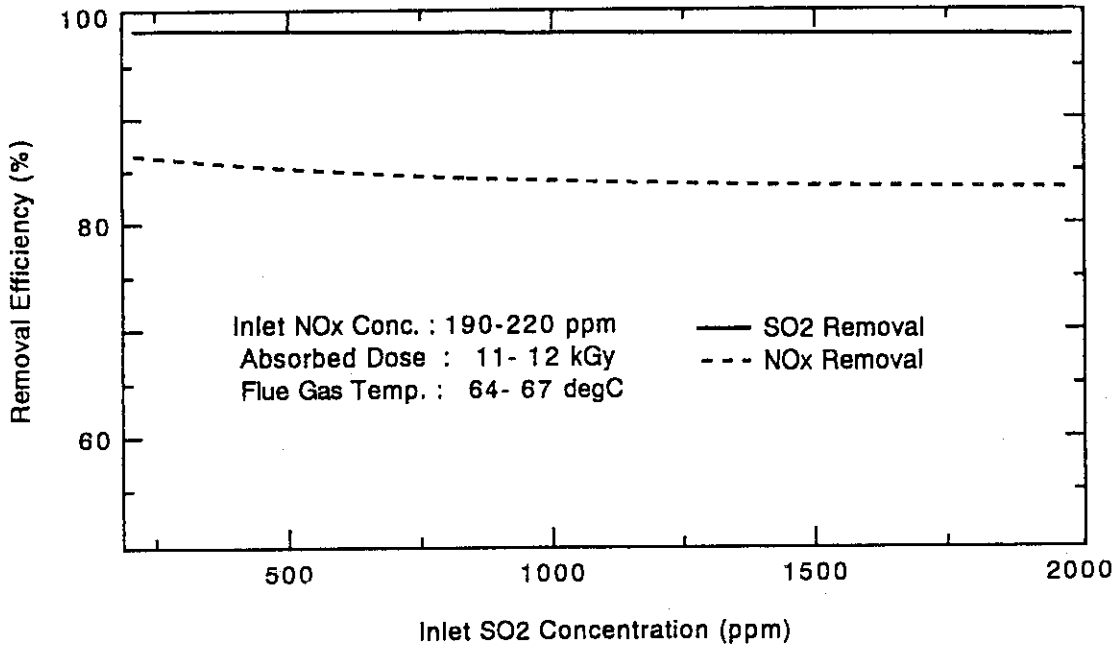

Fig. 2 Effect of inlet SO_2 on removal of NO_x and SO_2

190 to 220 ppm. The temperature of flue gas was ranged from 64 to 67 °C. Irradiation dose of electron beams was ranged from 11 to 12 kGy.

High SO_2 removal was confirmed even at high inlet concentration because of high thermal reaction at low temperature. On the other hand, NO_x removal slightly decreases with the increase of inlet SO_2 concentration.

1.2.4 NO_x concentration

Fig. 3 shows an example of NO_x removal efficiency as a function of initial NO_x concentration [5]. This result was also obtained by the pilot plant test which was carried out in the premises of the Shin-Nagoya Thermal Power Station, Nagoya. Higher NO_x removal was achieved with higher absorbed dose and with lower inlet NO_x concentration because the amount of NO_x molecules removed is corresponding to the amount of active species formed by electron beam irradiation.

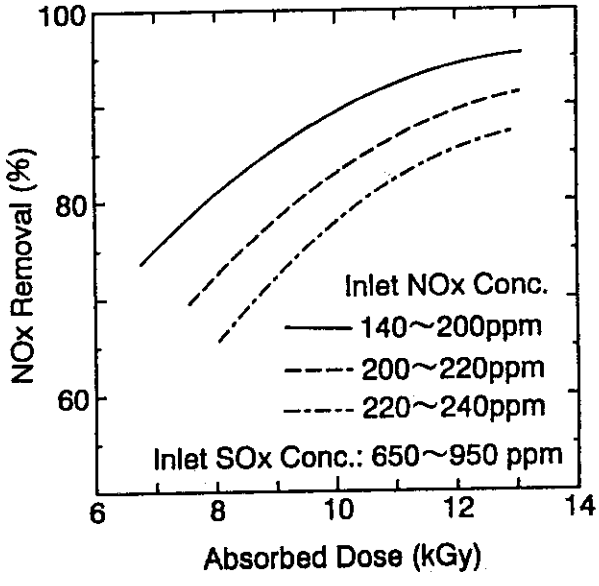

Fig. 3 Dose dependence of NO_x removal

1.2.5 Ammonia concentration

The NO_x and SO_2 removal efficiencies in the mixture of 350 ppm of NO and 1000 ppm of SO_2, 8 % of water vapor, 12 % of oxygen and 80 % of nitrogen irradiated in the presence and absence of ammonia are shown in Fig. 4 as a function of ammonia concentration.

The SO_2 removal efficiency increases markedly with the increase of ammonia concentration up to 0.6 mol. equivalent and increases gradually. On the other hand, the NO_x removal efficiency increases markedly up to 0.2 mol. equivalent ammonia concentration and also increases gradually.

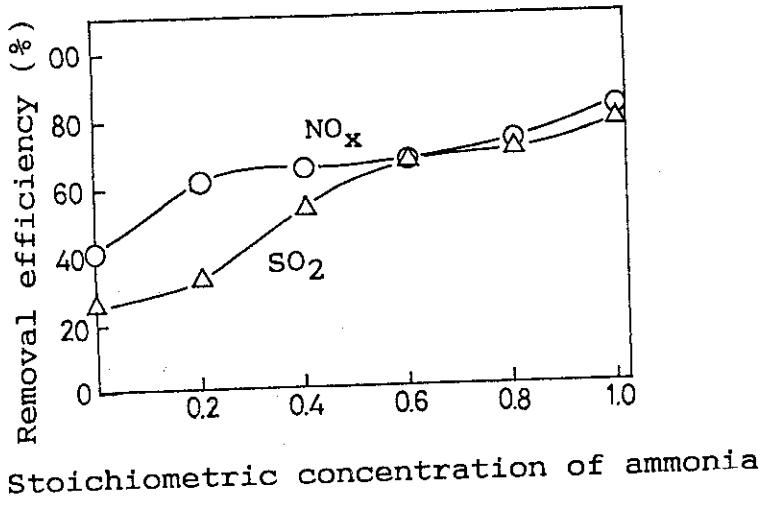

Fig. 4 Effect of ammonia on removal of NO_x and SO_2

1.2.6 Multi-stage irradiation

Figs 5 and 6 show dose dependence of NO_x and SO_x removal efficiencies in the condition of multi-stage irradiation [6]. The concentration of the gas components was set as follows; NO: 225 ppm, SO_2: 800 ppm, O_2: 6 %, H_2O: 12 %, N_2: balance. The NH_3 stoichiometry is one. The NO_x removal increased by multi-stage irradiation at the same dose, while no effect was observed on SO_2 removal.

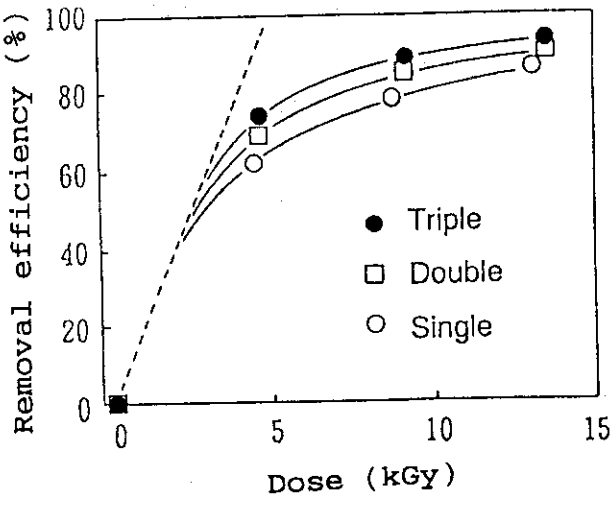

Fig. 5 NO_x removal in multi-stage irradiation

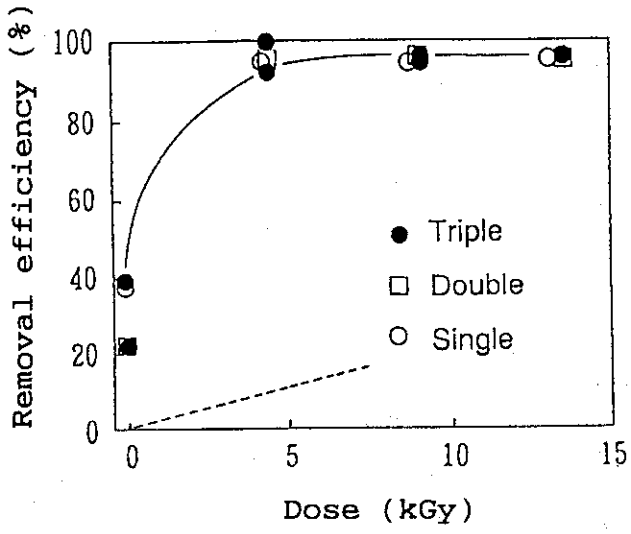

Fig. 6 SO_2 removal in multi-stage irradiation

The intermediates such as HNO_2, NO_2 and HO_2NO_2 are produced during the irradiation. These intermediates are important as precursors of final product HNO_3 or NH_4NO_3, except for HO_2NO_2 which mainly decomposes to produce NO_2 and HO_2. In some reaction pathways, these intermediates waste radicals in vain as shown in Fig. 7. For example, at higher NO_2 concentration, main part of O radicals are spent by the reaction with NO_2 instead of oxidizing NO to NO_2. Therefore it will increase the efficiency of NO_x removal by setting dwelling time between irradiations in order to oxidize and remove theses intermediates through thermal reactions.

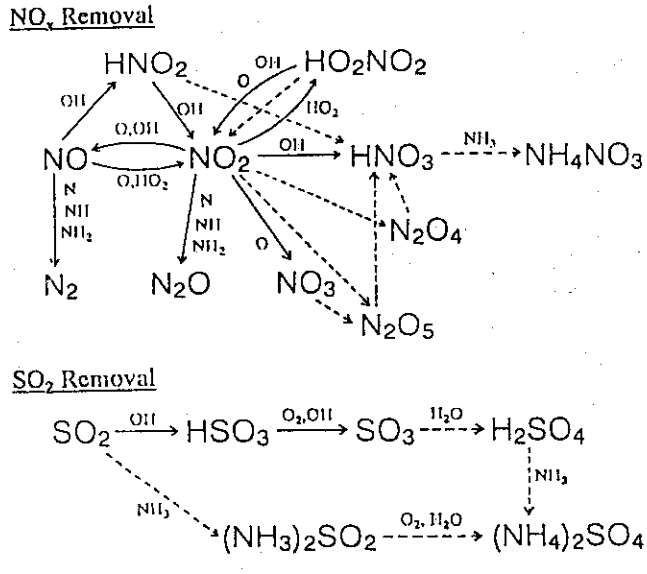

Fig. 7 Main reaction path to remove NO_x and SO_2

1.2.7 Moisture

Fig. 8 shows effect of moisture on removal of NO_x and SO_2 removal efficiencies from the irradiated mixture containing 350 ppm of NO, 1000 ppm of SO_2, 2350 ppm of ammonia, 8 % of water, 6 % of oxygen and balance of nitrogen [2]. SO_2 removal efficiency increases markedly with the increase of moisture content. This increase is explained by the reaction between ammonia and SO_2 without irradiation ("Thermal Reaction"). On the other hand, moisture content does not affect removal of NO_x.

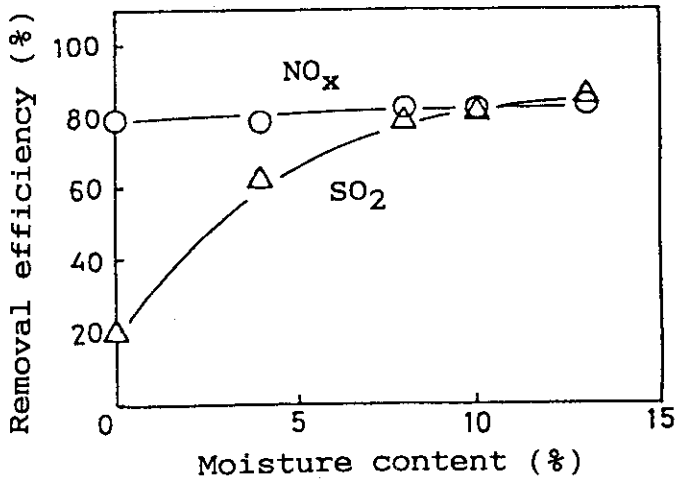

Fig. 8 Effect of moisture on removal of NO_x and SO_2

1.2.8 Oxygen concentration

Effect of oxygen on NO_x and SO_2 removal efficiencies are shown in Fig. 9 [2]. The composition of the gas is almost same as in 1.2.7. Under the oxygen concentration higher than 2 to 3 %, both NO_x and SO_2 removals are almost constant. These values become smaller with the decrease of oxygen concentration because the lack of oxygen decreases the oxidation reactions from NO to nitric acid and SO_2 to sulfuric acid.

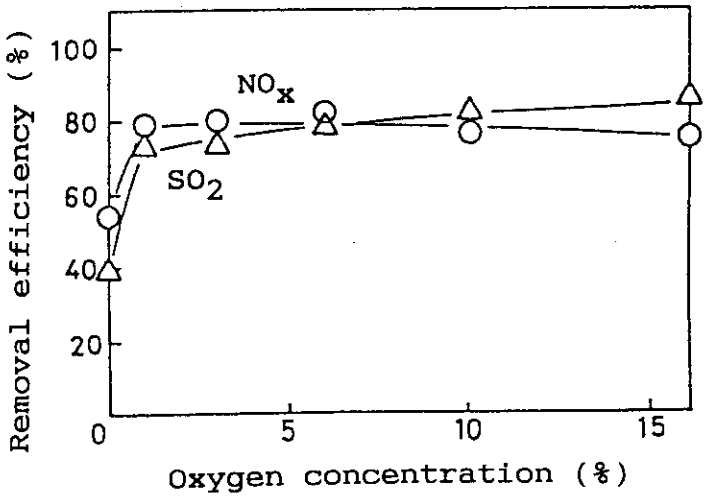

Fig. 9 Effect of oxygen on removal of NO_x and SO_2

1.2.9 CO concentration

The $G(-SO_2)$ in irradiation of the moist mixture of 1400 ppm SO_2, 1.3 % water vapor, 20 % of oxygen and 68.6 – 78.6% nitrogen containing carbon monoxide is shown in Fig. 10 as a function of carbon monoxide concentration [7]. The $G(-SO_2)$ decreased steeply from 5.3 with increasing carbon–monoxide concentration and attained a constant value of 2.8 at a concentration above about 3 %.

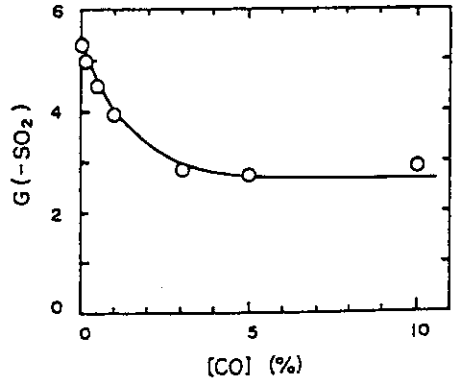

Fig. 10 Effect of carbon monoxide on $G(-SO_2)$

Figs 11 and 12 show decrease and formation of NO and NO_2 during irradiation with functions of carbon monoxide. The NO concentration decreased rapidly with the increase of carbon monoxide. While the formation of NO_2 by irradiation increased at higher concentration of carbon monoxide. As the removal of NO_2 converting to HNO_3 is not difficult, addition of carbon monoxide will be effective for the removal of NO_x.

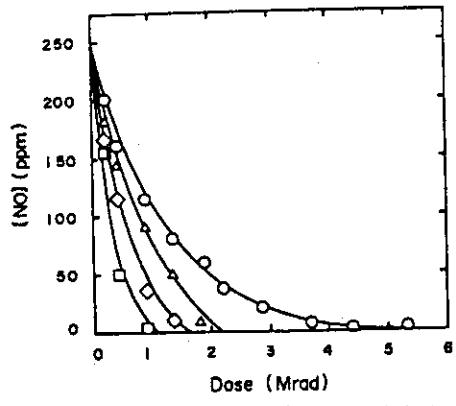

Carbon monoxide(0%(○), 0.29%(△), 0.59% (◇) and 1.17%(□)), NO(250 ppm), water vapour(8%), oxygen(12%) and nitrogen(78.8-80%). Irradiation temp. (120°C).

Fig. 11 Effect of carbon monoxide on removal of NO

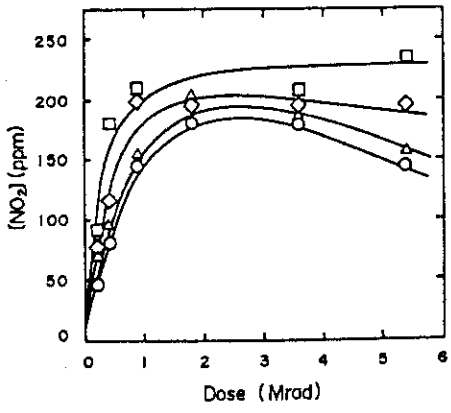

Carbon monoxide(0%(○), 0.29%(△), 0.59% (◇) and 1.17%(□)), NO(250 ppm), water vapour(8%), oxygen(12%) and nitrogen(78.8-80%). Irradiation temp. (120°C).

Fig. 12 Effect of carbon monoxide on removal of NO_2

1.2.10 CO_2 concentration

Addition of carbon dioxide shows no effect on removal of NO and formation of NO_2 [7]. Also, the rate of SO_2 removal was not affected by the addition of carbon dioxide up to 13.3 %.

1.3 Optimization of parameters

It will be possible to understand from the discussion mentioned above that the main factors to be decided for optimum control are as follows;

1) Irradiation dose
2) Gas temperature
3) Ammonia injection
4) Multi-stage irradiation
5) Humidity

Fig. 13 shows the relations between these factors. In actual plants, optimum conditions for above factors are limited.

1) Irradiation dose is directly relating to the removal of NO_x and SO_2 and larger dose gives higher removal efficiency. But, the dose should be reduced from economical point of view.
2) The lower temperature is better to remove SO_2 by thermal reaction. On the other hand, the higher temperature of the gas is favorable for avoiding corrosion of the reactor and pipes by the liquid condensation on the wall, and for easy handling of products in the form of dry powder.

The temperature for the treatment should be decided by considering these two factors.
3) Although it was clarified that the higher concentration of ammonia gives higher removal of SO_2 and NO_x, the ammonia injection is limited to reduce the ammonia leakage.
4) Multi-stage irradiation benefits the removal of NO_x and the geometry of the system should be decided at the stage of design from engineering point of view.
5) The humidity is decided by water injection to control temperature by evaporation and the variable range of the humidity is very limited for water-added temperature control system. So, this factor can be neglected.

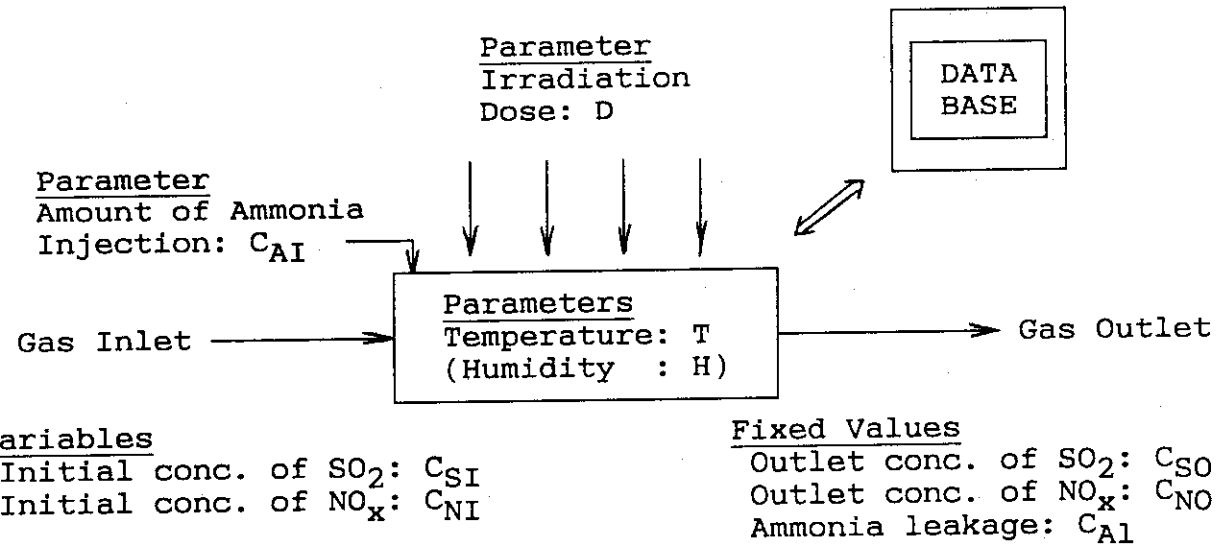

Fig. 13 Factors for optimum operation

For the optimum operation of the process, the factors should be decided by the following procedures and these values should be always recalculated and set to be proper values as the change of variables by computer system. A data base on the relation between these factors and NO_x and SO_2 removal efficiencies is necessary to establish the calculation with the computer system.

1) Decide the amount of SO_2 and NO_x to be removed from the gas.

$$C_{SR} = C_{SI} - C_{SO}$$
$$C_{NR} = C_{NI} - C_{NO}$$

2) Decide the amount of ammonia, C_{AI}, to be injected.

$$C_{AI} = 2 \times C_{SR} + C_{NR} + C_{Al}$$

3) Decide the irradiation dose, D, necessary to remove NO_x.

4) Decide the lowest temp. without condensation of water

5) Check whether the dose is enough to remove SO_2 at lowest temp.
If enough, check the possibility to increase the temp.
If not enough, decide the dose to remove SO_2 at lowest temp.

References

[1] H. Maetzing; "Chemical Kinetics Model of SO_2/NO_x Removal by Electron Beam", Non-Thermal Plasma Techniques for Pollution Control, NATO ASI Series G: Ecological Sciences, Vol. 34, Part A, p.59 (Proceedings of the NATO Advanced Research Workshop on Non-Thermal Plasma Techniques for Pollution Control, held at Cambridge, England, September 21-25, 1992).

[2] H. Namba, S. Hirosawa and N. Suzuki; Proceedings of the 30th Symposium on Radiation Chemistry, Japan, Oct. 21-22, p. 43, 1987 (Nagoya).

[3] H. Maetzing, H. Namba and O. Tokunaga; Radiat. Phys. Chem., Vol. 42, Nos 4-6, P. 673 (1993).

[4] K. Hirota et al.; J. Environmental Science, Vol. 6, No. 2, p. 143 (1993).

[5] S. Hashimoto et al.; "Pilot-scale Test for Electron Beam Purification of Flue Gas from Coal-combustion Boiler", Proceedings of the 1995 CO_2 Control Symposium by EPRI, March 30, 1995 (Miami, Florida).

[6] H. Namba, O. Tokunaga, T. Tanaka, Y. Ogura, S. Aoki and R. Suzuki; "Basic Study on Electron Beam Flue Gas Treatment for Coal-Fired Thermal Plant", Proceedings of the International Conference on Evolution in Beam Application, Nov. 5-8, 1991, p.476 (Takasaki, Japan).

[7] O. Tokunaga and N. Suzuki; Radiat. Phys. Chem., Vol. 24, No. 1, p. 145 (1984).

2. Collection of by-products by ESP and bag filter

S. Hashimoto, H. Namba and O. Tokunaga

Abstract

Effective methods of by-products collection in electron beam treatment of coal combustion gas are discussed. Main technologies used for the collection are filtration by a bag-filter and precipitation by an electro-static precipitator (ESP). From the experimental results, it was shown that ESP is the most excellent tools from the view points of high removal efficiency and no pressure drop of the gas.

2.1 Introduction

Establishment of the technology to collect by-product is very important to complete the process of the electron beam treatment of coal combustion gases. Main technologies used for the collection are filtration by a bag-filter and precipitation by an electro-static precipitator (ESP). In this report, effective methods for collection of by-products are discussed mainly based on the experimental results in Japan Atomic Energy Research Institute.

2.2 Distribution of particle size of by-products [1]

Size distribution of formed aerosol measured by an aerosol spectro-photometer is shown in Fig. 1. The concentration of the gas were as follows; SO_2 (1500 ppm), NO (350 ppm), O_2 (6 %), H_2O (10 %), NH_3 (3000 ppm) and N_2 (balance). The irradiated doses were 2.5 and 12

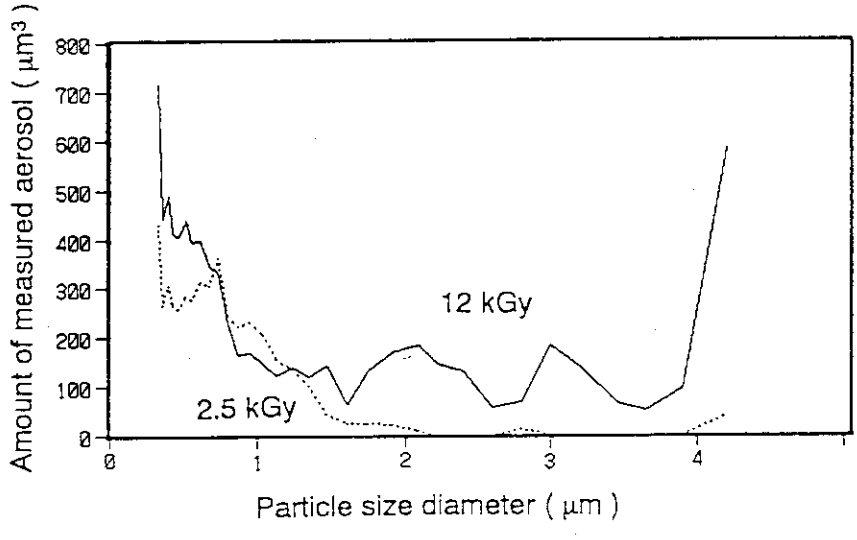

Fig. 1 Size distribution of the aerosol at 0.1 sec after irradiation

kGy. The measurement was carried out at 0.1 second after the irradiation. The detection limit of the spectro-photometer is 0.33 micro-meter. Small amount of totally measured aerosol and the tendency of the distribution curve indicate that the main part of the aerosol exists in smaller region than detection limit.

The size distribution of total amount of aerosol collected at 0.5 seconds after 8.6 kGy irradiation as well as chemical components were shown in Fig. 2. A large part of the aerosol were detected less than 0.46 micro-meter. The peak of the distribution of NO_3^- was detected between 0.22 to 0.33 micro-meter while more than one third of SO_4^{2-} was detected less than 0.06 micro-meter. The bimodal distribution of the aerosol is clearly correlated with its formation by condensation of sulfuric acid from the gas phase. The primary particle formation (below 0.06 micrometer) coagulates rapidly forming the mode between 0.22 to 0.46 micro-meter.

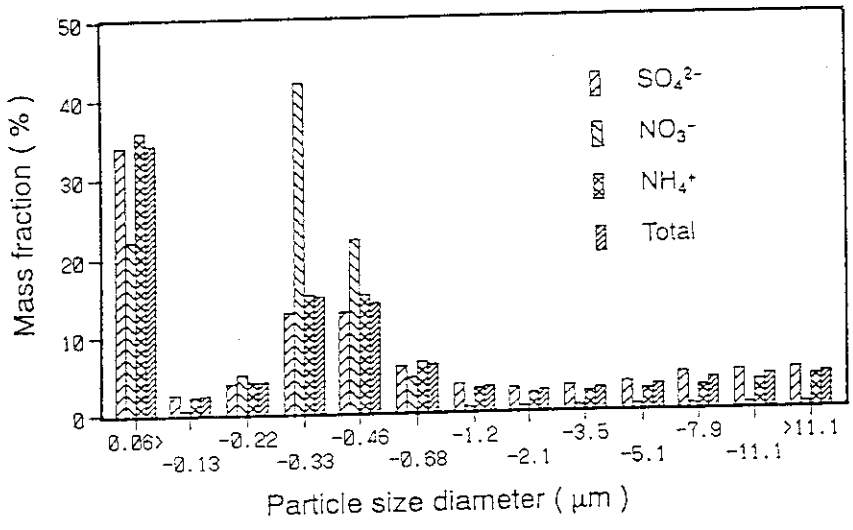

Fig. 2 Size distribution of the aerosol and its chemical components at 0.5 sec after irradiation with 8.6 kGy

Fig. 3 shows the size distribution of aerosol and its chemical components sampled at 30 seconds after the irradiation with 14 kGy. The distribution is significantly different from that observed at 0.5 second after the irradiation. This is probably due to a growth of the aerosol by coagulation of the primary aerosol and by condensation of sulfuric and nitric acid in the presence of ammonia on the surface of the primary particles forming the mode between 0.22 to 0.52 micro-meter. The ratio of ammonia components to total aerosol in the mode at 30 seconds is more than that at 0.5 second. This indicates gaseous ammonia is absorbed on the aerosol during the coagulation. It can be also said that some part of the primary aerosol may be deposited on the walls of the reactor and the ducts as will be mentioned later.

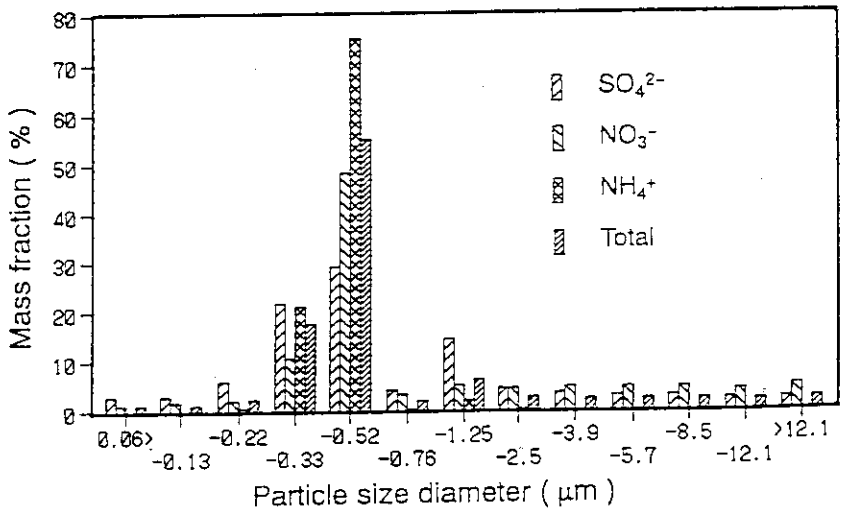

Fig. 3 Size distribution of the aerosol and its chemical components at 30 sec after irradiation with 14 kGy

2.3 Collection of by-products by bag filter [2]

Fig. 4 shows the relation between operation time and the pressure drop at the bag filter after starting irradiation. The mixed gases containing 400 ppm of NO, 1720 ppm of SO_2, 3840 ppm of ammonia, 13 % of water, 6.9 % of oxygen and balance of nitrogen were used as model of coal combustion gases.

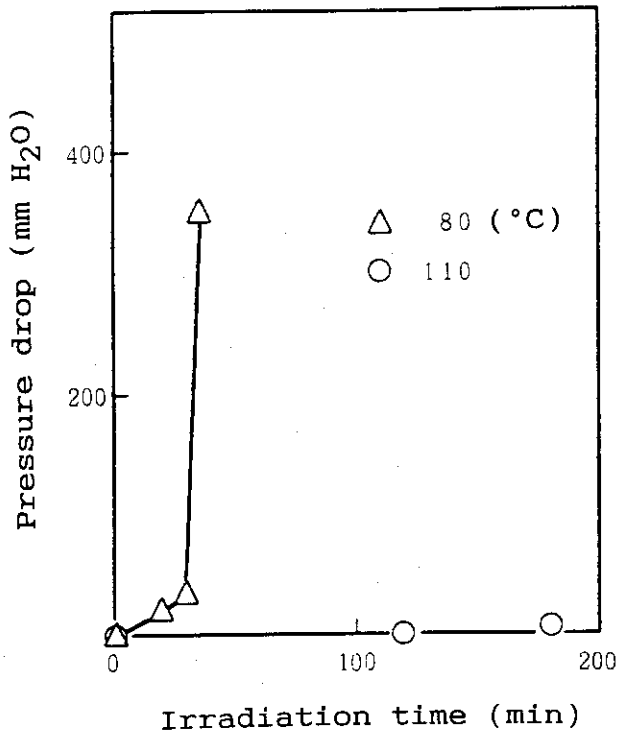

Fig. 4 Change of pressure drop at the bag filter

The pressure drop irradiated at 80 °C increased very quickly after 30 minutes and it was difficult to continue the operation. As shown in Photo. 1, the products are accumulated between the fibers of the bag filter at 80 °C. On the other hand, almost no pressure drop was observed at 110 °C and not so much accumulation of the products was observed (Photo. 2) in this case.

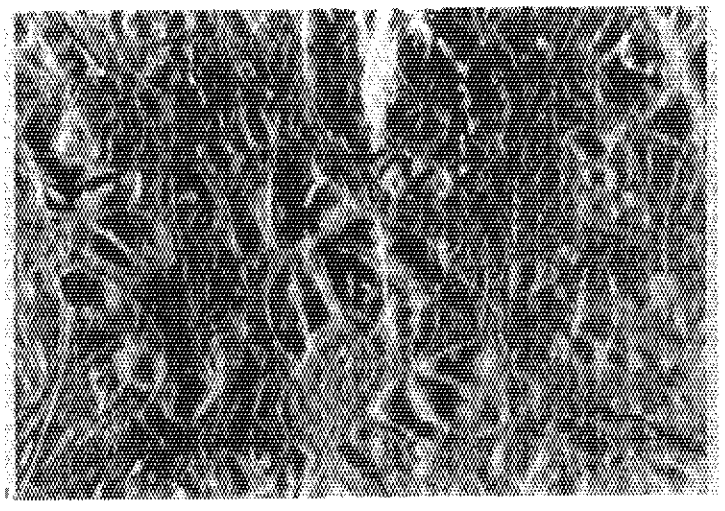

Photo. 1 Surface of the bag filter after use (80 °C)

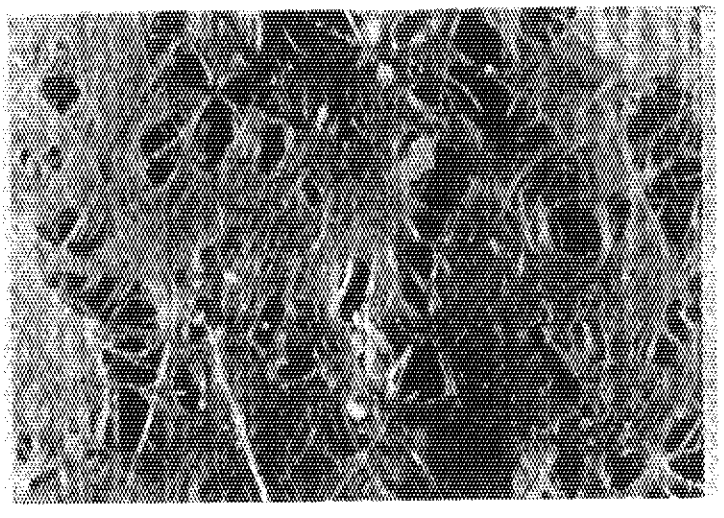

Photo. 2 Surface of the bag-filter after use (110 °C)

2.4 Collection of by-products by ESP

The mixed gases containing 3900 ppm of NO, 1530 ppm of SO_2, 1 stoichiometry of ammonia, 13 % of water, 6.9 % of oxygen and balance of nitrogen were used. The irradiation dose was 17 kGy at 80 °C. The concentration of dusts including by-products in the gas after ESP was 3.8×10^{-4} g/m^{3}N during the operation of ESP. On the other hand, the concentration of the dusts was 1.24 g/m^{3}N without operation of the ESP. So the efficiency of the collection was calculated to be 99.97 % and this value is very high compared with bag filter. In this experiments, the flow rate of the gas was 2.7 cm/sec and very small. More than 99.5 % of the dust collection was also performed in the pilot plant test which was carried out in the premises of the Shin-Nagoya Thermal Power Station, Nagoya even the treatment capacity was 12000 m^3/hr [3].

2.5 Deposit of by-product on the reactor and the duct [2]

Deposit of the products in the ESP and on the walls of reactor and ducts upstream and downstream of the ESP are shown in Table 1 together with the result of chemical analysis of the products. The most part of NO_3 was collected in ESP. But almost the same amount of SO_4^{2-} which was collected in ESP was also collected from the duct before ESP. This means that the large part of the sulfur deposited in the reactor and the ducts before attaining the ESP. It should be considered in an actual plant to install the removal system of the by-products accumulated on the walls of reactor and duct.

Table 1. Deposit of the product

Condition	Components	Upstream of ESP	ESP	Downstream of ESP
NH_3:1 St.	NH_4^+	201(43.6)	88.2(19.1)	17.9(3.9)
	SO_4^{2-}	99(21.5)	33.7(7.3)	7.9(1.7)
80 °C	NO_3^-	1.8(0.4)	11.3(2.5)	- (-)
NH_3:1 St.	NH_4^+	98.9(29.3)	107.8(31.9)	15.0(4.4)
	SO_4^{2-}	50.0(14.8)	51.3(15.2)	7.9(2.3)
70 °C	NO_3^-	0.2(0.1)	6.8(2.0)	0.1(0.0)
NH_3:0.5St.	NH_4^+	99.1(42.9)	48.3(20.9)	4.6(2.0)
	SO_4^{2-}	48.1(20.8)	21.8(9.4)	2.2(1.0)
70 °C	NO_3^-	0.3(0.1)	6.0(2.6)	0.5(0.2)

The values are shown in mmol., those in ( ) show ratios to the total value by %.
St.:Stoichiometry, SO_2:1570-1670ppm, NO:360-390ppm, Dose: 17kGy

References

[1] H. Namba, O. Tokunaga and H. R. Paur; J. Aerosol Sci., Vol. 22, Suppl. 1, p.S475, (1991).

[2] H. Namba et al.; JAERI-Tech, to be submitted.

[3] S. Hashimoto et al.; "Pilot-scale Test for Electron Beam Purification of Flue Gas from Coal-combustion Boiler", Proceedings of the 1995 CO_2 Control Symposium by EPRI, March 30, 1995 (Miami, Florida).

III. Kaweczyn Pilot Plant

1. Optimization of process parameters for efficient removal of SO_2 and NO_x
2. Collection of by-products by bag filter
3. Development of e-beam process monitoring system
4. Electron beam scanning and centering automatic control system
5. The dose distribution in the reactor of the Kaweczyn Pilot Plant
6. Experimental studies of the prototype internal beam monitor in Kaweczyn power station installation
7. Calculations of the spatial dose distribution during irradiation of a gas sample by low energy electron beam
8. Data acquisition and control system

1. Optimization of process parameters for efficient removal of SO_2 and NO_x

A.G. Chmielewski, J. Licki, B. Tymiński, E. Iller and Z. Zimek

ABSTRACT

The research on optimization of process parameters for efficient removal of SO_2 and NO_x is discussed in the chapter. Discussed tests has been performed on industrial pilot plant (20 000 Nm^3/h) at EPS Kawęczyn. The new humidification system has been built which allows to obtain gas humidity above 10% vol. Removal of NO_x depends very directly on mode of irradiation (multistage process) and dose distribution i.e. construction of irradiation vessel. Solutions applied in Polish pilot plant are pointed out.

The maximal measured removal efficiences were 98% for SO_2 and 80% for NO_x.

1.1. INTRODUCTION

1.1.1. Physico-chemical process principles

High-energy electrons, when moving in a gas , form hundreds of ions and free radicals along their path of motion. Amount of electron energy absorbed by the various components of such gas of mixed form is proportional to their mass fraction. Hence, in the case of flue gas more than 90% of electron energy is absorbed by nitrogen, oxygen, water vapour and carbon dioxide. The process chemistry was presented by Mätzing [1].

Since the acidic pollutants SO_2 and NO_x of interest are present at low concentrations (e.g. SO_2 up to 3000 ppm, NO_x up to 500 ppm), the energy transfer process is indirect as is illustrated by the following pathway:

$$\text{gas matrix } (N_2,\ O_2,\ H_2O,\ CO_2) \Rightarrow \text{ions, radicals} \Rightarrow \text{radicals} \Rightarrow \text{products} \qquad (1)$$

During simultaneous removal of SO_2 and NO_x from flue gas from coal combustion the values of G reach 20/100 eV in single-stage irradiation.

Ions formed as a result of an interaction of electrons with gas molecules react very rapidly with the predominant components of the gas matrix. This results in a redistribution of the absorbed energy so that the traces of the primary radiolytic reactions become extinct very rapidly. In reactions of the type: positive ion-molecule forms are most relevant in this redistribution.

Besides a simple charge transfer, many reactions of positive ion-molecules are coupled with dissociation of the one or both reaction components, leading to the formation of neutral radicals. Thus, the reactions connected with positive charge transfer are the most relevant source of radicals in the electron beam processing for flue gas treatment [1, 2, 3].

The most reactive is the OH radical, formed at the rate of hundreds of ppm/s at the power dose 10 kGy/s. About 90% of OH forms as a result of the reaction of positive ion-molecule, while only 10% are the result of direct decomposition of water vapour.

The overall rate of radicals formation is dependent on the dose, an increase in which results in higher process efficiency.

The formed radicals are reactive with respect to the matrix gases to a very small degree. They are, however, accessible for the desired decomposition and removal of the gaseous pollutants. The only exception is hydrogen atoms, which directly bond with oxygen producing HO_2 radicals. For a change, this radical reacts selectively at a high rate with NO yielding NO_2 and OH. The oxygen atom bonds relatively slowly with molecular oxygen forming ozone, which is used to oxidize NO and other pollutants.

The OH radical plays a key role in simultaneous removal of NO_x and SO_2 from flue gas. It is indispensable in forming sulfuric and nitric acid molecules, and in initiating their aerosol production. While OH is very reactive, four main trace components compete in bringing about its consumption:

$$NO + OH + M \rightarrow HNO_2 + M \qquad (1) \qquad k_1 \cdot [M] \approx 4 \cdot 10^{-12}\ cm^3/sec \qquad (2)$$

$$NO_2 + OH + M \rightarrow NHO_3 + M \qquad (2) \qquad k_2 \cdot [M] \approx 9 \cdot 10^{-12}\ cm^3/sec \qquad (3)$$

$$SO_2 + OH + M \rightarrow HSO_3 + M \qquad (3) \qquad k_3 \cdot [M] \approx 7 \cdot 10^{-13}\ cm^3/sec \qquad (4)$$

$$NH_3 + OH \rightarrow NH_2 + H_2O \qquad (4) \qquad k_4 \approx 3 \cdot 10^{-13}\ cm^3/sec \qquad (5)$$

The given reaction rate constants correspond to 1 bar pressure and 350°K temperature. The competition is very intensive since the differences in reaction rates are levelled off by the influence of the reagent concentration.

While SO_2 can be removed only by its oxidation to the sulfuric acid radical, removal of NO_x is accomplished both by oxidation as well as by reduction. Nitrogen atoms and NH_2 radicals can reduce NO_x to two stable gaseous products - molecular nitrogen and nitrous oxide [2].

$$NO + N \rightarrow N_2 + O \qquad (6)$$

$$NO + NH_2 \rightarrow N_2 + H_2O \qquad (7)$$

$$NO_2 + N \rightarrow N_2O + O \qquad (8)$$

$$NO_2 + NH_2 \rightarrow N_2O + H_2O \qquad (9)$$

In order to produce N_2O the reaction (9) is more important than the reaction (8), so the N_2O emission can be controlled by an appropriately controlled rate of ammonia injection. Amount of nitrogen usually shows a deficit amounting to up to 20% of the initial NO concentration, depending on the process conditions. The phenomenon of molecular nitrogen formation has been verified by application of the isotopic tracer N-15 [4].

The above described reaction path of NO_x removal is frequently disrupted by decomposition of the intermediate compounds. The most significant reaction of this type is

$$NO_2 + O \rightarrow NO + O_2 \qquad (10)$$

This reaction results in a non-linearity of the relationships quantifying NO_x removal as a function of the irradiation dose. Formation of the intermediate product HNO_2 has been experimentally verified [5], however, the amount of its generation was less than that predicted from the model calculations [1]. Main reactions leading to SO_2 and NO_x removal from flue gases are summarized in [6].

The presented mechanism does not account for mass transfer. The process of the reaction product removal is affected by absorption and adsorption, dissolution etc. These phenomena are strongly exhibited under operating conditions closely matching optimal values of process parameters, i.e. at 60-70°C and high absolute humidity (over 10% vol. of water vapour) [7]. Oxidation reactions of SO_2 are catalyzed at the interfacial surface [8,9,10].

From the discussion dealing with the process mechanism one can conclude that the overall SO_2 removal effectiveness is affected by two factors:
- thermal reactions and
- reactions induced by irradiation:

$$\eta\ SO_2 = \eta_1\ (\varphi,\ T) + \eta_2\ (D,\ \alpha_{NH3},\ T) \qquad (11)$$

The yield of the thermal reaction is then determined by gas humidity and temperature T. Depending upon the process conditions this value may reach 20-70%.

It should be pointed out that without electron beam irradiation sulfites are also formed [9].

1.1.2. Pilot plant of flue gases cleaning from SO_2 and NO_x at the Kawęczyn Power Plant

(1) Plant location

The plant is located at the Kawęczyn Power Plant site in Warsaw. It cleans up flue gases of the volumetric flow rate up to 20 000 Nm^3/h from SO_2 and NO_x. The flue gases are extracted from the WP-120 type boilers. Location of the plant facility close to the electrofilters removing fly ashes from the flue gases fed to the stack allows gas stream to be collected from the discharge pipings from both WP-120 boilers. The layout of this situation is shown in Fig.1.

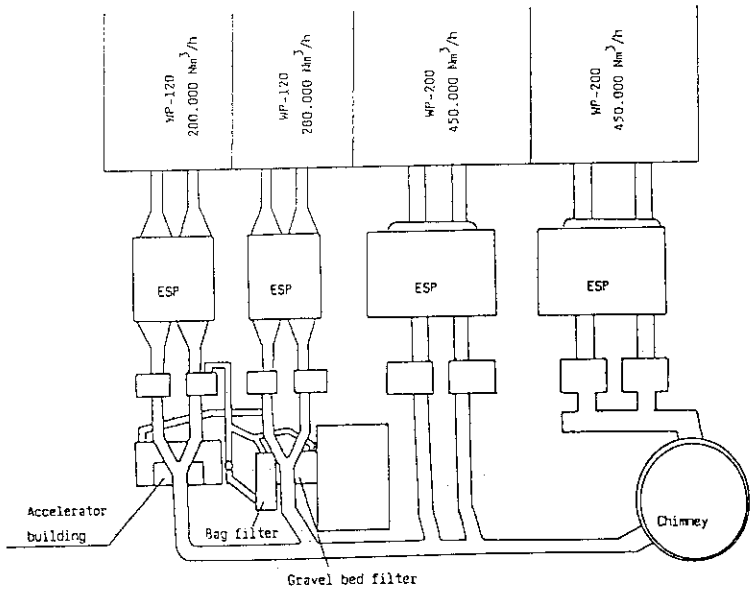

Fig.1. Power Plant Kawęczyn-Warszawa. Location of the installation.

After passing through the electrofilters the discharged gas, partially free of fly ash, are fed to the installation where the simultaneous removal of SO_2 and NO_x takes place [12]. Typical composition of discharged gas from the WP-120 boilers working at Kawęczyn Power Plant is listed in Table 1.

Table 1. Typical flue gas composition from a WP-120 boiler.

CO_2	10-12 vol.%
O_2	8-10%
H_2O	30-50 g/Nm^3
SO_2	0.9-1.2 g/Nm^3
NO_x	0.2-0.55 g/Nm^3
N_2	from balance
dust concentration before ESP	25 g/Nm^3
dust concentration after ESP	0.2-0.6 g/Nm^3

(2) General layout of the installation

The installation consists of four main sections:
1. humidifying-cooling tower,
2. system of ammonium dosing,
3. reactor chamber with two accelerators,
4. filtration section - bag filter, and gravel bed filter.

It was designed by the designing companies PROATOM and ENERGOPROJEKT, and assembled by Elektromontaż and Betonstal. The investment overview was performed by the Kawęczyn Power Plant. A layout of the installation equipped with a bag filter is shown in Fig.2.

In 1992 a wet gravel bed filter of capacity 5000 Nm^3/h was added to the facility. This modification is shown in Fig.3.

The detailed description of the pilot plant is given in [12]. However in the frame of IAEA-JAERI-INCT collaboration the humidification system was improved. The description of new system is given in next paragraph.

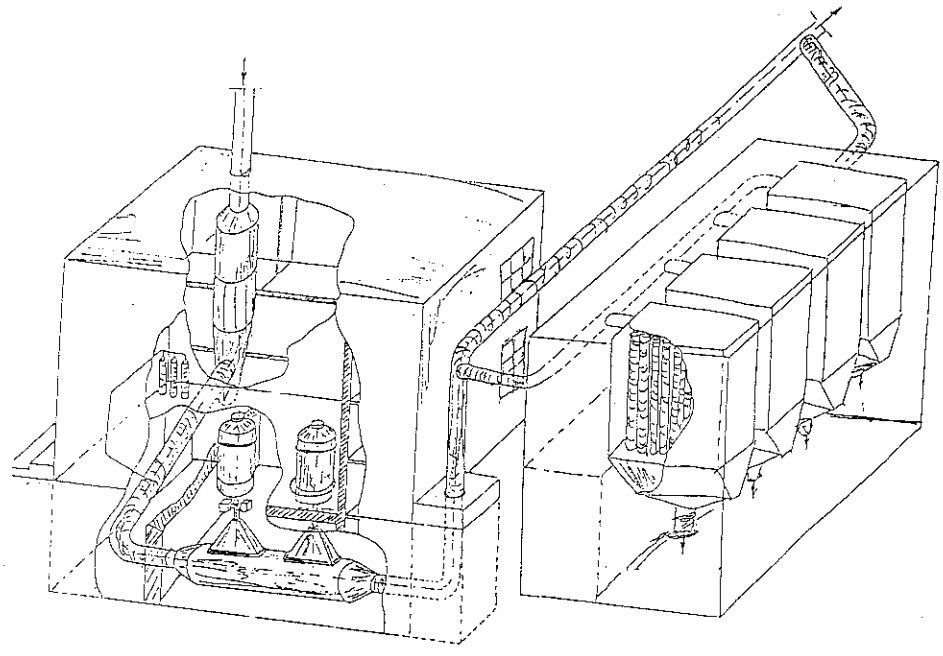

Fig.2. Scheme of an installation for simultaneous removal of SO_2 and NO_x equipped with a bag filter.

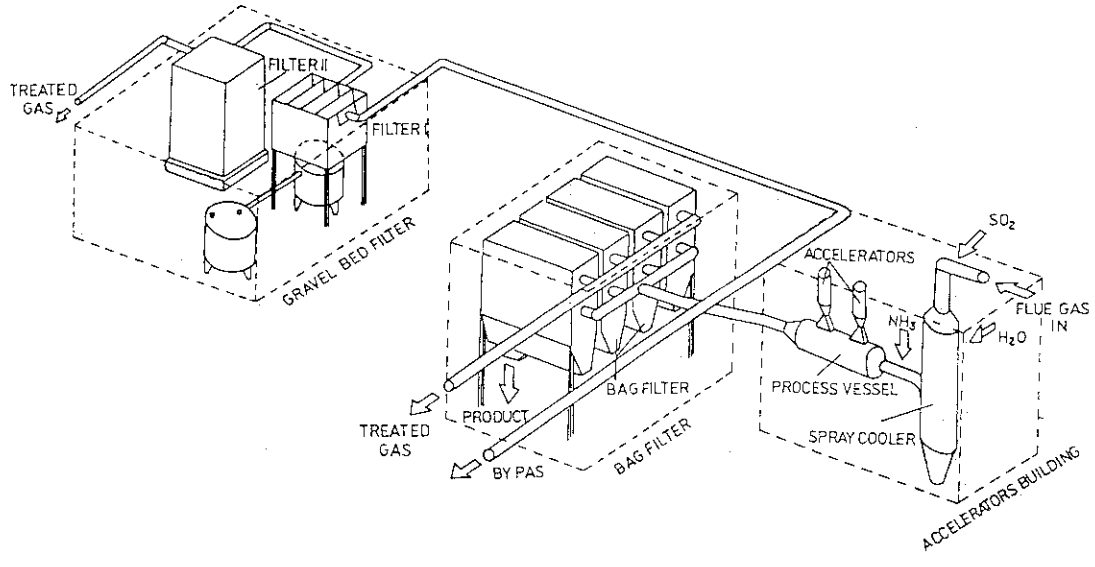

Fig.3. General scheme of the pilot plant at the Kawęczyn Power Plant.

1) Spray cooler

The apparatus is a cylinder of diameter ca. 1.5 m and height about 6 m, with volume of 9 m^3. It is equipped with a Caldyn nozzle which sprays water by means of compressed air into droplets of about 50 μm in diameter. Complete evaporation of the sprayed water and subsequent gas cooling occur in the tower.

The outlet gas, which leaves the electrofilter, contains fly ash amounting from 80 mg/Nm^3 to 600 mg/Nm^3, depending on the type of coal and electrofilter dust removal efficiency. The inlet gas temperature is between 95 and 120°C, while humidity does not exceed 5.5% vol. of water vapour. In the sprayed tower gas flowing in parallel to the sprayed water is cooled down to about 65-70°C and their humidity is increased to 8% vol. water vapour. Water introduced by of the two-phase nozzles is completely evaporated so that the tower operates at a "dry bottom".

Before the testing period 1992/93 the way of feeding water into the nozzles was changed and cold water was replaced by hot water supplied from a central heating system. The water is introduced to the nozzles at 80°C which allows to increase water vapour content in the outlet gas stream up to 9% vol. (Fig.4).

As it follows from the laboratory-scale tests the greatest removal effectiveness for SO_2 is achieved if humidity of the gas stream fed into the reaction chamber reaches 11-12% vol. Hence, a new system of flue gas conditioning has been designed and installed. It comprises of a column layer packing of Białecki rings, while the water fed from the top through the spraying nozzles is circulated and heated in a heat exchanger (Fig.7).

Flue gas of temperature 140-145°C should be cooled down 70 to 65°C in a direct heat transfer process with a sprayed water, while increasing water vapour content to 10-12% vol. This process can be carried out in a sprayed tower (scrubber) where water is sprayed by means of the water nozzles and flows cocurrently with the gas stream.

The amount of water introduced is controlled with a controling computer-aided system, and the operational impulse is temperature of the gas leaving the tower after its humidification. The layout of this system, together with the other measuring points, is shown in Fig.4.

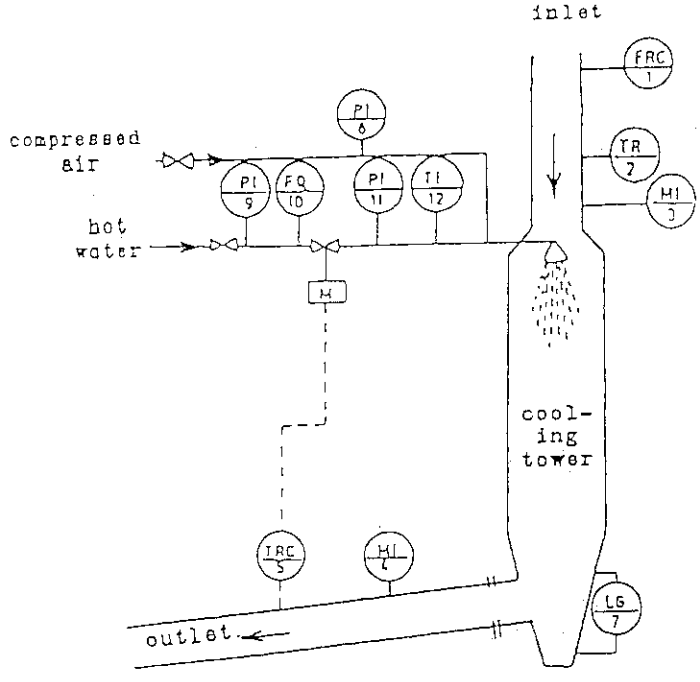

Fig.4. Flue gas humidifying system with hot water.

In the course of the column operation the following parameters are measured and controlled: inlet gas volumetric flow rate (FRC-1), its temperature (TR-2) and humidity (MI-3), pressure of air introduced to the nozzles (PI-8), pressure of the hot water feeding the nozzles (PI-9), amount of the water fed to the nozzles (FQ-10), pressure of the hot water after the regulating valve (PI-11) and its temperature (TI-12). In the gas stream leaving the column its humidity is also measured (MI-4, MR-6) - at present a recorder for a continuous measurements of humidity is assembled. The readings of the recorder TRC-5 via a computer system control a regulating valve through which the water is fed into the nozzles. Such a computerized control system enables to secure a reliable work of the flue gas conditioning section.

New constructed system, schematically shown in Fig.5, is a flue gas conditioning system based on a heat exchanger and water recirculation. This allows for an additional (beside the ESP) removal of fly ash from the flue gas and is applicable in the case of small effectiveness of the dust removal section (at fly ash concentration in the gas > 150 mg/Nm^3).

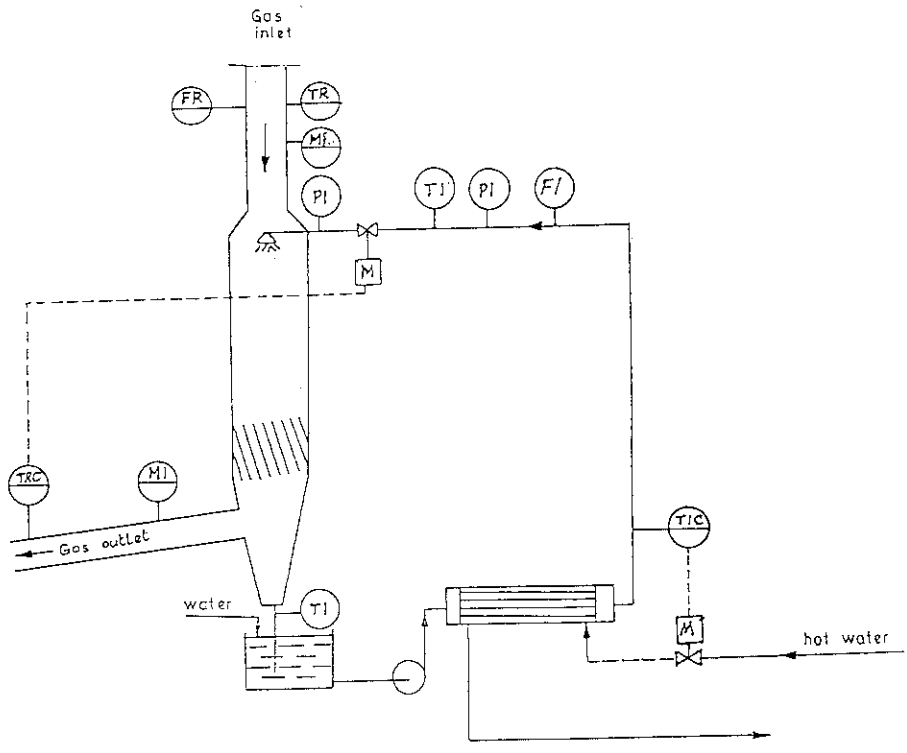

Fig.5. Flue gas conditioning system with recirculation of hot water.

2) Reaction chamber and system of accelerators

Removal efficiency of NO_x depends very much on dose distribution and mode of gas irradiation (single or double). The dose distribution is discussed in another chapter. Here only some details of irradiation system are presented.

In spite the fact that the process of flue gases cleaning using electron beam irradiation has been studied for many years, there are numerous problems which require technical solutions and optimization before an industrial implementation of this technology. These problems deal mainly effective filtration of the product, optimal energy spending and flue gases conditioning. One of the

most important idea, of fundamental significance of the Kawęczyn pilot plant design, was an application of a two-stage exposition of gases to the electron beam. This leads to a meaningful decrease in energy demand supplied to the gas and indispensable for active radicals formation which induce radiative reactions (cf. Chapter 2.1).

Another important solution was a longitudinal gas irradiation by the electron beam and application of air impingement (air curtain) below the second window of the electron beam introduction system to the irradiation chamber.

The new solutions applied in the Polish plant are shown in Fig.6.

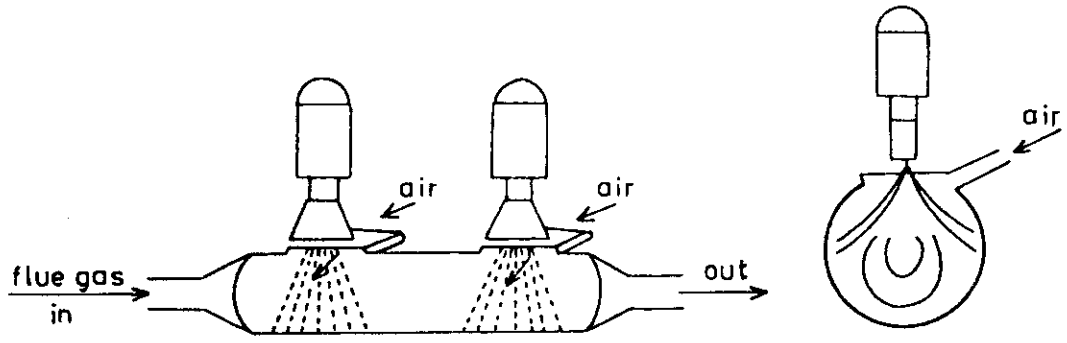

Fig. 6. Arrangement scheme of accelerators and irradiation chamber.

The reaction chamber is a horizontal cylinder of diameter 1.6 m and lenght 7 m. Two windows made of titanium foil of thickness 50 μm are cut in the wall of the chamber. The outlet-scanning sections of the accelerators are located above the surface of the foil. A double window system has been applied, and both windows are cooled by impinging air streams. Air impinging below the bottom window secures it against corrosive action of flue gases. The reactor layout is depicted in Fig.7.

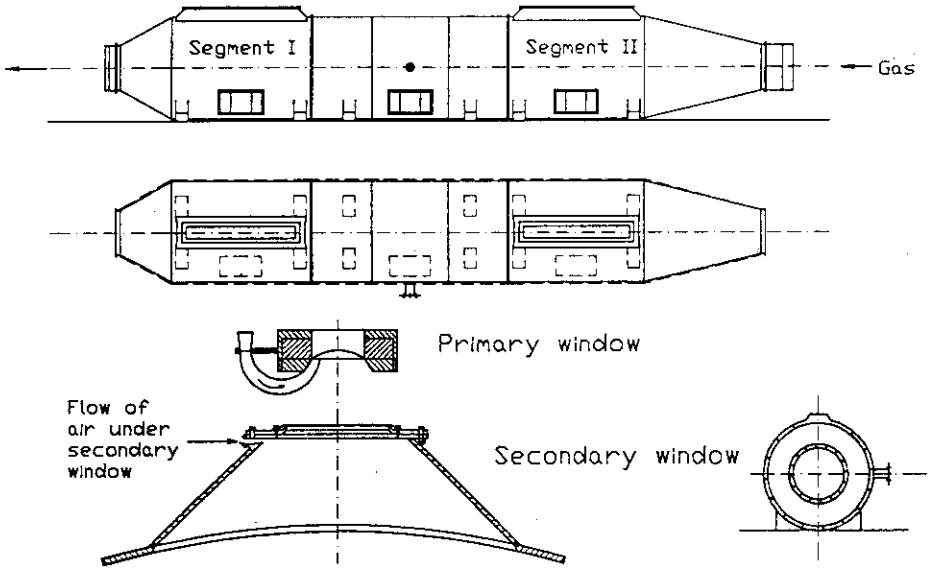

Fig.7. Reactor for gas cleaning by means of electron beam in the pilot plant of the Kawęczyn Power Plant.

Two accelerators ELW-3A, manufactured by the Novosibirsk Institute of Physics of Academy of Science, operate in the installation. Their main characteristics is given in Table 2.

Table 2. Basic parameters of the accelerator type ELW-3A.

Energy of electrons	0.5-0.7 MeV
Energy instability	5%
Power of electron beam	0-50 kW
Beam current	0-100 mA
Instability of beam current	5%
Window size	75 x 1500 mm
Power	70 kW
Dimension of the accelerating section	
diameter	1320 mm
length	2400 mm
mass	3700 kg
Dimension of the control console: 1370 x 1040 x 1340 mm Mass 250 kg	
Pressure of SF_6	1.1 MPa
Cooling water demand	1.5 m^3/h
Cooling air demand	200 m^3/h
Total mass of the equipment	7000 kg

1.2. INFLUENCE OF PROCESS PARAMETERS ON SO_2 REMOVAL

Primary tests for SO_2 were performed with low humidity (5-7% vol.). The effect of dose on removal efficiency is given in Fig. 8. According to the function (15) the influence of ammonia stechiometry is observed as well which shows Fig. 9 (low SO_2) and Fig. 10 (high SO_2). The effect of temperature is remarkable (Fig. 11 and Fig. 12) as effect of gas humidity is (Fig. 13).

After new humidification system has been introduced at EPS Kawęczyn's pilot plant the efficiences of SO_2 removal over 98% were observed (Fig. 14).

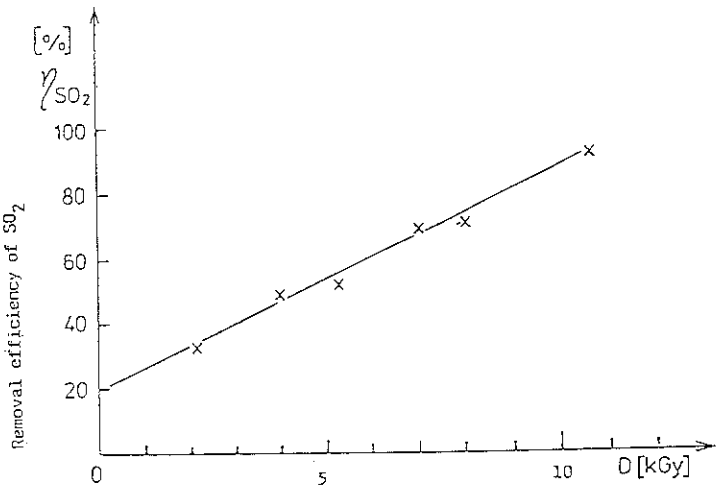

Fig.8. Effect of irradiation dose power on SO_2 removal effectiveness.

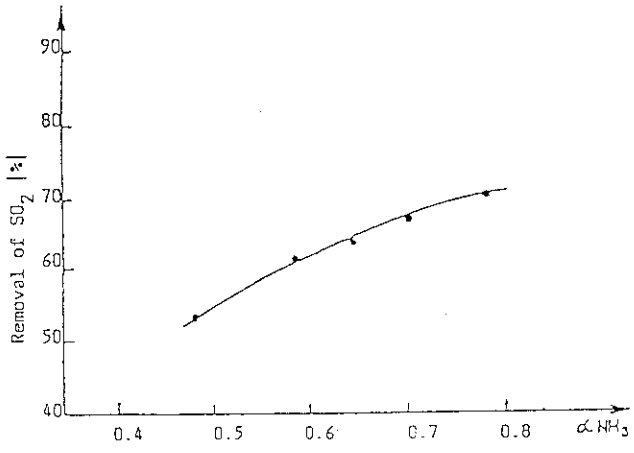

Fig.9. Effect of ammonia stoichiometry (with respect to NO_x and SO_2) on SO_2 removal.
V - 17 100 Nm^3/h, t_{inlet}=70°C,
SO_2° - 387 ppm, NO_x° - 187 ppm,
dose - 4.8 kGy.

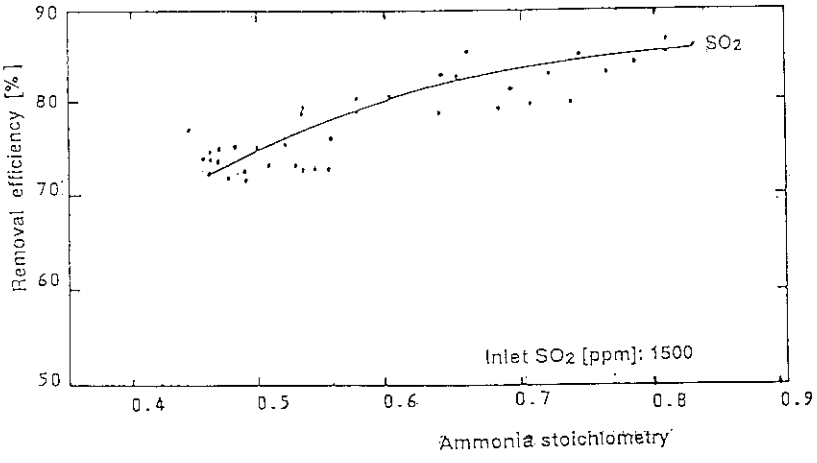

Fig.10. Effect of ammonia stoichiometry on SO_2 removal.
t_{inlet} = 70°C, inlet SO_2° = 1500 ppmV,
NO_x° - 135 ppm, dose 11.5 kGy.

An effect of temperature on SO_2 removal is illustrated in Fig. 11.

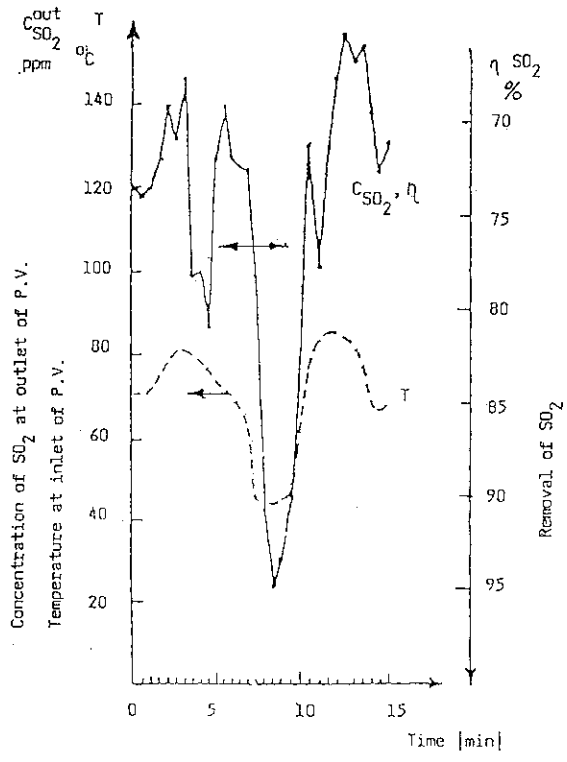

Fig.11. Effect of temperature on the SO_2 removal process.
V = 17 000 Nm^3/h, t^o = 110°C, SO_2^o - 460 ppmV,
NO_x^o - 185 ppmV, α_{NH3} = 0.57, dose - 4.7 kGy.

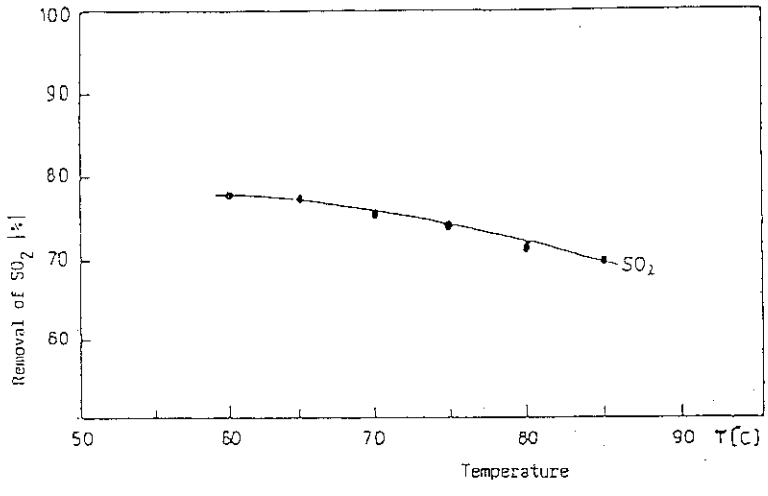

Fig.12. Effect of temperature on SO_2 removal process.
inlet SO_2^o - 1000 ppm, dose - 11.5 kGy.

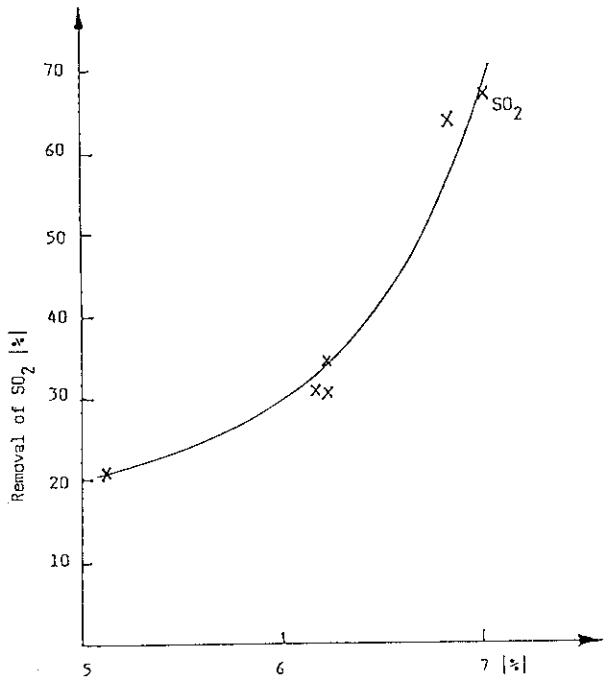

Fig.13. Influence of gas humidity on SO_2 removal (low humidity case).

The investigations of removal SO_2 and NO_x with high humidity of flue gases achieved 10-12% vol. of water vapour content confirmed 95-98% removal efficiency of SO_2. In Fig. 14 the dependency of process parameters on the removal efficiency of SO_2 are shown.

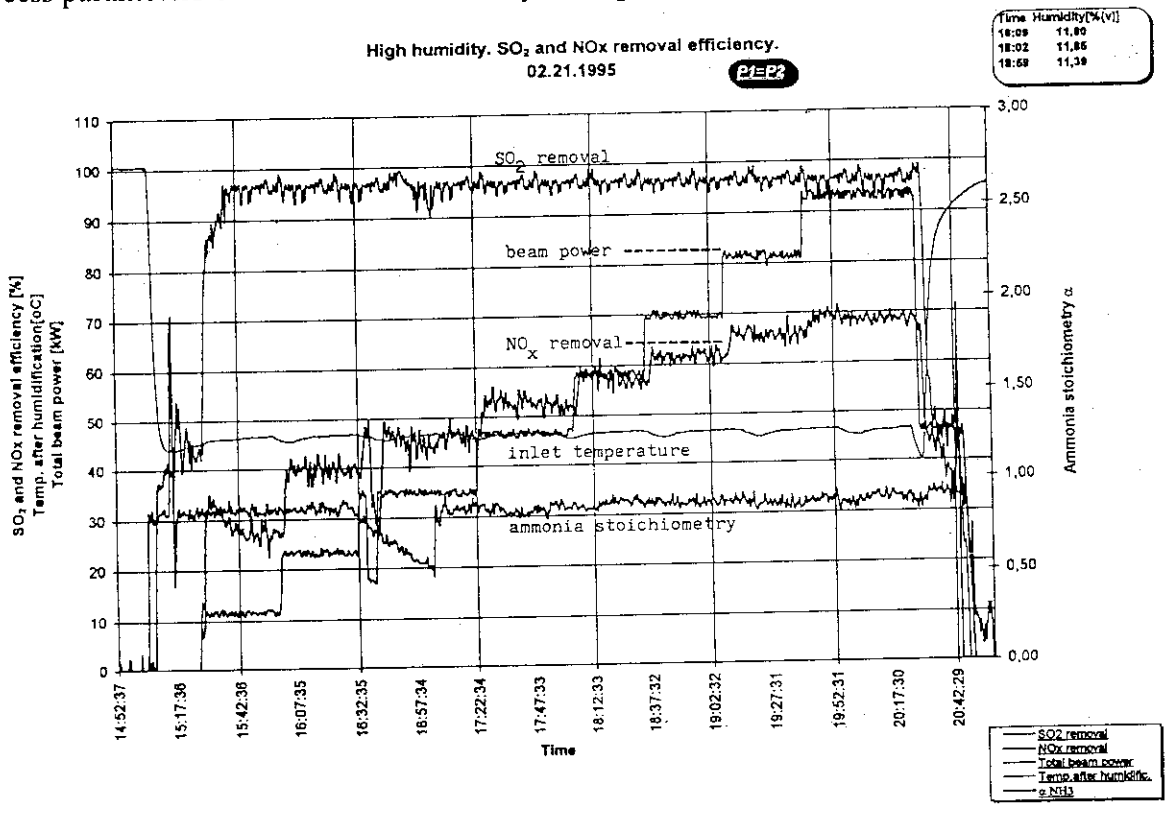

Fig.14. Dependence of SO_2 and NO_x removal on electron beam power. Humidity 11.8 % vol.

1.3. EFFECT OF PROCESS PARAMETERS ON NO_x REMOVAL EFFECTIVENESS

In contrast to SO_2, removal of NO_x occurs mainly as result of electron interaction. Such a dependence for a one-stage gas irradiation by an electron beam is presented in Fig.15.

An effect of temperature on NO_x removal effectiveness is slightly different than that for SO_2. In the range 60-85°C we can observe a small increase of the NO_x removal effectiveness (Fig.16).

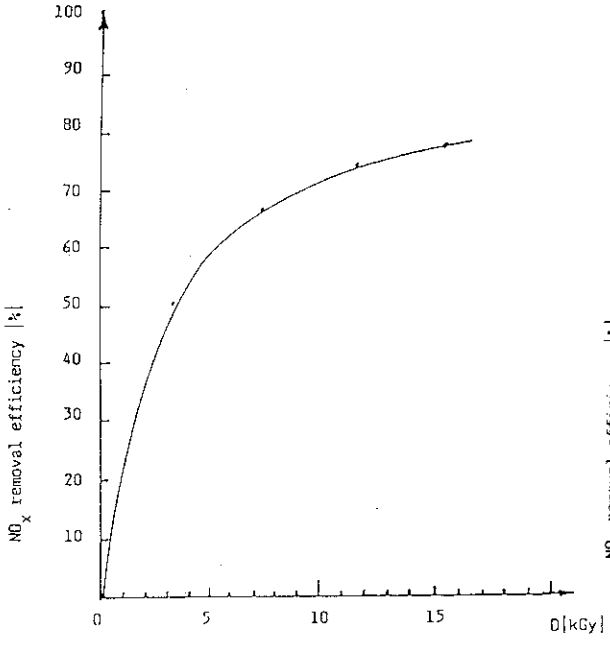

Fig.15. Degree of NO_x removal as a function of dose.
inlet SO_2^o = 1000 ppm,

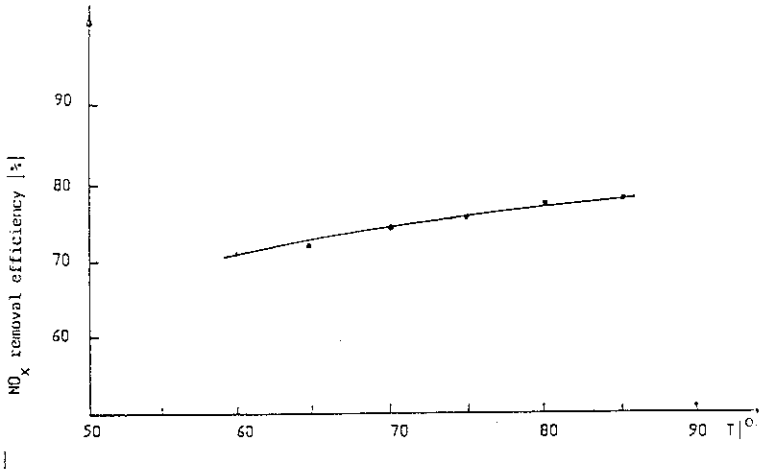

Fig.16. Effect of temperature on the NO_x removal efficiency.

A value of the ammonia stoichiometric factor does not affect greatly the NO_x removal effectiveness (Fig. 17).

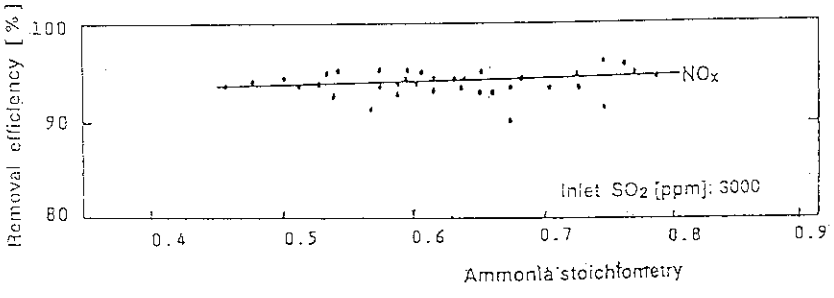

Fig.17. Effect of ammonia stoichiometry on NO_x removal.

An inlet SO_2 concentration largely influences the NO_x removal effectiveness. With the increasing concentration of SO_2 the NO_x removal effectiveness is higher, hence the energy demand drops. This phenomenon is illustrated in Fig. 18. It can be explained by an OH radicals consumption (causing a reverse reaction of NO_2 reduction into NO) by SO_2. The other reason can be H_2SO_4 mist formation in which NO_2 is well soluble. This enables to conclude that the technology under considerations is particularly advantageous (lower energy demand) when flue gases emitted during combustion of coals with high sulfur content should be cleaned.

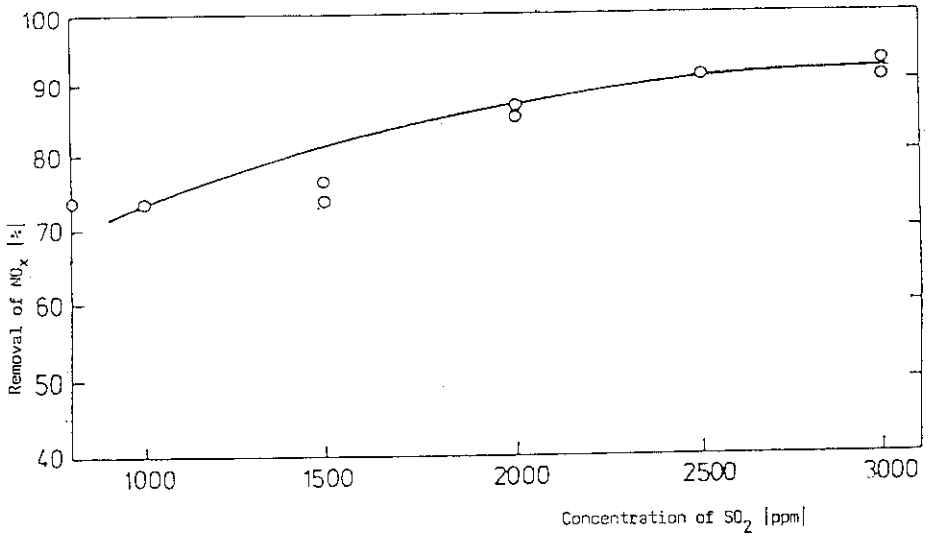

Fig.18. Effect of the inlet SO_2 concentration on the NO_x removal effectiveness.
t_{inlet} = 69.5 - 71°C, inlet NO_x° - 135 ppm, α_{NH3} = 0.59 - 0.65, dose 11.5 kGy, double irradiation.

1.3.1. Effect of the new design on SO_2 and NO_x removal effectiveness from flue gases

Application of a double irradiation of flue gases with an electron beam enabled to achieve high degrees of NO_x removal at about 20% lower energy demand (dose) for the reactions taking place as compared with that for a single stage exposition process. This dependence is presented in Fig. 19.

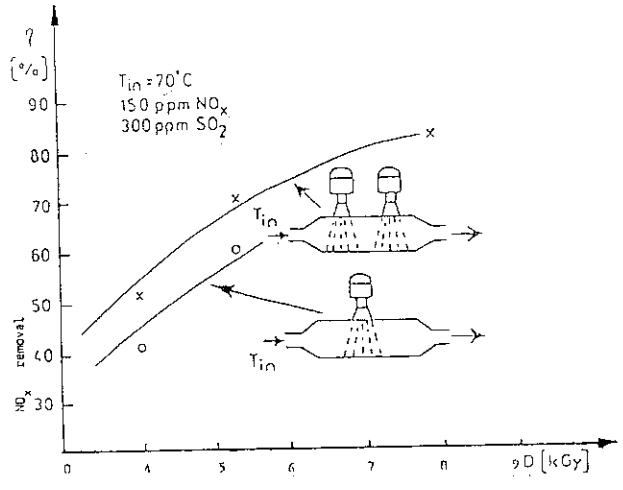

Fig.19. Effect of double irradiation on the NO_x removal effectiveness.

The relationships valid for a system of multistage chemical reactors in series has been used to interpret the results of the multiple irradiation exposition experiments of the gas mixture. In the case of a single irradiation the NO_x removal efficiency is expressed as follows:

$$\alpha = 100\ \Delta\ NO_x/(NO_x)_0 = K_1[1\text{-}\exp(-k_2D/NO_x)_0] \tag{12}$$

where
α - NO_x removal efficiency,
$(NO_x)_0$ - concentration of NO_x in the inlet gas (ppm),
$\Delta NO_x = (NO_x)_1 - (NO_x)_0$ - concentration decrement of NO_x (ppm),
$(NO_x)_1$ - concentration of NO_x after a single gas irradiation exposition by an electron beam,
D - electron energy dose (kGy),
100 - K_1 - measure of NO_x removal (%),
K_2 - parameter characterising the NO_x removal reaction (ppm/kGy).

For a two-stage exposition we get:

$$\alpha = 100[(NO_x)_0 - (NO_x)_2]/(NO_x)_0 = 100 - 0.01\ Y_e Y_f \tag{13}$$

where

$(NO_x)_2$ - NO_x concentration after the second stage of irradiation,

$$Y_e = 100 - K_1[1\text{-}\exp(K_2D/2] \tag{14}$$

$$Y_f = 100 - K_1[1\text{-}\exp(K_2D/0.02\ Y_e)] \tag{15}$$

$$K_2 = k_2/(NO_x)_0 \tag{16}$$

In the case

$$\alpha = 100[(NO_x)_0 - (NO_x)_3]/NO_x)_0 = 100 - 0.0001\ Y_b\ Y_c\ Y_d$$

where

$(NO_x)_3$ - concentration of NO_x after the third stage of gas irradiation by an electron beam,

$$Y_b = 100 - K_1[1\text{-}\exp(K_2D/3)] \tag{17}$$

$$Y_c = 100 - K_1[1\text{-}\exp(K_2D/0.03\ Y_b)] \tag{18}$$

$$Y_d = 100 - K_1[1\text{-}\exp(K_2D/0.3\ Y_b\ Y_c)] \tag{19}$$

Figure 20 shows the result of the model calculations for the data collected at the Kawęczyn Plant. Comparison of the experimental data for a single-stage and two-stage irradiation indicates good agreement. The case of three-stage irradiation concerns only the data theoretically calculated since at the pilot plant only the cases of a single-stage and a two-stage irradiation can be studied.

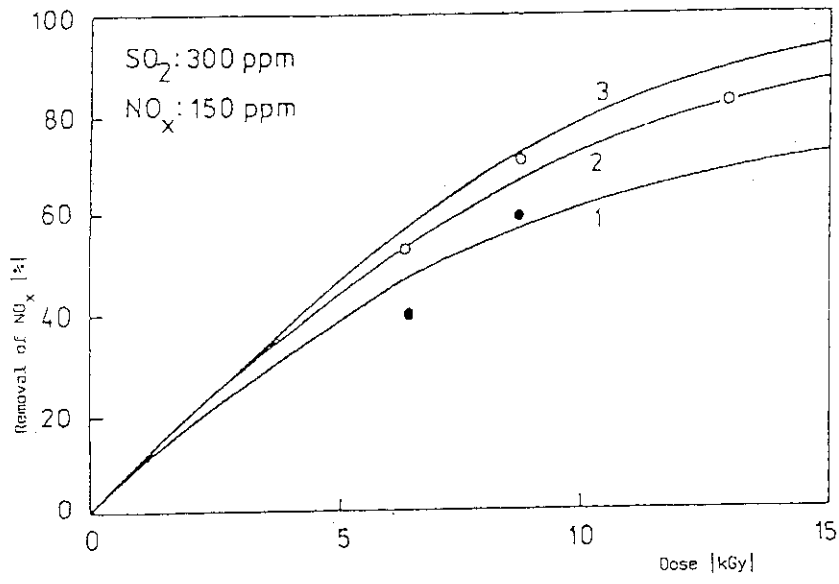

Fig.20. Theoretical curves for a single- and multiple-stage irradiation according to the experimental data obtained in INCT.

Calculations performed for the KfK data [13], and the JAERI data [14], gave also good agreement between the experiment and the model considerations.

The Japanese data confirmed conclusions following from the model that an application of three-stage irradiation yields only small increase in NO_x removal as compared with the two-stage one. It does not seem possible that the three-stage irradiation will find practical application because of much higher capital costs which do not justify the effectiveness achieved. The two-stage irradiation is of great practical significance.

Deeper analysis of the multistage process of the flue gases exposition by an electron beam revealed that in the case of NO_x removal non-uniform power distribution of the accelerators at the successive stages will provide further energy savings (Fig. 21).

An optimal distribution of the electron energy dose supplied to the gas has been calculated using the dependences for NO_x removal after its two-stage and three-stage exposition by an electron beam of a given energy.

The Hook-Jeeves procedure has been applied to find a minimum value of the aim function defined as:

$$f(T,K_1,K_2,D) = \int \mid 100 - \alpha(T,K_1, K_2, D) \mid dD \qquad (20)$$

where
$f(T,K_1,K_2,D)$ - the aim function,
$\alpha(T, K_1, K_2,D)$ - degree of NO_x removal (the model curve),
T - vector of the searched parameters,
T = T[x,y] - for two-stage gas exposition,

T = T[x,y,z] - for three-stage gas exposition,
D - dose (variable parameter),
K_1 and K_2 - constant process parameters,
D_g - upper limit of D variation.
From the analysis the following conclusions can be drawn:
- for two-stage gas exposition by an electron beam the optimal ratio of the dose distribution is x = 0.56, y = 0.44;
- for three-stage irradiation : x = 0.394, y = 0.332, z = 0.274.

The experiments have confirmed theoretical computations, and the results are shown in Fig. 21. However, the energy savings are not so significant as in the case of substitution of a single-stage irradiation by a two-stage one (Fig. 22).

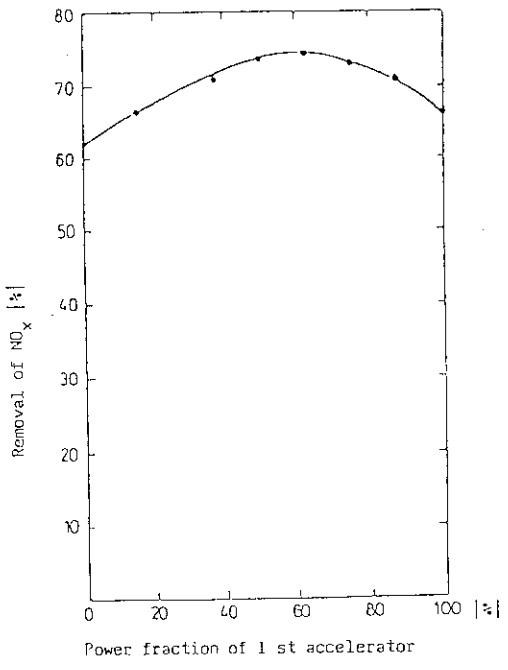

Fig.21. Effect of the accelerator power distribution on the NO_x removal effectiveness.
V = 14 300 Nm^3/h, α_{NH3} = 0.8,
SO_2^o - 395 ppm, NO_x^o - 176 ppm,
t_{inlet} = 70°C, dose = 5.6 kGy.

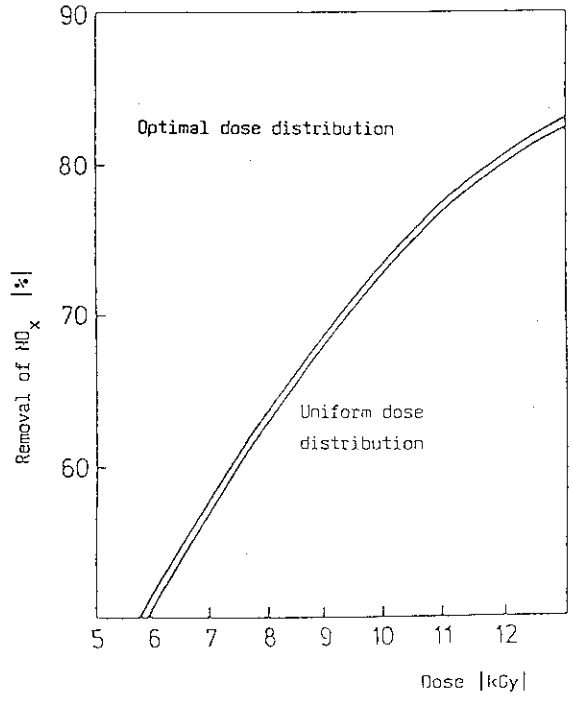

Fig.22. Effect of the electron dose distribution at a two-stage gas irradiation on the NO_x removal effectiveness.

The removal efficiency of NO_x depends on NO_x inlet concentration (Fig. 23).

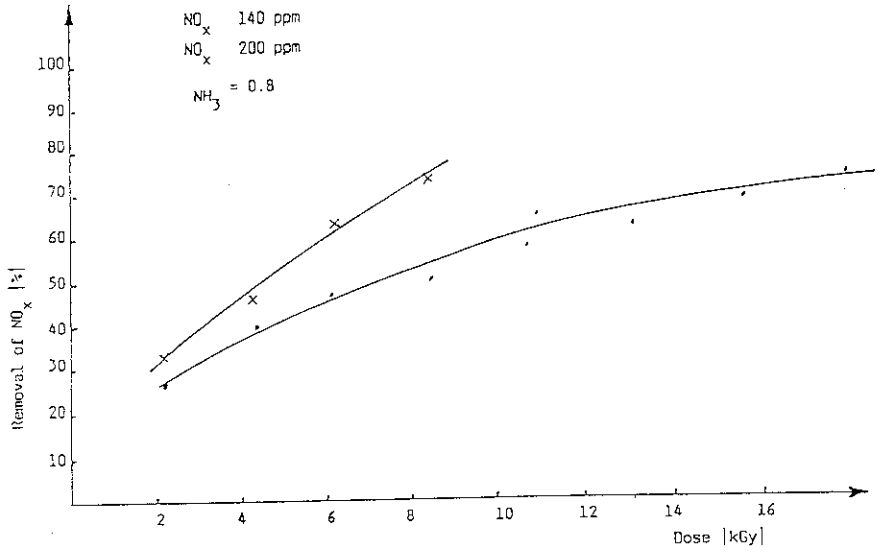

Fig.23. NO_x removal efficiency vs. dose for different NO_x inlet concentrations.

1. 4. CONCLUSIONS

The removal efficiency of SO_2 as high as 98% can be achieved at low temperatures and high humidity. In the case of NO_x removal efficiency depends mostly on dose and mode of energy delivery (single or multistage irradiation). Up to 80% NO_x can be achieved what depends on the process parameters and inlet NO_x concentration.

REFERENCES

1. H. Matzing;
Non-thermal plasma techniques for pollution control. Part B: Electron beam and electrical discharge processing. pp. 59-64.
(Edited by Bernie M. Penetratne and Shirley E. Schutheis) NATO ASI Series. Series G. Ecological Sciences. Vol. 34, part A/B. Berlin: Springer-Verlag 1993.
2. H.R. Paur, H. Namba, O. Tokunaga, H. Matzing;
Aerosol formation and material balance in the electron beam dry scrubbing process. In: Aerosols (S. Masuda, K. Takahashi eds.). Oxford: Pergamon Press, 745-748.
3. J.W. Gentry, H.R. Paur, H. Matzing;
Radiat. Phys. Chem., 31, 95-100 (1988).
4. H. Namba, O. Tokunaga, R. Suzuki, Sh. Aoki;
Appl. Radiat. Isot., Int. J. Radiat. Appl. Instrum., Part A, 41(6), 569-573 (1990).
5. H. Matzing, H. Namba, O. Tokunaga;
International Symposium on Applications of Isotopes and Radiation in Conversion of the Environment. Karlsruhe, Germany, 1992. IAEA-SM-325/1889.
6. H. Namba;
UNDP/IAEA/RCA Regional Training Course on Radiation Technology for Environmental Conservation. JAERI, Takasaki 27.09-8.10.1993, pp. 9-104.
7. A.G. Chmielewski;
Rad. Phys. Chem., (4-6), 46, 1057-62 (1995).
8. P.S. Christensen, N.M. Madsen, H. Livbjerg;
J. Aerosol Sci., Vol. 23, Suppl. 1 pp. 5261-264 (1992).
9. K. Hjuler, K. Dam-Johansen;
Ind. Eng. Chem. Res., Vol. 31, No 9, 2110-2118 (1992).
10. K. Hirota, T. Niina, E. Anvar, H. Namba, O. Tokunaga, Y. Tabata;
SO_2 reaction with ammonia. IAEA-JAERI- INCT Meeting, Takasaki, Japan, February 1994.
11. H. Namba et al.;
Rad. Phys. Chem., 36, 669-672 (1993).
12. A.G. Chmielewski, E. Iller, Z. Zimek, J. Licki;
Proceedings of on International Symposium on Applications of Isotopes and Radiation in Conservation of the Environment. Karlsruhe pp. 8192 (1992).
13. H. Paur, W. Schikarski;
see [5] IAEA-SM-325/187.
14. S. Sato et al.;
see [5] IAEA-SM-325/116.

2. Collection of by-products by bag filter

A.G. Chmielewski, B. Tymiński, G. Zakrzewska-Trznadel, O. Tokunaga and S. Sato*

ABSTRACT

In the paper design, operation and results of investigation of the bag filter in the process of filtration of irradiated flue gas has been presented. Bag house consists of 4 filters with 128 bags, 150 m^2 of filtration area each. Three filters are in operation and the forth in regeneration mode. During experiments 6 kinds of bags and 5 modifications of cages were examined.
The significant influence of garland effect on bag regeneration was found. The removal of filtration cake from the surface of bags by jet-pulse method is not effective enough and other methods of cake removal should be searched.

2.1. INTRODUCTION

The filtration using bag filters is very well known method of dust removal from the gas phase. This method of filtration have a very good efficiency of the range 99,5 to 99,9% [3,4] relative simple construction of apparatus and simple in operation. The product from the bag filter is solid particulate easy to storage and distribute. It was also found that in filter, cake occur intensive reactions of removal of SO_2 and NO_x [4]. Filtration take place mainly in the layer of filter cake deposited on bag surface. The structure, thickness of the cake and its adhession to the filter surface have essential influence on pressure drop during filtration. For reducing pressure drop, aerosols collected on filtering surface should be removed. The most popular method of removal of deposits from the bag surface is pulse jetting. However, other methods like shaking are known. The method of pulse jetting was applied in all bag filters used in EB flue gas treatment plants.
Operation of removal system depends on the kind of filtered aerosols. Removal of sticky deposits which are formed in EB flue gas treatment process makes some problems. This problem was solved by selection of proper bag material, precoating, addition of filtration aid and maximizing of separation forces during jetting by proper garland effect and proper selection of size of jetting valve, pressure of air and time of jetting pulse. In Indianapolis [4] one tested 11 types of bag materials with different finishing of their surface were tested. It was found that acrylic felt singed bags are the best for this purposes. In Badenwerk [3] polyacrylic felt with foam membrane finishing was applied. Manufacturers of filter materials for filtration of such aerosols usually suggest acrylic felt with teflon membrane. The same powder was used for precoating and as filtration aid. In Indianapolis diatomaceus earth was used and in Badenwerk fine grounded lava as well as grounded product of filtration. Diatomaceus earth and lava were the inert materials and they reduced concentration of ammonium salts in the product.
During pulse jetting a bag expands and inertion forces as well as blow of air from the inside should separate cake of product. The separation efficiency depends on a number of operation and design parameters. Distances between wires of the cage and differences of diameters of the bag and the cage are essential for garland effect [6]. The pressure of air, time of jet and size of jetting valves were examined in Badenwerk [3]. One found that too low pressure, too small size of jetting valves and too short or too long jetting time reduce significantly separation efficiency.

* JAERI

2. 2. PROPERTIES OF THE AEROSOL FORMED IN EB PROCESS

The properties of the aerosol created by the electron beam dry scrubbing of flue gas at Kawęczyn Pilot Plant were examined physically and chemically. Particle size distribution was tested with Andersen Stack Sampler connected with 8-stage cascade impactor. The device works according to the EPA standard method and assures the isokinetic sampling. Using this equipment it is possible to measure the size distribution of particles and mass concentration of aerosol, as well.

Aerosol measurements were conducted at the reaction chamber outlet, before the gas entered the baghouse. All samples collected in experiments were analyzed gravimetically and after extraction of filters with bidistilled water, chemically.

The investigations performed at the Pilot Plant confirmed the high fly ash concentration in flue gas introduced into the purification system. The significant fly ash content remains at the reaction chamber outlet, too. The concentration of fly ash depending on the sort of coal used in the boilers varried from 5 up to 50%, and sometimes reached even 70% (Table 1).

The mass concentration of aerosol formed in the process for standard concentration of SO_2, e.g. 250-350 ppmv varied from 169 to 208,8 mg/m^3. For higher SO_2 inlet concentration (1500-3000 ppm) the content of soluble part of aerosol was correspondingly higher.

Table 1. Mass concentration of aerosol measured at the reaction chamber outlet.

Dose	Humidity of gas	Total aerosol	Soluble part of aerosol	Fly ash content
kGy	%	mg/ Nm^3	mg/Nm^3	%
16	7,1	478	208,8	56,3
12	6,8	370	186	49,7
9,2	6,3	262,5	248	5,2
7,3	7,7	434,9	280,2	35,6
4	9,14	591	169	71,5

To determine the concentration of particles for any size range, first the percentage of total particulates for each stage was calculated. Then the cumulative percent was determined beginning with the last stage of the impactor. The data from experiments are presented in Figures 1 and 2. There are two curves in each figure: one curve performs the cumulative percentage of soluble particles versus median diameter, the second cumulative percentage for total aerosol in sample (soluble particles and fly ash together). From Figure 1 it can be seen that approximately 80% of soluble particles are in submicron range, while only 73% of total sample are submicron.

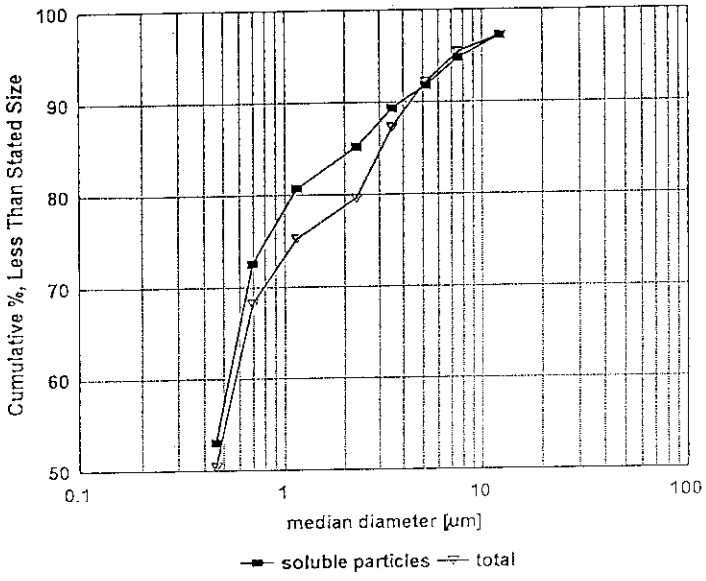

Fig.1. Particle size distribution in flue gas after the reaction chamber. Initial SO_2 concentration 250 ppmV, NO_x - 20 ppmV, flow rate 14 400 Nm^3/h, dose 5.1 kGy, humidity 7.74 % vol., NH_3 stoichiometry - 0.9.

For higher initial SO_2 concentration (3000 ppmv) one can observe the shift into the higher size range: only 40% of aerosol is composed of submicron particulates (Figure 2).

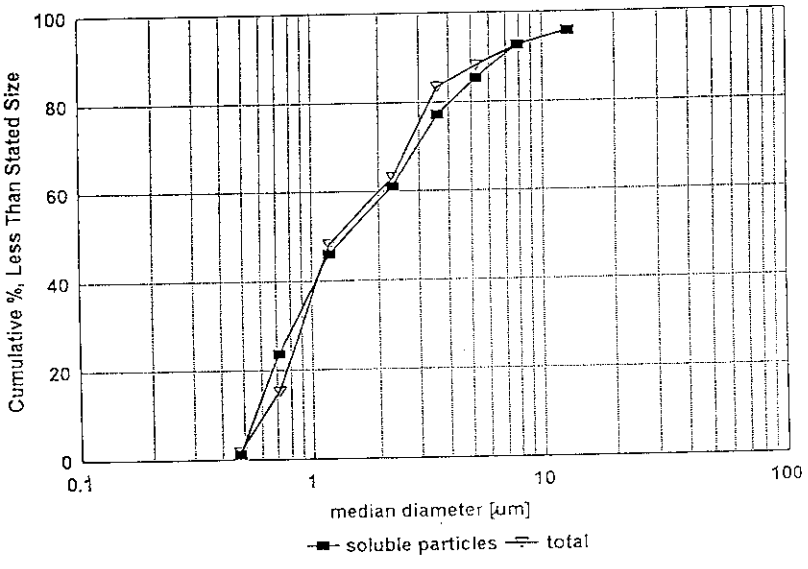

Fig. 2. Particle size distribution in flue gas after the reaction chamber. Initial SO_2 concentration 3 000 ppmV, NO_x - 125 ppmV, flow rate 6 800 Nm^3/h, dose 12.54 kGy, humidity 6.52% vol., NH_3 stoichiometry - 1.14.

In high concentration the particles of primary aerosol formed by the nucleation of acids in the presence of water vapour, more likely condense creating the bigger particles.

The chemical analysis of the aerosol collected in impactor was performed by ion chromatography. According to the analysis the main components of aerosol created in the process were: $SO_4^{(-2)}$ (about 66%), NO_3^-(~ 7%) and NH_3^+ (~ 26%). Small admixtures of other ions like Cl^-, Na^+ or K^+ were detected.

The size distribution of total aerosol and all components as well, is presented in Figure 3.

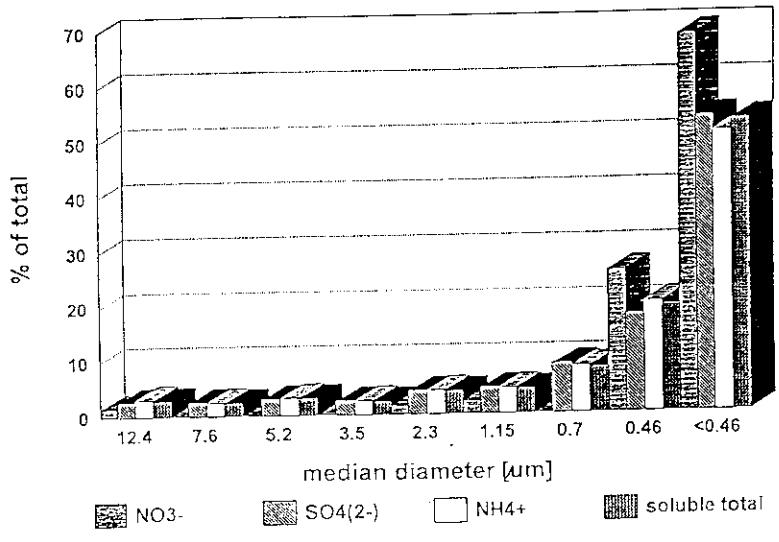

Fig. 3. Size distribution of the components of aerosol collected in flue gas after the reaction chamber. Initial SO_2 concentration 250 ppmV, NO_x - 220 ppmV, flow rate 14 400 Nm^3/h, dose 5.1 kGy, humidity 7.74 % vol., NH_3 stoichiometry - 0.9.

The samples were collected one second after irradiation by 7.3 kGy dose. Under this conditions the great part of aerosol (53%) was less than 0.46 μm, and about 80% was submicron. The peak of distribution of the main components was detected in the least fraction, < 0.46 μm. About 70% of nitrate was in that range. The results are in a good agreement with those reported by the other authors [1,2]. Jordan et al. detected up to 93.4% of nitrate in the fraction smaller than 0.65 μm. Namba et al. noticed the great part of nitrate between 0.22 and 0.33 μm. Having the chance to distinguish the smaller particles he found the peak of sulfate in fraction smaller than 0.66 μm.

In Figure 4 the results of experiment with 3000 ppmv inlet concentration of SO_2 are presented. The samples were collected in the same point, behind the reaction chamber after the 27,3 kGy irradiation. The size distribution is slightly different from those presented in Figure 3. Only about 45% of total aerosol is submicron. There is no distinct peak of $SO_4^{(-2)}$, but a great amount of this ion (45%) is in submicron range. A clear peak of nitrate was detected between 0,48 and 0,72μm. Almost ~90% of total nitrate particles in the aerosol is smaller than 1,2 μm. The experiments with high concentration of SO_2 showed the tendency of the shifting of $SO_4^{(2-)}$ distribution into the bigger size range when inlet SO_2 concentration increased. Such shift was also noticed in the case of NO_3^- ions, that means the influence of initial concentration of SO_2 on NO_x removal was observed.

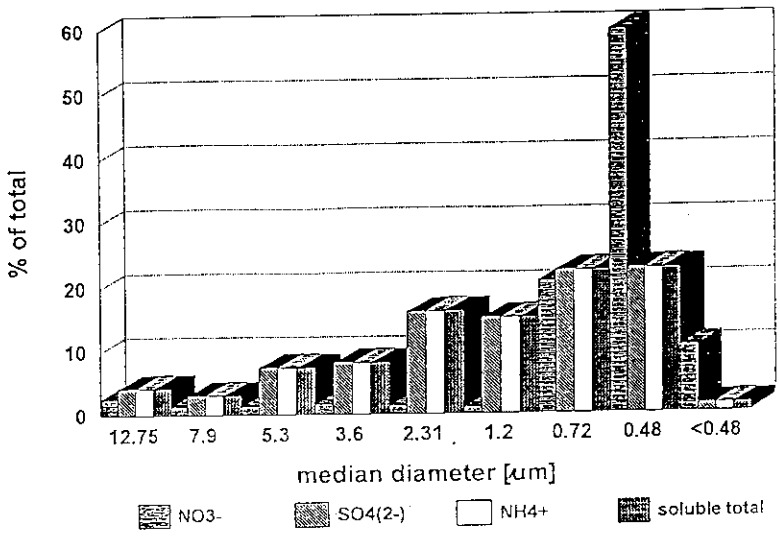

Fig. 4. Size distribution of the components of aerosol collected in flue gas after the reaction chamber. Initial SO_2 concentration 3 000 ppmV, NO_x - 125 ppmV, flow rate 6 800 Nm^3/h, dose 12.54 kGy, humidity 6.52 % vol., NH_3 stoichiometry - 1.14.

2. 3. BAG HOUSE DESCRIPTION

The bag filter and the accompanying equipment has been designed by the Designing Company of the Steel Industry "BIPROHUT", Warsaw Branch, which specializes in designing of dust removal equipment. The filter has been manufactured by the Factory of Dust Removal Techniques owned by Mr. Z. Golanko (Eng.) in Końskie. The layout of the bag filter in shown in Fig. 5.

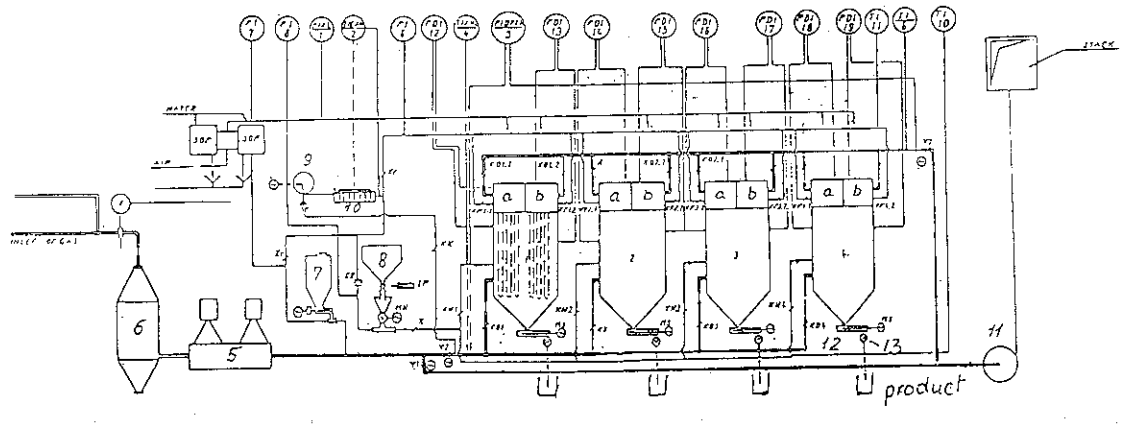

Fig. 5. Scheme of baghouse.

The filtration system consist of four filters F1 to F4, three of which remove aerosol particles from flue gases while the fourth one is regenerated. Each filter contains 128 bags with the total filtration area of 150 m^2. The total area of all of the filters equals 600 m^2, and 150 m^2 is disconnected and subjected to regeneration. The bags are fixed to the wire cages and adjusted to a plate separating the clean part of the filter by means of collars or elastic rings. The clean chamber of each filter is separated into two equal parts from which the clean gas are discharged to a common mainfold and further, through a valve Y3, they flow to the blower 11. A filtration aid can be added to the cleaned flue gas. This addition is aimed at an improvement of the dust layer structure which is deposited on the bag surfaces by increasing its gas permeability. The filtration aid is continuously introduced by means of a screw conveyer from a hopper 7. The amount of the filtration aid can be varied with a multistage gear. The filtration aid is conveyed to the flue gas stream with a hot air stream supplied from a blower 9 and heated in a heat exchanger 10.

During the course of the filtration process the deposition of aerosol particles results in flues gases pressure drop increase. Thus they should be temporarilly removed. This removal is accomplished in a cyclic regeneration. Each filter is successively subjected to regeneration in an "off-line" system. The regeneration cycle comprises of 4 stages: (Fig. 6)

- breaks to change the valve position,
- jetting,
- reverse flow of a hot air,
- precoating.

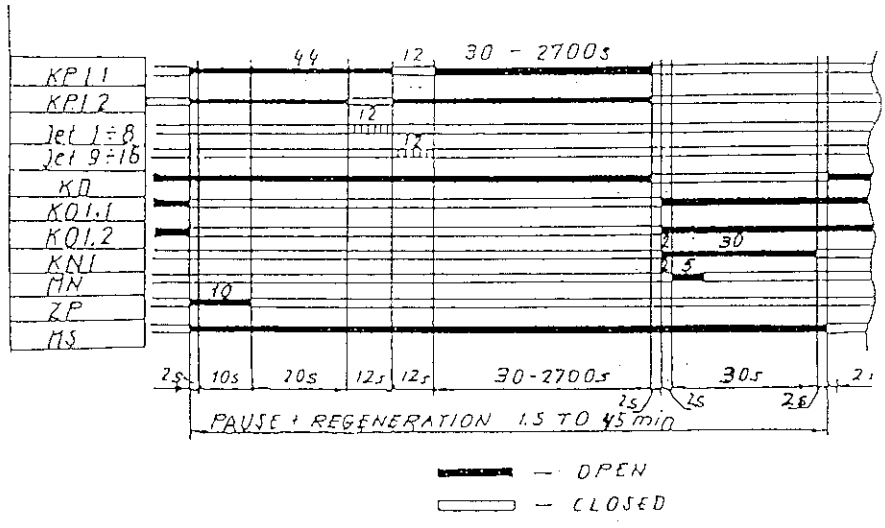

Fig. 6. Run of cleaning cycle.

During the break the valves position is changed and the screw conveyer 12 is activated to transport the product from the filter cone. The valve location is shown in the control panel by the control lights. Jetting of filters means introduction of a compressed air to the filtration bag in form of an impulse lasting 0.2 - 0.3 s. These compressed air impulses are simultaneously introduced to 8 bags by means of a pipe with holes situated along the bag axis. Venturi nozzles are located in the upper part of the cages, due to which the filtered flue gas are also entrained during the compressed

air impulse action. As a result of this operation a temporary increase of pressure inside the bag occurs, the latter expands and the deposited layer settles down. The time lapse between the jetting of the sucessive raws of bags can be controlled by means of an electronic control system. The total jetting time of each half part of a filter can also be fixed with an appropriate adjustment of a time relay. In paractice from one to three jettings were applied. The jetting air is taken from the general compressed air net. Before its use it is dried and cleaned in a dehumidification device SOP. This air is also applied to control the valves. After jetting hot air supplied from a blower 9 and heated in a heat exchanger 10 is fed to the clean part of the bag. The air temperature ranges from 80 to 100^{0}C. The air flowing in an opposite direction with respect to the flue gas flow causes also product being tored from the bag surface. The time of the reverse hot air flow can be adjusted at 3 to 45 minutes.

The precoating stage starts from opening the valve ZP which results in filling up the storage tank located above the cell conveyer MN with the filtration aid. Then this conveyer is activated for a few seconds. Change of the time of rotation of the time of rotation of the conveyer is possible, so that the amount of the filtration aid fed into the system can be varied. The filtration aid is fed to the filter by means of the hot air supplied from a blower 9. After precoating the valves location is changed and the filter is ready for work, and next is subject to regeneration.

The valves control system comprises of the time relays. During the filter work a number of parameters are measured. The most important, like pressure drop for the whole filter and the inlet gas temperature, are recorded by a computer. There are also the measuring devices enable to measure pressure drop and flow rates of flue gases in each of the eight parts of the filter.

2. 4. FILTRATION OF THE AEROSOL FORMED IN THE PROCESS

A very high dust removal effectiveness in the bag filters has been achieved in the process. The removal effectiveness of a standard dust in the bag filters applied in this study has been determined in the Institute of Textile Materials MORATEX in Łódź. Table 2 presents a list of types of the investigated filters bag as well as their dust removal effectiveness after a period of work. The table informs also about the types of cages inserted in the bags (see also Fig. 8).

The inlet gas temperature ranged from 70 to 85^{0}C. The outlet gas temperature was by 10 to 20 degrees lower. The filter capacity ranged from 8000 to 12 000 m^3/h and the total working filtration area, was 440 m^2.

Variation of the gas pressure drop during filtration is one of the most important process parameter. The gas pressure drop depends on the flue gas flow rate which varies with aerosol deposition and switching in the regenerated filters. The effect of the gas flow rate on pressure drop can be dealt with by analysing not only the value of Δp, but rather ratio $\Delta p/V$ (pressure drop and volumetric gas flow rate).

In April and May 1993 a continuous three-shift work of the installation was conducted. Fig. 7 shows variations of the pressure drop in the different sections of the filter.

Table 2. Kinds of bags and cages - used in EB Pilot Plant Kawęczyn.

	Filter 1		Filter 2		Filter 3		Filter 4		Year
	a	b	a	b	a	b	a	b	
Bags Efficiency Cages	Polyester new 99.99 a	Polyester new 99.99 a	Acryl used 99.98 a	Acryl used 99.98 a	Acryl used 99.98 a	Acryl used 99.98 a	Acryl used 99.98 a	Acryl used 99.98 a	1992
Bags Efficiency Cages	Goretex / Moratex EC new 99.95/99.91 b	Goretex / Moratex EC new 99.95/99.91 b	Goretex new 99.94 b	Goretex new 99.94 b	Moratex EC-1 new 99.89 a	Moratex EC-2 new 99.90 a	Polyester used 99.9 a	Polyester used 99.9 a	1993
Bags Efficiency Cages	Moratex EC new 99.93 b	Moratex EC new 99.93 c	Goretex used 99.95 b	Goretex used 99.95 d	Moratex EC-1 used 99.92 a	Morteleque new 99.91 e	Polyester used 99.9 a	Morteleque new 99.91 a	1994

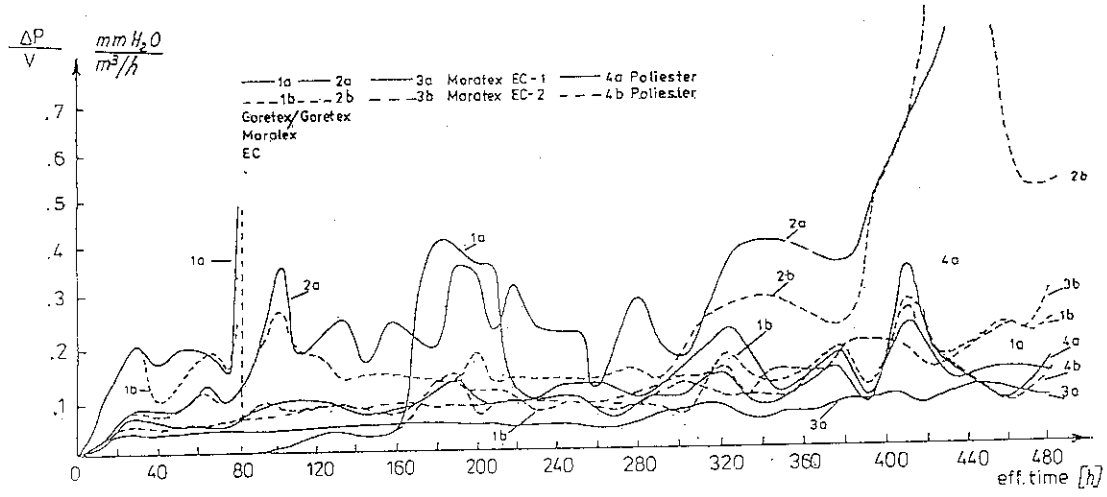

Fig. 7. Pressure drop of gas flowing through the various filtration bags.

As it follows from this figure, the performance parameters of the bags reveal changes. The smallest pressure drop was observed for the bags EC-1 in the filter 3a, while the biggest were recorded for the Goretex bags, initially inserted in the filters 1 and 2. After 80 hours of work of the filter 1 the Goretex bags were replaced by the Moratex EC bags. It is also typical that for the best bags EC-1 the variations of the values Δp/V were the smallest, so that this part of the filter is responding most stably. The variations result both from the disturbances as well as from the changes of the process parameters. The bags EC-2 have the same properties as those of the polyester bags of Polish production. Similar behaviour was observed for the EC bags, however, they indicated greater susceptibility for the factors which results in the greater pressure drop. The Goretex bags with a teflon coat show significantly highest pressure drop and are the most susceptibe for disturbances and variations in the aerosol concentration.
Setting of the product particles on the fibers of the filtration felt may also affect the pressure drop. The microscopic photographs 1 to 4 show a clean felt and with product.

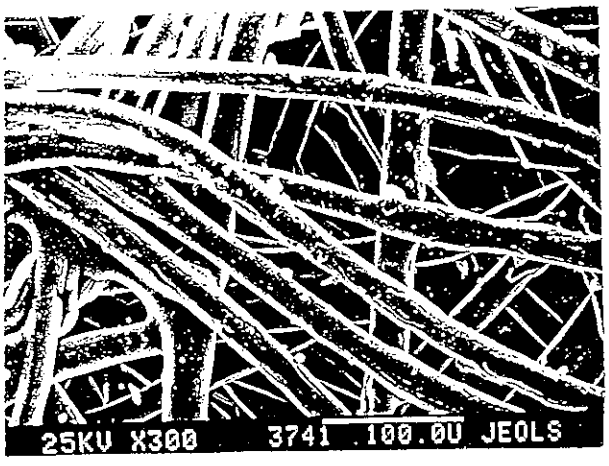

Photo 1. Clean surface of EC-2 felt.

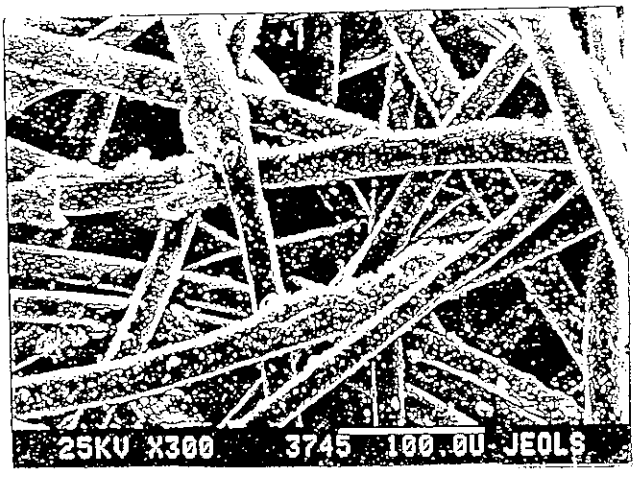

Photo 2. Filtration felt EC-2 with product.

Photo 3. Filtration felt Goretex with product.

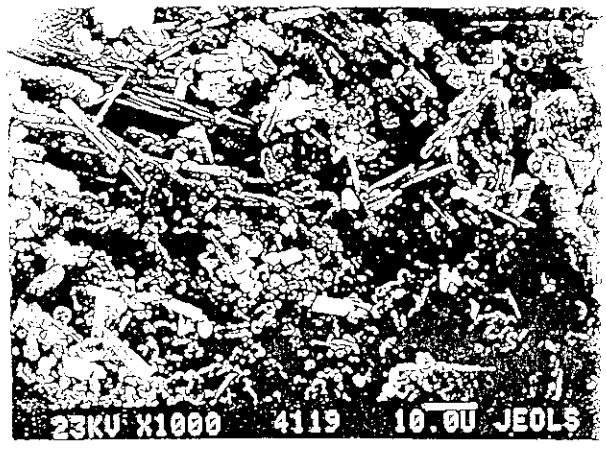

Photo 4. Filtration felt Moratex with product.

A visual survey of the bags revealed that the EC bags are very tightly attached to the cages which causes great difficuties with their dismantling. The EC-1 bags as well as those of polyester can be dismantling without difficulties, while the EC-2 bags, in spite their closer attachement to the cages wires, can be easily removed. The Goretex bags were also quite tightly attached to the cages.
The product sticks to the bag surfaces in form of a thick fractured layer. The fractures appear mainly at the points of attachement of bags to the cages wires.
It seems that a better behaviour of the EC-1 bags results from the larger garland's effect, i. e. an inertial effect of product splitting caused by the bag expansion during the jetting.
During the next season (1994) partial modifications of the German cages manufactured by H. Giesbert GmbH and Co. KG were performed, leading to enlarge loose space between the bags and the cages as well as to increase the garland effect (Fig. 8).

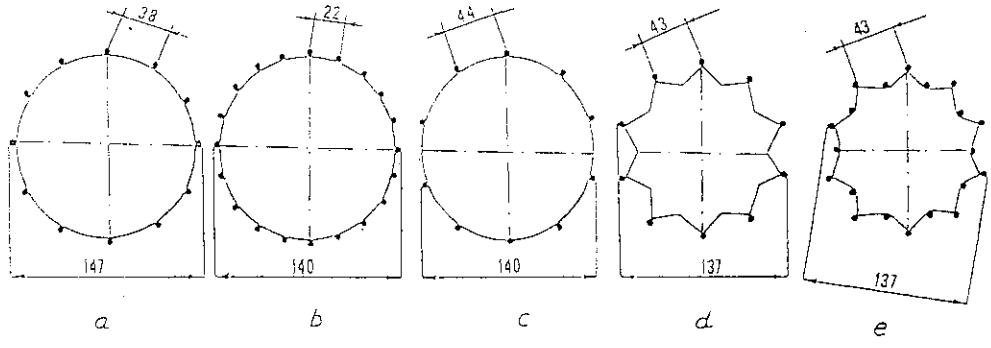

Fig. 8. Modifications applied in the bag filter cages design.

For comparison in filters 1, 2 and 3 in one part of the filter the cages were remained unmodified.and in the second modified. In filter 4 in both parts were unmodified cags a (see Tab. 2).

Cages modifications in filters 1b evidently diminished gas pressure drop during filtration (curve I), (Fig.9). The introduced modification consisted only on the two two-fold increase of a distance between the wires. As a result the pressure drop in the EC bags decreased by 30 to 60%. In the filter 2 the distance between the wires as well as differences between the cages and bag diameters were increased. Similarly to the first filter, in this case diminishing of the pressure drop during filtration occured (curve II). In case of Moratex EC-1 bags in filter 3 and Polyester bags in filter 4 both on cages of type 2 drop pressure was almost the same (curve III) Similar results were obtained for Morteleque bags in filters 3b and 4a. In this case the difference between diameter of cages and bags were 18.4 mm and 9.4 mm. So over some value of Δp its further increase for a filter jetting system, used does not result in the diminishing of the filtration pressure drop.

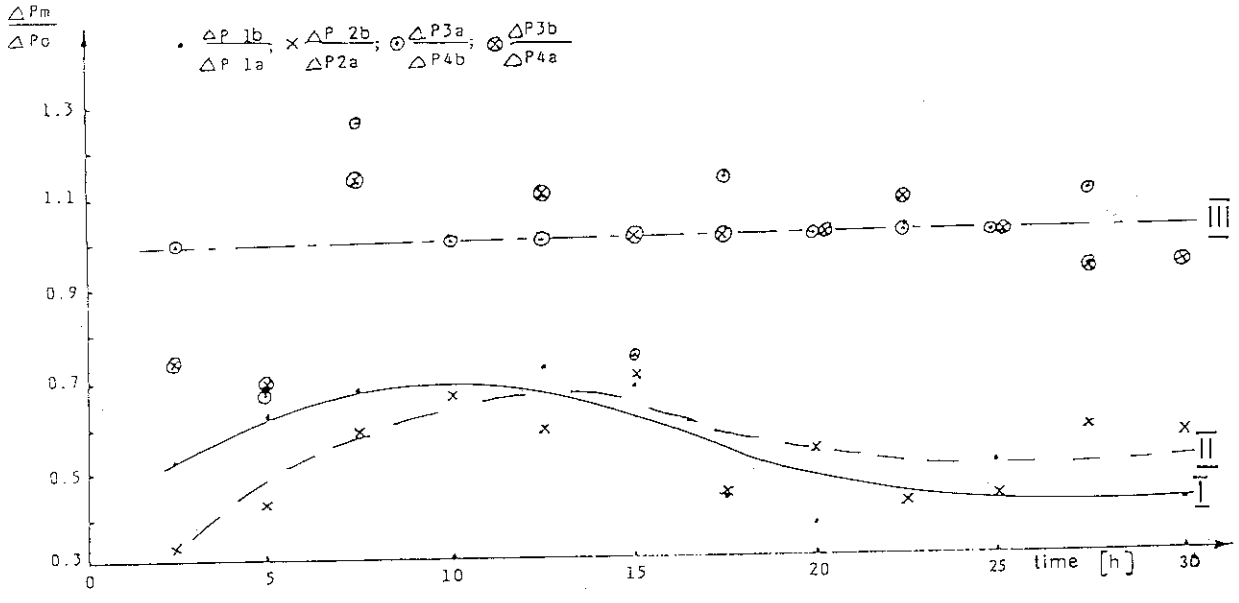

Fig. 9. Influence of cages modifications on drop pressure during filtration.

The Moratex EC-1 bags and polyester bags attached to the Z. Golanko's Co. cages revealed similar filtration pressure drop to the tests carried out in the previous year. No break down of the bags caused by chemical demage of the felt or sews was detected during these investigations. Only 1 to 2% shinkage of EC and polyester bags was observed.

2. 5. CONCLUSIONS

The results of the bag filter tests allow to draw the following conclusions:

- The difference between the diameters of the cages and bags should not be smaller than 5-6 mm.
- When cages with larger gap between the wires are applied jetting effectively removes product layer from the bag surface. This leads to a significant decrease of filtred gas pressure drop. An optimum distance between the wires should be in the range of 35 to 40 mm.
- The difference between the diameters of the cages and bags and the distance between the wires can be mutually equivalent.
- bags with the lower filtration pressure drop are more resistant for clogging when the jetting system is disturbed.
- It seems likely that methods other than jetting, e.g. mechanical cleaning of bags may be more effective.
- Filtration felts used exhibited sufficient chemical resistance with respect to the chemical substances present in the gas.
- When designing filter bags one has to account for 1 to 2% of material shrinkage.
- Application of a suitable filtration aid makes filter performance more stable, however, it usually diminishes its agricultural value.

2.6. LITERATURE

1. S. Jordan, H.R. Paur, W. Cherdon, W. Lindner: J. Aerosol Sci. Vol 17, No 4, 699-75 (1986).
2. H. Namba, O. Tokunaga, H.R. Paur: J. Aerosol Sci. Vol 22, Suppl.1, p S 475-78 (1991).
3. H. Angele, J. Gott Stein, K. Zellner, Flue Gas cleaning by EB Process at the RDK Pilot Plant, 4th Symp. on Intergrated Env. Control, Washington, March 2-4, 1988
4. S. Jordan: On the state of the art of flue gas cleaning by irradiation with fast electrons. Radiat. Phys. Chem. Vol. 35, No 1-3, 409-15, (1990).
5. Ebara electron beam flue gas treatment process. Final report, June 1988. DOE # AE 22-830 PC 60259 (USA).
6. E. Loffler, H. Dietrich, W. Flatt: Dust Collection with Bag Filters and Envelope Filters, Friedr. Vieweg and Sohn Braunschweig/Wiesbaden (1988).

3. Development of e-beam process monitoring system

J. Licki, A.G. Chmielewski, E. Iller, O. Tokunaga, S. Hashimoto and S. Sato*

ABSTRACT

The results of reliable and precise measurements of gas composition in different places of e-b installation are necessary for its proper operation and control. Only the composition of the flue gas coming into e-b installation is adequate to composition of flue gas emitted from coal-fired boiler. At other points of e-b installation the gas composition is strongly modified by process conditions therefore the specific measuring systems (sampling and conditioning system and set of gas analyzers) for its determination are required. In the paper a two systems for gas composition measurements, in place localized after process vessel or after filtration unit, are described. One of them is designed for measurement the concentration of SO_2, NO_x, CO_2, CO and O_2 and other one for measurements of NO, NO_2, NO_x and NH_3 concentrations. Both systems have been installed at pilot plant at EPS "Kawęczyn".

3. 1. INTRODUCTION

For monitoring and controlling of the electron beam process the reliable and accurate measurements of flue gas composition at the critical points of e-b installation are indispensable. In the selection of suitable measuring equipment for gas analysis it is neccessary to consider the specifics of treatment process.

A normal composition of flue gas emitted from coal-fired boiler and dedusted by ESP is analysed at the installation inlet. Normally the SO_2 and NO_x concentrations are high and exceed the allowed emission level. The flue gas emitted from a coal-fired boiler consists of only two types of nitrogen oxides namely: nitric oxide (NO) and nitrogen dioxide (NO_2). NO is the dominant constituent of NO_x. The main factors which complicate these gas composition measurement are: water vapour content about ~ 5% (V), fly ash loading, CO_2, CO and O_2 concentration. The suitable flue gas analyzers could be used for such measurement.

In the spray cooler the humidity of flue gas increases to level 10 - 12% (V). The elevated humidity complicates the gas analysis both at outlet of humidifier and subsequent ones. At the process vessel an essential change of flue gas composition occurs as a result of physico-chemical processes caused by the electron beam irradiation of flue gas. The stream of gas leaves the irradiation vessel is a multicomponent three-phase system. The gas phase is characterized by significantly reduced SO_2 and NO concentration, a slightly increased NO_2 concentration, on the presence of unreacted ammonia and nitrous oxide-N_2O (a gas treatment by-product) and nearly unchanged CO_2, CO, O_2, N_2 and water vapour content. The liquid phase is consists of sulphuric acid and nitric acid aerosols. The solid phase is formed of a by- product particulates of ammonium sulphate and nitrate. The particulate matter consists of hygroscopic particles of diameter primarily in the range 0,4 to 4 μm. The magnitude of above mentioned changes of flue gas composition depend on irradiation dose, ammonia stoichiometry and gas humidity at the irradiation vessel inlet. In most cases it is necessary to measure the similar concentrations of SO_2, ammonia and nitrogen oxides. The measurements of gas composition at this point are extremely difficult. The main purpose of this paper was to design the proper mesuring system. At the filtration unit nearly 99% of by-product particulate mass is removed.

* JAERI

The other flue gas parameters are not changed and for measurements of gas composition the same system as at the process vessel outlet could be used.

3. 2. APPROACH

The basic factors which may adulterate the measurement of flue gas composition at outlet of process vessel as well as after the filtration unit (bag filter or gravel bed filter) are as follows:

- low gas temperature (60 - 90°C) and its high absolute humidity (at the level 10 - 14% (V)). Therefore in the sampling system as well as in the gas analyzers of the water and sulphuric acid condensation may occurs. Three gas components: NH_3, SO_2 and NO_2 are water soluble and their concentrations could be reduced on transportation way from the sampling point to the sample cell in the analyzer. It is especially relevant in the case of a long sample gas line. The water solubility of above components decreases with the increase of gas temperature. To prevent this influence, the temperature of sample gas should be kept above the acid dew point at all sampling processes. In the conditioning system the water vapour should be carefully removed from sample gas and the condensate should be automatically discharged by pumping it off.
- the presence of unreacted ammonia (in the gas leaving the process vessel). Ammonia may complicate such measurements in two ways:
  - NH_3 readily reacts with SO_2 and water. Efficiency of this thermal reaction decreases with gas temperature. However at above 120°C this factor is negligible [1].
  - the specific absorption spectra of ammonia takes place in the ultraviolet and infrared spectral ranges ([2], Fig.1). Its spectra overlaps the spectra of some other component of analyzed gas. In this case the special techniques should be employed for improve the selectivity of flue gas analyzer, for example: gas filter correlation or two wavelengths comparision technique. Recently, two producers of gas analyzers: Shimadzu (Japan) and Thermo Environmental Instruments Inc. (USA) offers the ammonia scrubber which is designed for selective absorption of ammonia gas from sample gas without the changing the concentration of other component. These solutions are applicable for our monitoring system.
- gas leaving the process vessel contains the particles of the final products which are hygroscopic and have of submicron size. They may clog and incrust the gas sample line and sample cell in the gas analyzer. To separate them, a set of gas filter must be inserted at the begining of the sampling line. These filters should have the proper pore size and must also be kept above the acid dew point.

Numerous consultations were carried on with manufacturers of gas analyzers from Japan, USA and Europe. Finally two following sets of instruments were selected and purchased from the JAERI funds:

- set of four flue gas analyzers for SO_2, NO_x, CO/CO_2 and O_2 with optional accessories from Shimadzu Corporation (Japan).
- set for measurement of NO, NO_2, NO_x and NH_3 concentration from Thermo Environmental Instruments Inc. (USA).

3. 3. SET OF FLUE GAS ANALYZERS FROM SHIMADZU CORP.

The system consists of:
sampling probe - the pipe is made of SUS 304. Probe insertion length - 1200 mm,
heated gas filter - carborundum 7,5 μm, heated electrically up to 120°C,
heated sampling line - teflon tube with internal diameter 6 mm, outside diameter 8mm, heated electrically,
ammonia scrubber - to selectively absorb ammonia from sample gas. Absorption efficiency - 98% or more, sample gas flow rate - max 3 l/min,
drain separator - to remove of water from sample gas,
gas analyzers - to measure concentration of interest component of sample gas.
There are four following gas analyzers:
SO_2 analyzer type URA - 107
Measuring principle: non-dispersive infrared absorption method, single light source, 2 light beam (ratio method).
Measuring ranges: 1000/200 ppm SO_2
NO_x analyzer type NOA - 305A
Measuring principle: atmospheric pressure chemiluminescent method.
Measuring ranges: 50, 100, 250, 500, 1000, 2000, 2500, 5000 ppm NO_x.
CO/CO_2 analyzer type CGT - 10 - 1A
Measuring principle: non-dispersive, infrared absorption method, two light source and two light beam.
Measuring ranges: CO - 1000/5000 ppm, CO_2 - 15% (V)
O_2 analyzer type POT -10
Measuring principle: paramagnetic.
Measuring ranges: 10/25%(V)
Figure 2 presents scheme of this system. This system of gas analyzers is devided into two lines because max. gas flow rate through ammonia scrubber is only 3 l/min. The standard gases in the cylinders are used for calibration of these analyzers.

3. 4. SET FOR MEASUREMENT OF NO/NO_x/NH_3 CONCENTRATION

For this measurements the ammonia analyzer Model 17 from Thermo Environmental Instruments Inc. (USA) was selected. It is a chemiluminescence NH_3 analyze, equipped with microprocessor system and other innovative design (both hardware and software) to obtain higher sensitivity, reproducibility and specificity. The minimum detection limit is 1 ppb, precision of measurement - 0.5% of full scale and linearity ± 1% of full scale. The Model 17 utilizes a three channel approach to provide continuous analogue output signals for NO, NO_x and NH_3. The instrument is configured as two separate modules, a converter and an analyzer module, to allow for site-specific ammonia conversion. This is an analyzer with nine measuring ranges but the max. range is only 5 ppm. In the gas leaving of the process vessel the ammonia concentration may be up to 100 ppm. For the measurement of higher NH_3 concentrations, the sample gas should be diluted before its inlet to ammonia converter module. It is necessary to use two additional Thermo Environmental Instrument Inc. products: heated sample gas dilution and conditioning unit Model 900 and Model 111 Zero-Air Supply. Figures 3 presents scheme of measuring set.

The sample gas contains unreacted ammonia which readily reacts, particularly in lower gas temperatures with SO_2. To avoid this reaction during sample gas transportation to an analyzer as well as sulphuric acid condensation, ingoing parts of the system (the probe, ceramic filter and sampling line) are kept at a temperature 180°C that is higher than the sulphuric acid dew point temperature. The sample gas contains also hygroscopic submicron particles of final products. Means for a periodic blow-back of, so called zero air is provided through heated line, preliminary filter and probe to clean their surface. In the Model 900, sample gas enters heated section and passes through a sample filter and then is blended with clean dry air (zero air). The blended sample is pumped to the analyzer for analysis. In our system the dilution ratio 100:1 was selected. Chemiluminescence NH_3 analyzer Model 17 contains off two converters. The stainless steel converter is kept at temperature 825°C and used to convert ammonia and NO_2 to NO. The molybdenum converter is kept at temperature 325°C to convert NO_2 to NO. NO concentration analysis is carried out directly in the chemiluminescent chamber of the analyzer. The analysis of flue gas sample is carried out according to the following procedure:

The inlet sample gas is devided into a three equal parts at the analyzer inlet. One part flows to chemiluminescent chamber where NO concentration is measured. A second part passes through molybdenum converter and chemiluminescent chamber. This allows to determination of NO_x concentration: $NO_x = NO + NO_2$.

The third part of sample goes through the stainless steel converter and chemiluminescent chamber, and then is used for determination of $N_t = N_{NH3} + NO_x$ concentration. A microprocessor calculates the individual concentration of NO, NO_2 and NH_3 from these three measured signals. An analyzer is equipped with three analogue output signals for NO, NO_x and NH_3 as also with five digital output signals for NO, NO_2, NO_x, NH_3 and N_t. For calibration of this system four standard should be used gases: zero gas (or pure nitrogen 99.999%), NO in nitrogen, NO_2 in nitrogen and NH_3 in nitrogen. Fig. 4 presents flow diagram in the converte module and in the analyzer Model 17.

3.5. CONCLUSIONS

The composition of flue gas leaving of process vessel outlet may be determinated by the both sets of gas analyzers. These measurements will be reliable and accurate when all the requirements presented by the approach will be fulfiled. Both systems are installed in pilot plant at EPS "Kawęczyn". During experiments their work was checked by the simultaneous measurements of gas composition using the manual analytical methods [3]. The good agreements between these methods were obtained. Both sets of gas analyzers were installed in the mobile racks then they were used for measurements of gas composition at the process vessel outlet or the filtration unit (bag filter or gravel bed filter) outlet. Fig. 5 presents the scheme of full gas analyses system installed at the e-b pilot plant at EPS "Kawęczyn".

Both systems were used in the long-term test of the installation. Fig.6 presents the results of this test.

REFERENCES

[1] O. Tokunaga and H. Namba; Application of radiation technology for flue gas treatments. In Proceedings of Advisory Group Meeting on New Developments and Trends on Radiation Chemistry and Technology, organized by the IAEA, Tokyo, 4-7 April 1989.
[2] R.H. Person, A.N. Fletcher, E.St. Clair Cantz, Catalog of infrared spectra for qualitative analysis of gases, Analytical Chemistry, vol. 28 (1956), 1218-1239.
[3] J. Licki, A.G. Chmielewski, G. Zakrzewska-Trznadel, N.W. Frank; Monitoring and control systems for an e-b flue gas treatment pilot plant - Part I. Analytical system and methods. Radiat. Phys. Chem., Vol. 40 (1992), 331-340.

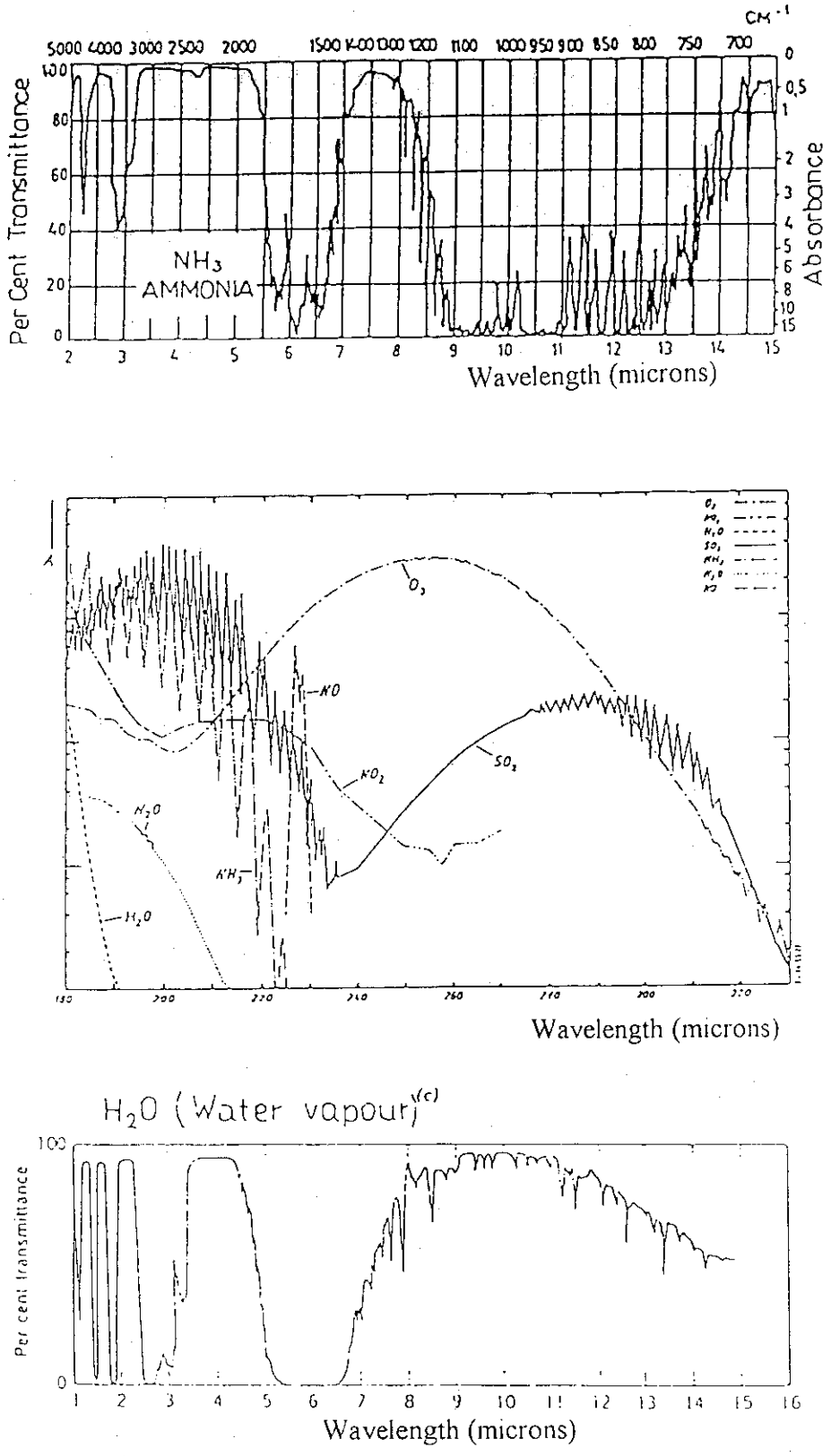

Fig. 1. Specific absorption spectra of ammonia and water vapour in the ultraviolet and infrared regions.

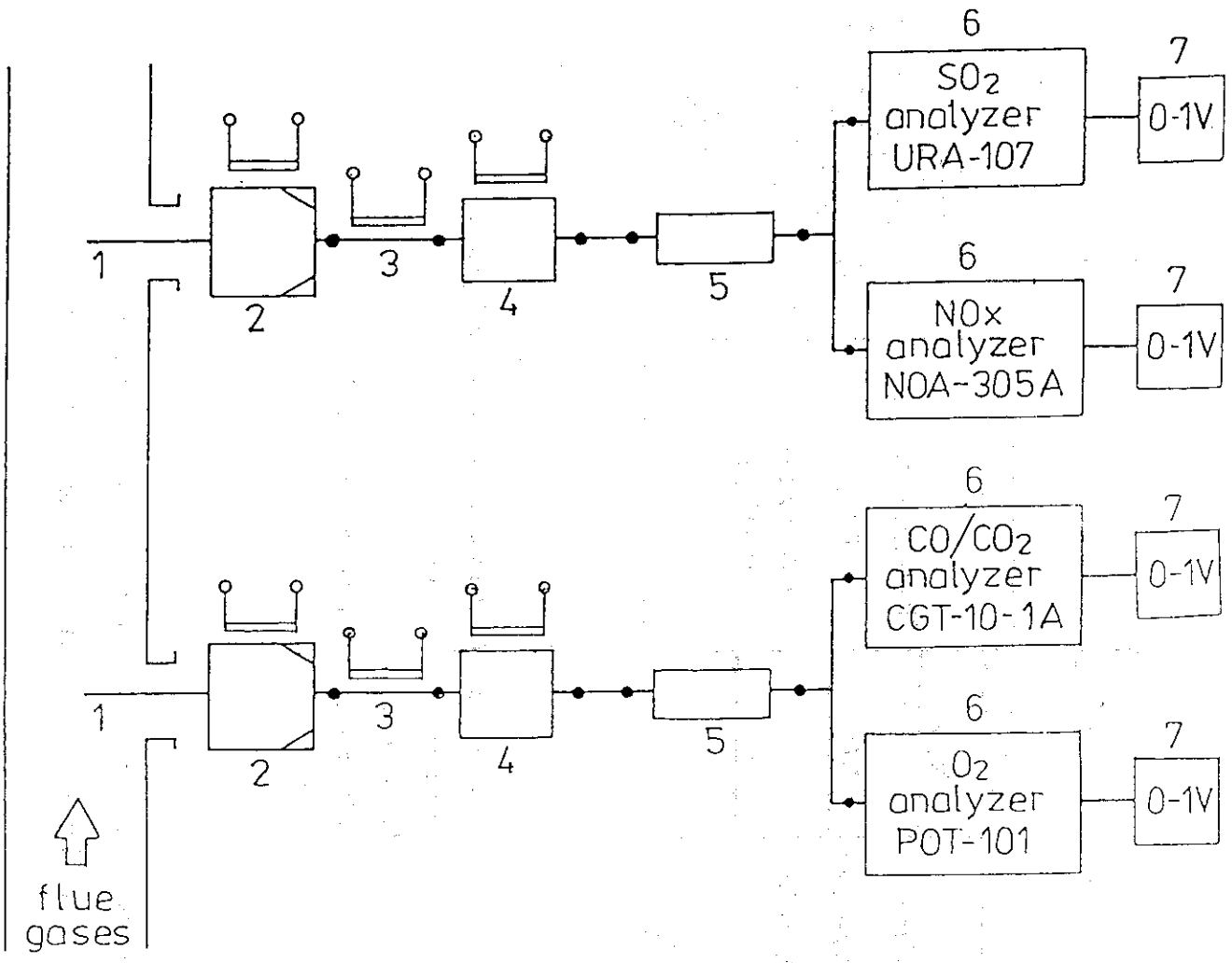

1- sample probe (SUS 304)

2 - heated ceramic filter (carborundum 75 μm)

3 - heated sample line (teflon tube 6/8 mm)

4 - ammonia scrubber

5 - drainer

6 - portable gas analyzer

7 - indicators (recorder)

Fig.2. System for the measurements of SO_2, NO_x, CO/CO_2 and O_2 concentration in the gas at the process vessel outlet or at outlet of installation, based on the Shimadzu Co. (Japan) portable analyzers.

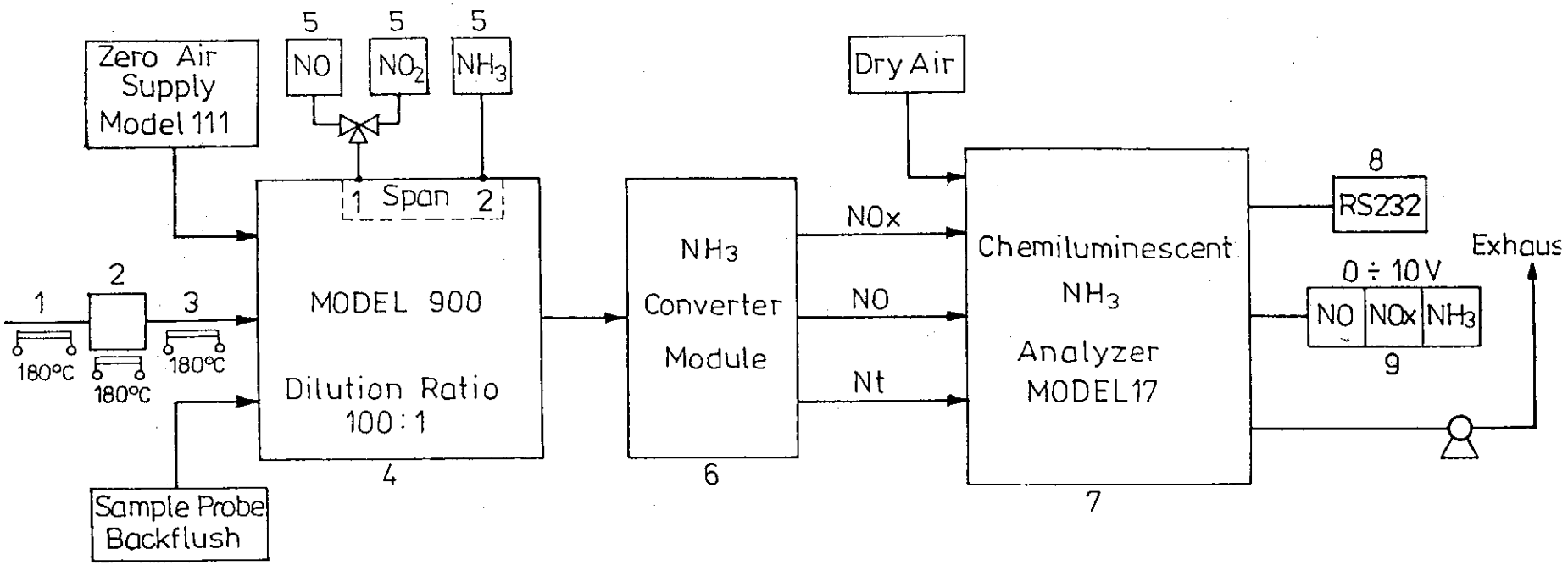

1 - heated sample probe,

2 - heated ceramic filter,

3 - heated sampling line,

4 - heated sample gas dilution and conditioning unit,

5 - standard gases for calibration,

6 - converter module (stainless steel converter and moly converter),

7 - ammonia analyzer Model 17,

8 - digital output,

9 - analogue output signals for NO, NO_x and NH_3.

Fig.3. System for measurement of $NO/NO_x/NH_3$ concentrations in the gas leaving of process vessel or outlet of installation, based on the Thermo Environmental Instruments Inc. (USA) equiment.

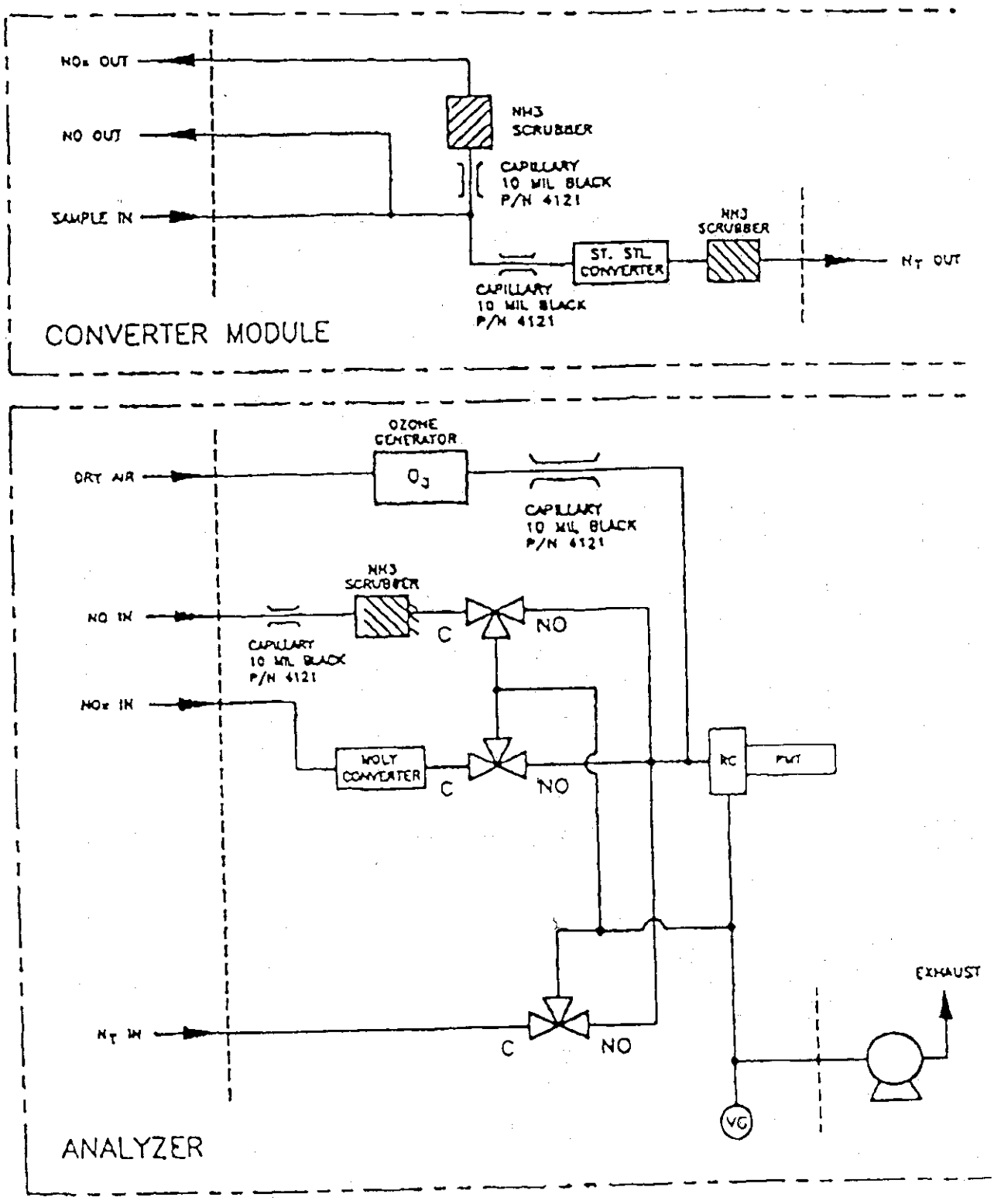

Fig.4. Scheme of Model 17 chemiluminescence ammonia analyzer.

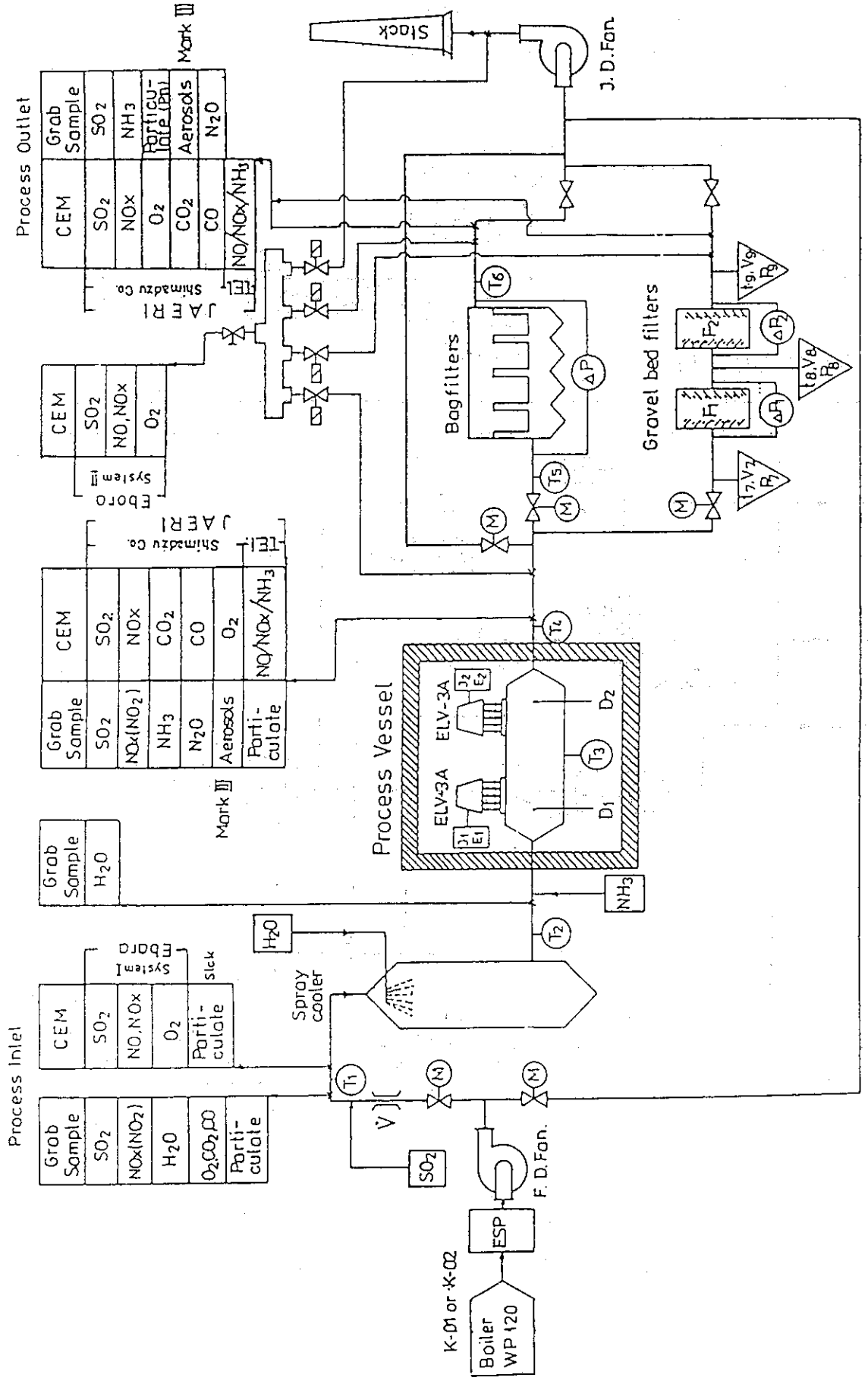

Fig.5 Gas analyses system installed at Kawęczyn pilot plant.

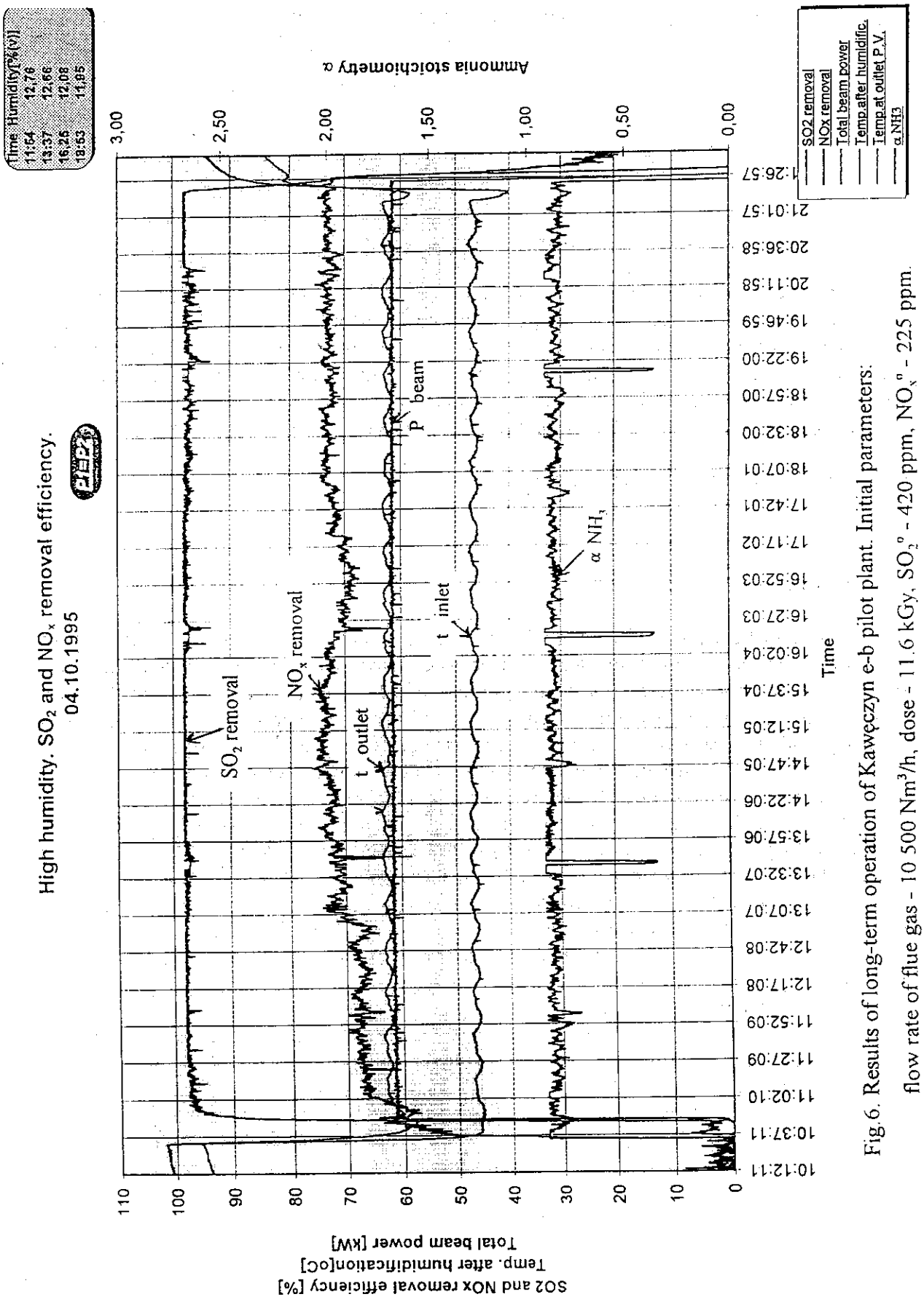

Fig.6. Results of long-term operation of Kawęczyn e-b pilot plant. Initial parameters: flow rate of flue gas - 10 500 Nm^3/h, dose - 11.6 kGy, SO_2^o - 420 ppm, NO_x^o - 225 ppm.

4. Electron beam scanning and centering automatic control system

Z. Zimek, S. Bulka and S. Hashimoto

Abstract

The automatic control of electron beam scanning and centering system was designed and tested in ELV 3A electron accelerators installed in pilot plant for flue gas treatment. It helps to minimize beam power losses and to avoid destruction of the output devices by overheating the window output foil due to non proper beam centering and scanning pattern homogenity. The purpose of the system is to provide the control of the electron beam scanning and centering parameters and transmit a logic signals to main computer when malfunction is detected and recognized. When acceptable levels are passed the electron beam is stopped automatically to prevent beam losses or possible damages of accelerator components.

Keywords: Accelerator, Electron beam, Control

4.1. Introduction

Automatic control of electron beam scanning and centering should be applied for high power low energy industrial type electron accelerators not only to minimize beam power losses but also to avoid destruction of the output devices. The fault in scanning pattern can overheat the window output foil when full beam power is applied. Non proper beam centering leads to destruction of scanning horn and vacuum in accelerating structure. It means not only the cost of service and spare parts but also time when accelerator is out of work.

Fig. 1 illustrates possible electron beam shape distortions due to improper sweeping amplitude. When the beam pattern is too large (Fig. 1. a and b) beam losses are observed and vacuum sealing can be destroyed as a results of local overheating. When beam spot pattern is to small (Fig. 1. c) the window output foil can be destroyed by thermal energy deposited by higher than acceptable electron beam density. The output foil can be effectively overheated and destroyed by non homogeneous beam spot pattern as well (Fig. 2). It can be seen on photos (Fig. 3) where overheated spot on titanium foil indicates local overheating casued by non homogeneous scanning pattern.

The centering system malfunctions are illustrated by Fig. 4. Beam losses are observed and vacuum sealing can be destroyed in a results of local overheating. In the worst case the wall of scanning horn can be damaged what may need appropriate time to replace the destroyed component.

The purpose of the monitoring system is to provide the control of the electron beam scanning and centering parameters and transmit a logic signals to main computer when malfunction is detected and recognized. When acceptable levels are passed the electron beam is stopped automatically to prevent beam losses or possible damages of accelerator components.

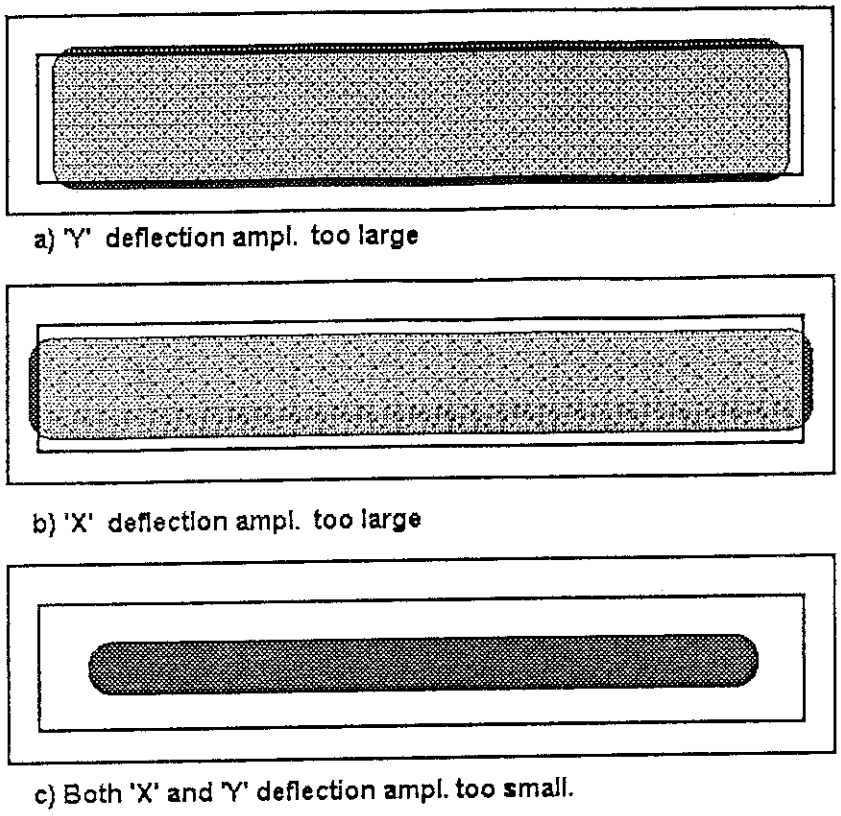

Fig. 1. Possible electron beam output shape distorions due to sweeping amplitude improper adjustment

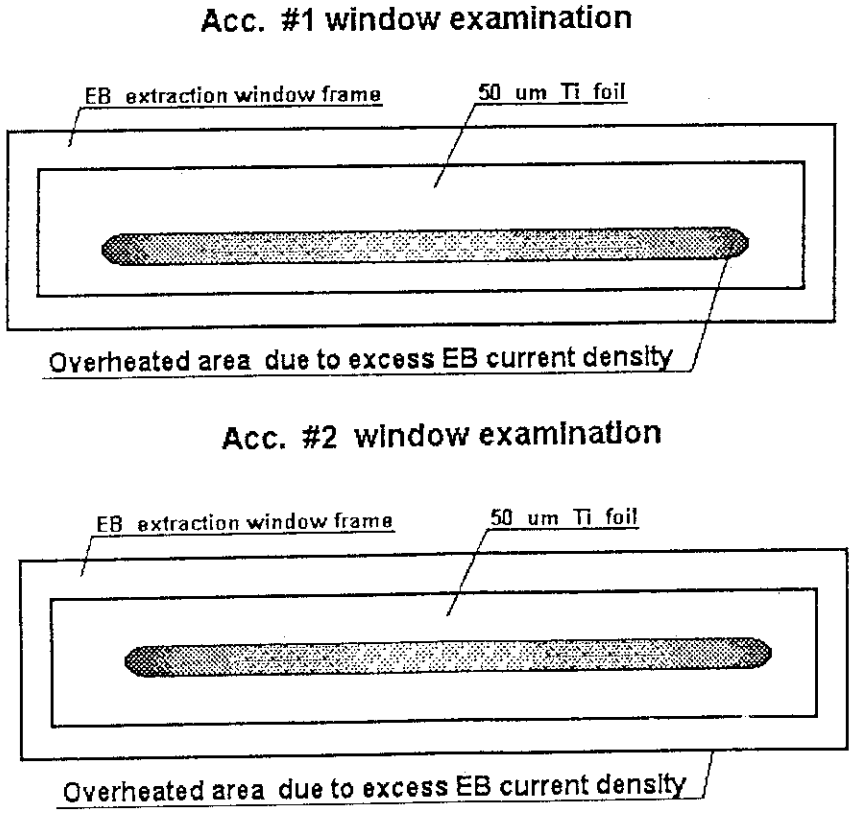

Fig. 2. Non homogenous electron beam pattern on window foil

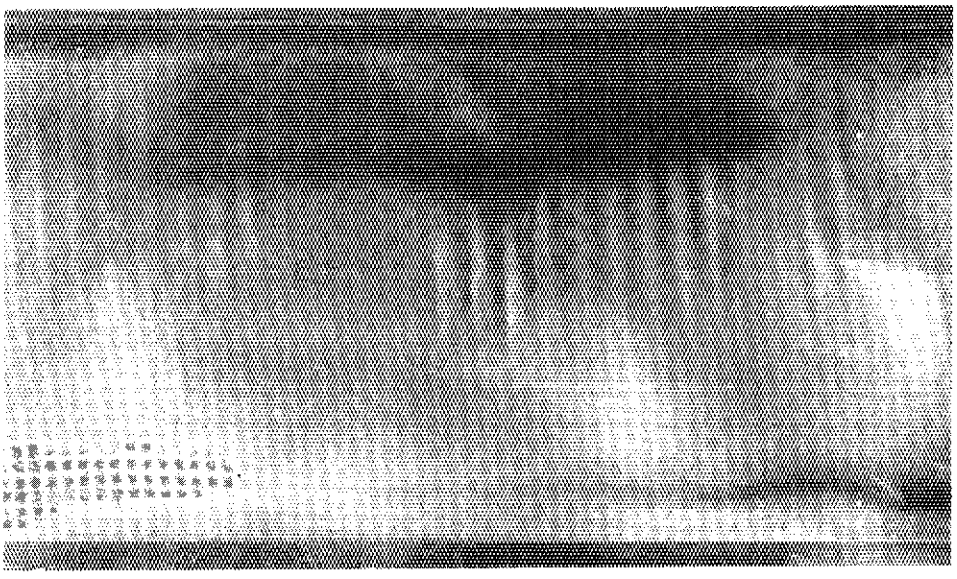

Fig. 3. Overheated spots on titanium window foil (photo)

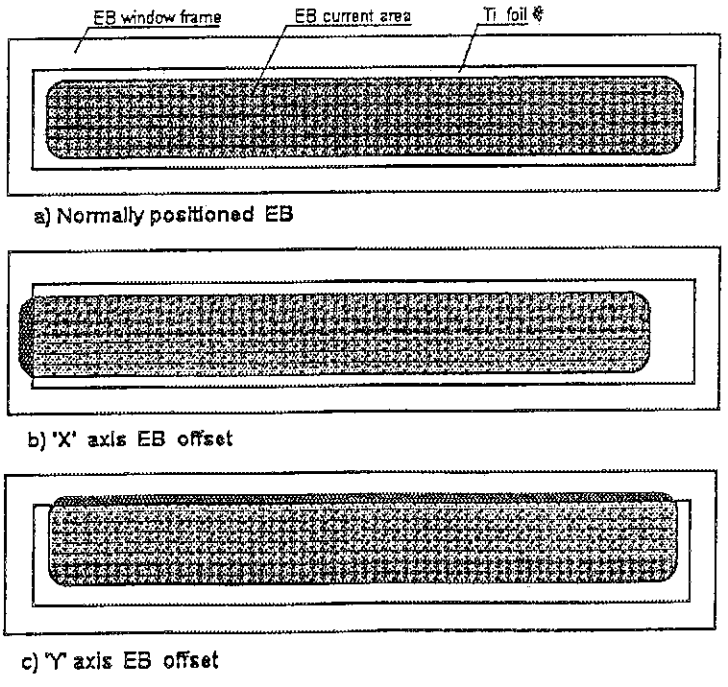

Fig. 4. Possible electron beam position distortions due to centering system malfunction

4.2. The principles of the control system

The modern industrial accelerators are equipped with computer control systems. Automatic systems may provide adequate multiparameters control of separate accelerators components, installations, safety interlock systems and electron beam parameters. It allows to perform remote control electron beam current and energy depends on technological process requirements. The schematic diagram of accelerator control system applied in Pilot Plant installed in Power Station EC Kweczyn is presented on Fig. 5. Separate computers are used to control each accelerator and central computer was applied to provide technological process control and keep necessary links with accelerators control systems.

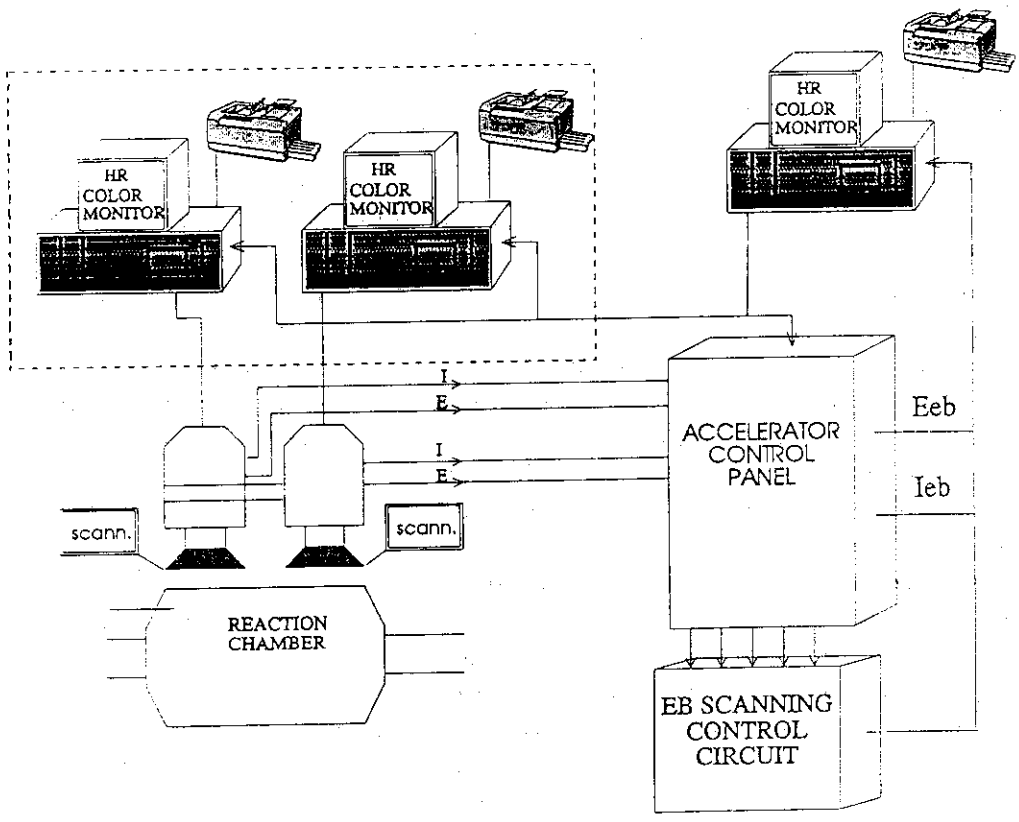

Fig. 5. The control system of ELV3A electron accelerators

The EB scanning control circuit applied additionally to existing components of accelerator control panel is located on separate printed board. The circuit is connected by multiwire cable with central computer to provide logic signals depends on status of electron beam scanning and centering. Particular the circuit is used to obtain:
- electrical separation between electron beam scanning and centering control systems, accelerator and central computer,
- detection of the status of low and high frequency scanning signals,
- detection of the electron beam location against output chamber walls on x and y directions and signaling off limit position,
- generation the logic signals,
- transmission of the logic signals to computer.

4.3. The construction of EB scanning and centering control circuit

The system consists of five separate channels for signals conversion. Each signal is taken as a sample representing the value of current provided to EB centering or sweeping coils. In case of accelerator's EB centering or sweeping control devices malfunction, the improper value of mentioned signals is detected and appropriate ALARM signal is set on. The description of monitoring board incoming signals is as follows (all signals are DC voltage-type):

1. 'X' scanning (along EB extraction window) current amplitude
2. 'Y' scanning (across EB extraction window) current amplitude
3. 'X' centering current value
4. 'Y' centering current value
5. EB scanning horn and window frame leak current
6. EB current.
7. External RESET from computer (TEL)

A channels of input signals 1 thru 4 type are limited/amplified to obtain suitable value to drive further IC's and then filtered in order to reject noise and broom. After that a set of comparators is tracing signals and detecting out-of-range variations. In that case the comparator output signal is memorized in RS flip-flop until computer reads it during nearest data acquisition cycle. Then RS is reset to be ready for the next event, the signal 7 has also meaning as the confirmation of successfully finished computer READ-IN operation .

Signals 5 and 6 are amplified with inverse amplification coefficient before further processing, and a part of signal 6 represents the reference value for signal 5 level comparison, this way it is possible to obtain information about Electron Beam -to- scanning horn mutual co-ordination.

RC filtering circuits frequency bandwidth is calculated on assumption that 20 millisecond (one sweep cycle) of scanning hang-up should be sufficient to set ALARM on. The monitoring unit can also act in auto - RESET mode, then the latched ALARMs are kept at the board logical outputs for 500ms before resetting.

Detailed schemes of separate circuits are shown on Fig. 6 to 9. Fig. 10 shows the overall view on printed board and its location in one of accelerator control panel circuit.

4.4. Conclusions

The performed tests confirmed the ability of the electron beam scanning and centering control system to detect and signal the unproper electron beam position which may lead to serious accelerator damage. The cost of the circuit is relatively low to compare with the cost of accelerator parts which can be destroyed. The installation of the circuits eliminates one more possibility which may stop accelerator for relatively long period of time.

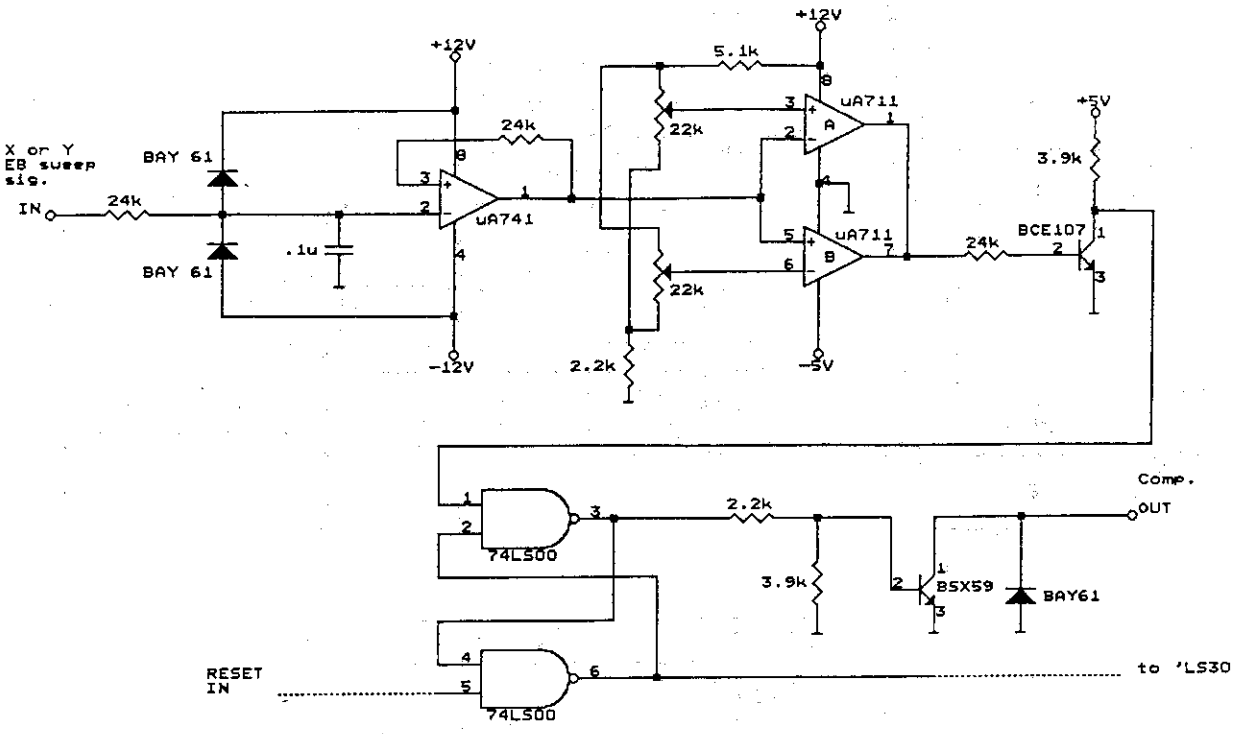

Fig. 6. Electron beam sweep amplitude monitoring circuit

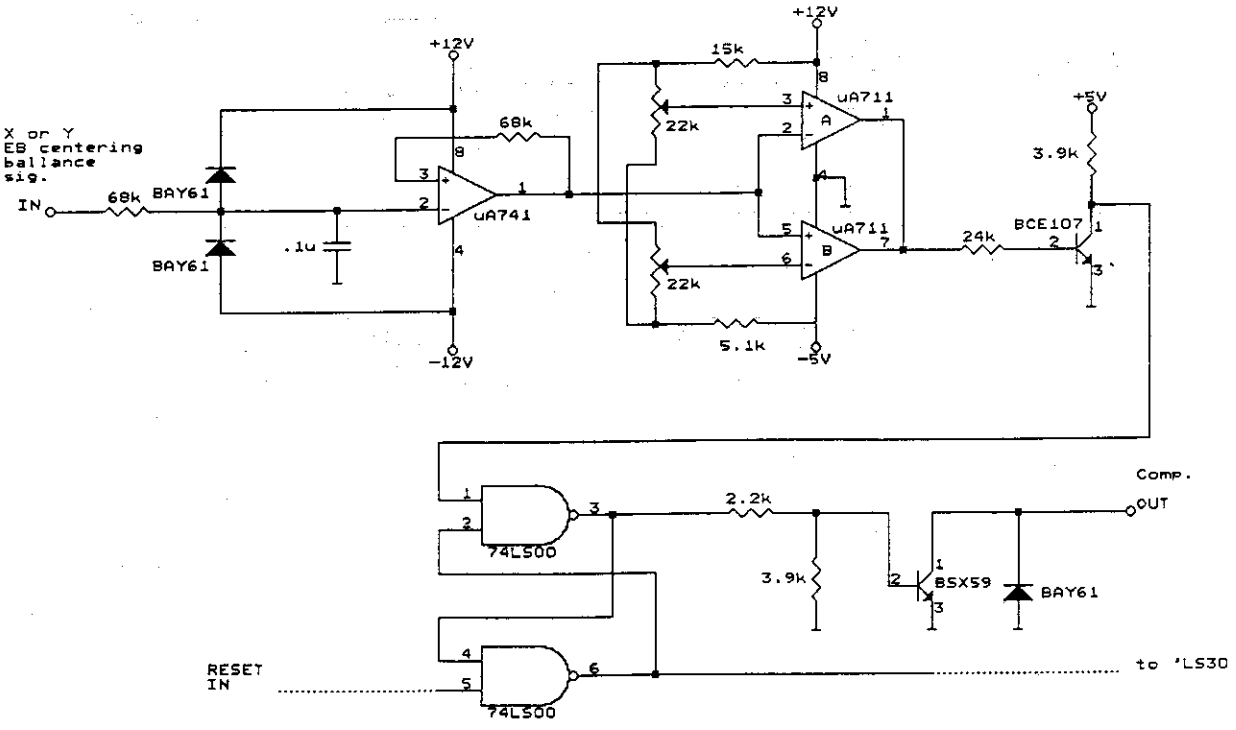

Fig. 7. Electron beam centering ballance monitoring circuit

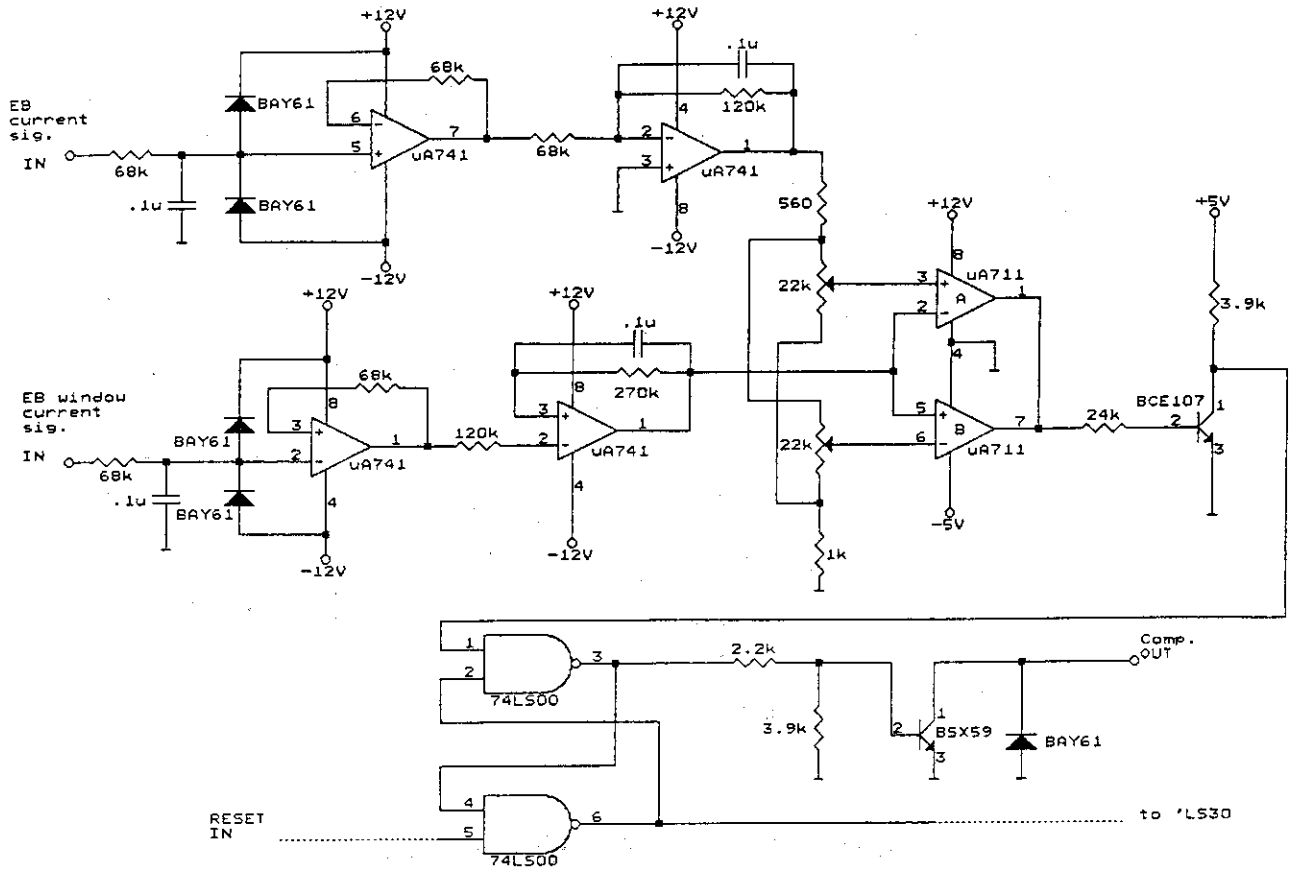

Fig. 8. Electron beam current leak monitoring circuit

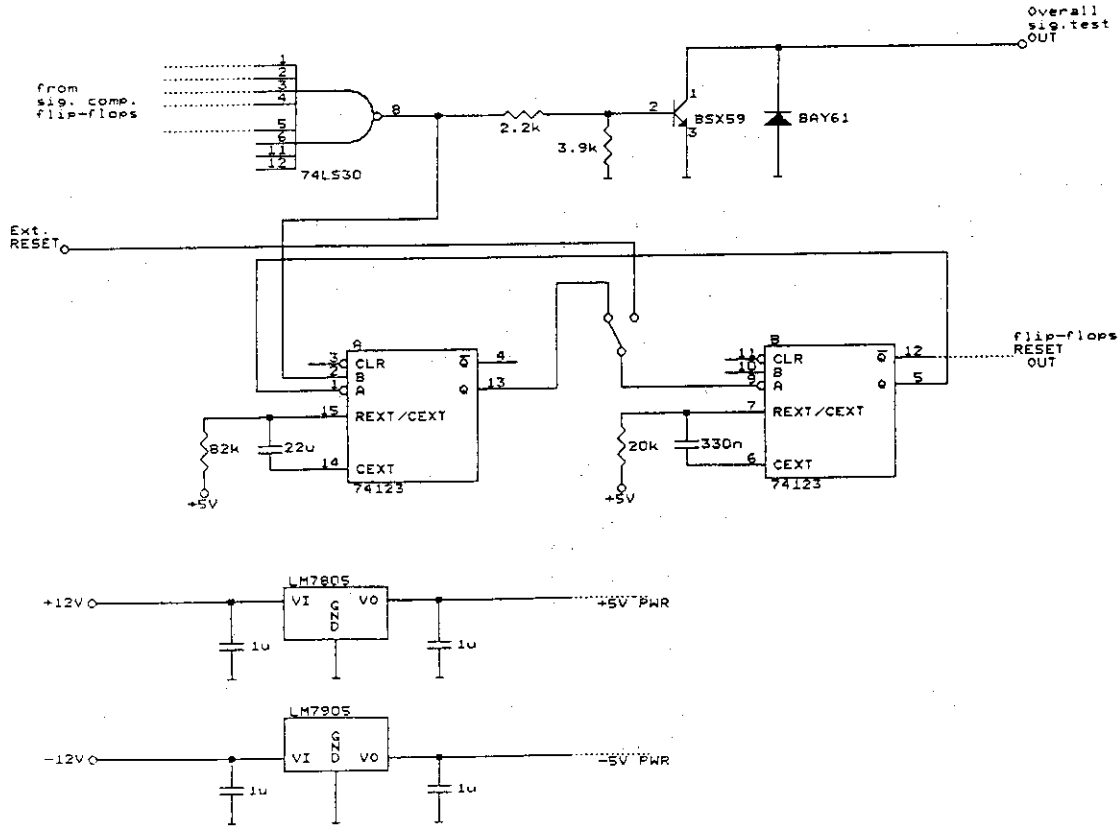

Fig. 9. Auto-reset and power circuits

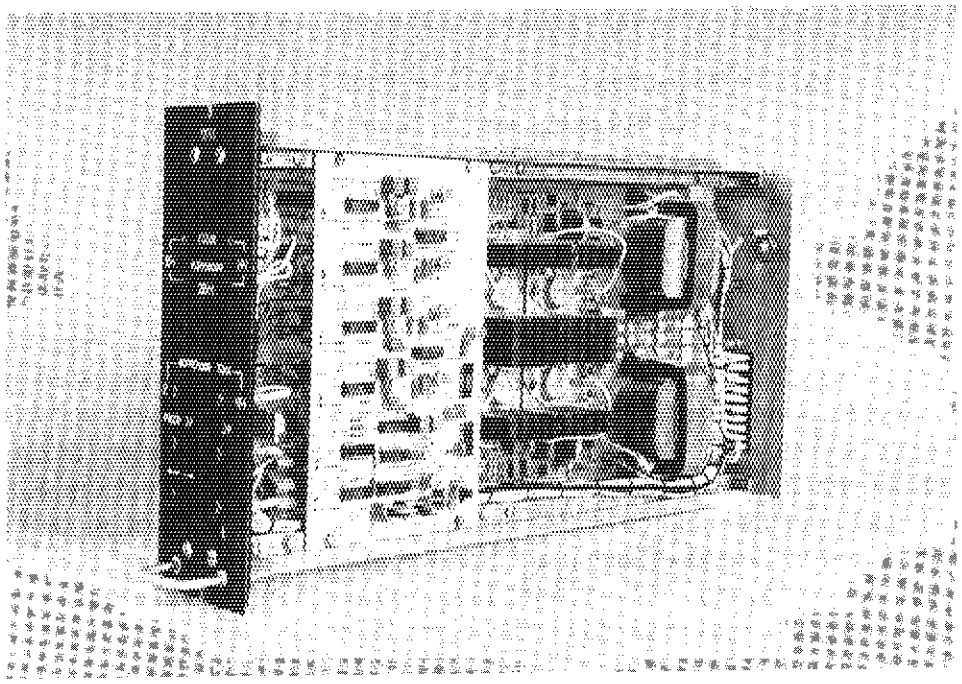

Fig. 10. Overall view on printed board and its location in one of accelerator control panel circuit.

5. The dose distribution in the reactor of the Kaweczyn Pilot Plant

A. G. Chmielewski, Z. Zimek, P. Panta, S. Bulka,
O. Tokunaga and H. Namba

Abstract

Detail experimental study was performed to measure dose rate and dose distribution in reaction vessel installed in Pilot Plant EC Kweczyn. Beam power losses caused by electron scattering and absorption in window system and reactor walls were evaluated to optimize process efficiency and maximize electron beam energy deposited in flue gas being purified. The experimental verification of the calculated optimization has been performed. The dose distribution in longitudinal irradiation of flue gas in reaction chamber applied in Pilot Plant was measured. The effectiveness of such irradiation system was discussed and dosimetry results were presented. Approximately 64% of total beam power with initial electron energy 0,7 MeV was delivered into the gas phase due to the losses in double window (two 50 :m titanium foils and 70 mm air gap between them) and process vessel definite diameter 1.6 m.

Keywords: SO_2, NO_x, Flue Gas, Dosimetry, Electron-beam, Radiation, Reaction Vessel

5.1. Introduction

The radiation processing applied for environmental protection as a method of clean-up industrial flue gases through the oxidation of SO_2 and NO_x is very intensively developing field. Research started in Japan is being conducted in USA, Germany, Italy, Poland and many other countries. The small scale experiments and results obtained in pilot plant facilities showed that SO_2 and NO_x can be simultaneously removed from irradiated flue gas from coal-fired, crude-oil and gas fired power plants. The direct technological goal of flue gas irradiation is the formation of highly reactive species like ions, low energy electrons, molecular ions, free radicals and also excited atoms and molecules, which are capable to oxidize SO_2 and NO_x to SO_3 and N_2O_5 and to convert them into acids with water presence. There are numerous gas phase reactions (up to 1500) which describe the process. The dose distribution optimization within entire volume of irradiated gas is essential for successful development of the electron beam flue gas treatment system.

It is worth to describe some physical relations regarding interactions between fast electrons and matter. Electrons interact with matter in several ways, main of which are inelastic and elastic collisions and also the emission of electromagnetic radiation (important at higher energy of electrons). The low energy electrons (bellow several MeV) lose their energy by inelastic collisions with electrons of the stopping material resulting in ionization and excitation in the irradiated material. The equation describing the rate of energy loss of an electron by ionization and excitation was first derived by Bethe, 1930 and completed by Bloch, 1933 is given by following formula:

$$dE/dx = \frac{2ANe^4Z}{m_0v^2}\left[\ln\frac{m_0v^2E}{2I^2(1-\beta^2)} - \ln 2\{2\sqrt{(1-\beta^2)}-1+\beta^2\}+1-\beta^2+\{1-\sqrt{(1-\beta^2)}\}^2/8\right] \quad [1]$$

where:
E - energy of the electron
x - distance travelled by the electron in the material
N - number of atoms per cm^3
e - charge of the electron
Z - atomic number of the stopping material
m_0 - rest mass of the electron
v - velocity of the electron
I - mean excitation potential for the atoms of the stopping material
$\beta = v/c$ where c is velocity of the light

The quantity dE/dx i.e. the rate of loss of energy with distance is known as the stopping power. It can be expressed in $MeVcm^2/g$ or in MeV/cm. The main conclusion from Bethe's equation is that the product NZ is equal to number of electrons in cm^3, i.e. stopping power is directly proportional to the electron density and will therefore be much lower in gas phase than in solids and liquids. Electrons due to their small mass are readily deflected by the Coulombic field of a nucleons. Although there is no energy loss in elastic collisions of this kind, such collisions are important and they result in non-linear passage of the electron through the irradiated medium.

The rapidly decreasing graph is obtained with a "tail" which merges with background when the percent of transmitted electrons is plotted as a function of absorber thickness. The absolute maximum range R_0 is determined by the intersection of the tail of the transmission curve with the background. The extrapolated or practical range R_p is determined by the extrapolation of the linear portion of the transmission curve to intersection with the background. The electron range can be calculated by numerical integration of the collision energy loss (equation 1). On the other hand some empirical relations can be used to calculate the electron range:

$$R = AE - B \quad [g/cm] \quad [2]$$

or

$$R = AE^n \quad [g/cm] \quad [3]$$

where:
E - electron kinetic energy in MeV
A, B, n - fitted constants

However, better accuracy offers more complex experimental formula:

$$R_0(E,Z,\upsilon) = a\,(1 + 25E^2 - 0{,}9865) \quad [g/cm^2] \quad [4]$$

where:
υ- incidence angle of the primary electrons in reference to the perpendicular line to the reflecting surface

$$a = \frac{0{,}161}{Z^{0.2}}\cos(h/2) \qquad \text{for } 0{,}03 < E < 3 \text{ MeV},\ 0 < \upsilon < 60°$$

As one can see, the last formula takes into account effects of Z and incidence angle υ. The angle υ depends on beam scanning parameters and on electron scattering in curved window foils. Electrons and also beta particles incident on a material are deflected either by electrons (electron-electron scattering) or by atomic nuclei (nuclear scattering). Scattering from a sample due to electron-electron interaction varies with Z/A and is slowly dependent on atomic number Z whereas nuclear scattering increases with Z. The total back-scattered intensity depends in a complex way on these two phenomena. Besides backscattering increases with increasing angle υ.

The thickness dependence of the most probable energy E_p can be approximated by simple expression:

$$E_p = E_0 (1 - x/R_p) \qquad [5]$$

where:
E_0 - initial electron energy
x - absorbing layer thickness
R_p - practical electron range.

5.2. Pilot plant facility

The Polish Pilot Plant for flue gas treatment, of capacity 20 000 Nm^3/h has been build at Power Station Kaweczyn in Warsaw (Chmielewski, Iller, Romanowski, 1991); Chmielewski et al., 1992). The installation was constructed on the by pass of the main stream of the flue gas with total flow rate 260 000 Nm^3/h from the boiler. This plant is the first industrial type of installation in which two stage longitudinal irradiation by electron beam was applied (Chmielewski et al, 1993; Chmielewski, Licki et al., 1995) and significant decrease of energy consumption was obtained in result.

Two electron accelerators transformer type ELV 3A were installed. The basic parameters of those accelerators are presented in Table 1.

TABLE 1. Technical characteristics of ELV 3A electron accelerator

Electron energy	500 - 700 keV
maximum beam power	50 kW
beam current	up to 100 mA
energy instability	+/- 5 %
beam current instability	+/- 5 %
accelerating voltage ripple	+/- 2 %
homogeneity of linear density of scanned beam at a distance of 50 mm from output window	+/- 10 %
extraction window dimension	1500 x 75 mm
max electron beam scanning angle	30°
titanium window thickness	50 μm
consumption AC power	60 kW

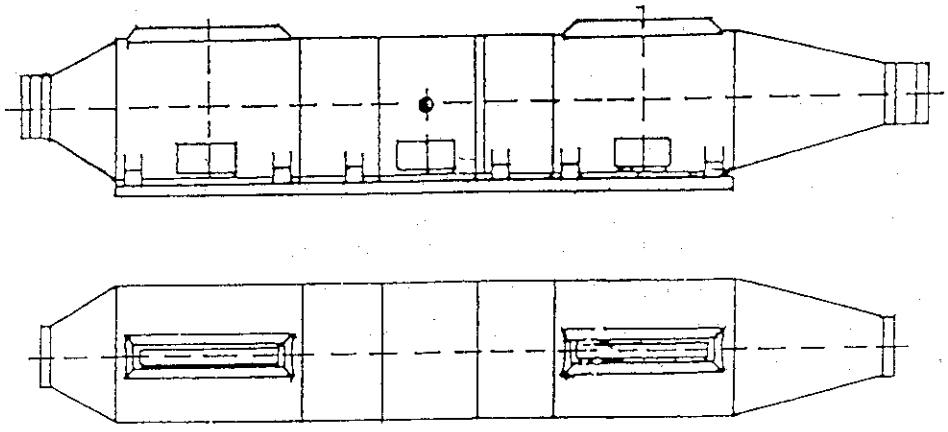

Fig. 1. The reaction vessel of the Pilot Plant EC Kaweczyn

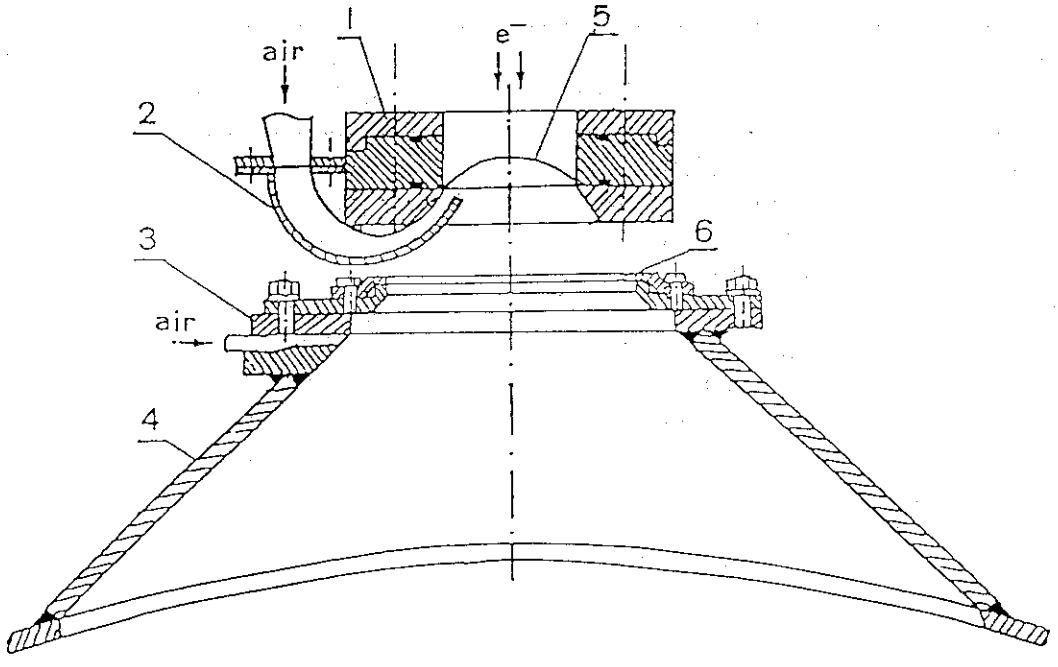

Fig.2. The double window construction applied in Polish Pilot Plant facility: 1 - accelerator output device, 2 - air cooling inlet (accelerator), 3 - air cooling inlet (process vessel), 4 - process vessel, 5 - accelerator window, 6 - process vessel window

The accelerators were installed in such distance that electron beams of both accelerators donot interfere with each other since their mutual distance along the axis of the process vessel is 2 m, what was confirmed by dosimetric measurements (Chmielewski, Zimek, Panta, 1991; Panta, 1992). The secondary windows made of titanium foil 50 μm thick were installed on the process vessel. The total length of the process vessel is 9960 mm with 1600 mm in its diameter. The distance between two accelerator is 5100 mm. The secondary windows dimensions are 1566x136 mm. Two streams of air with volume flow of 800 Nm^3/h each are blown into the process vessel under each of the secondary windows to make air curtain and prevent solid deposition on the foils. The air gap distance between primary and secondary windows is 70 mm. The reaction chamber and double window construction applied in Polish Pilot Plant facility are shown on Fig. 1 and 2.

5.3. Dose distribution measurements

The actual dose distribution everywhere within the entire volume of the treated flue gas is very important for the successful development of electron beam flue gas irradiation system. PVC and CTA dosimetric foils were chiefly used for spatial dose distribution measurements after critical selection of published dosimetric methods. The main characteristic of PVC and CTA foils are presented in Table 2.

TABLE 2. The intercomparison of main characteristics of PVC and CTA film dosimeters

Polymer foil	CTA JAERI6948/1977 (1)	PVC Riso 141/1966 (2)
composition	$(C_{12}H_{16}O_8)_n$ cellulose triacetate 85%, triphenyl phosphate, about 15%	$(C_2H_3Cl)_n$ polyvinyl chloride 98%
manufacturer	FUJI Co., LTD	KuntsoffwerkeS.
thickness	0,125 mm (+/- 5%)	0,26 mm
width of tape	8 mm	8 mm
specific weight	1,32 g/cm^3	1,4 g/cm^3
electron density	3,18x1023 e/g	3,15x1023 e/g
effective atomic number	Z 6,7	11,37
effective Z/A (A - atomic weight)	0,526	0,5
mass stopping power: 1 MeV	1,75-1,8 $MeV/g/cm^2$	1,64 $MeV/g/cm^2$
linearity range	10 - 200 kGy	5 - 50 kGy
wavelength of measurements	279,5 nm	394 nm
precision of measurements	8 - 10%	6 - 10%

(1) Tanaka et al., (1977)
(2) Popovic, (1966); Bulhak, (1976)

Dose spatial distribution inside the process vessel was measured by both PVC and CTA film dosimeters, which were cutted on stripes with length about 115 cm. The dosimetric film stripes were placed in a special designed square frame (holder) with external dimension approximately 113x113 cm in seven levels of 20 cm step. The frame construction excluded

selfscreening of dosimetric film strips. The frame position was perpendicular to the geometrical axis of process vessel in the middle of double titanium window during the radial dose distribution measurements.

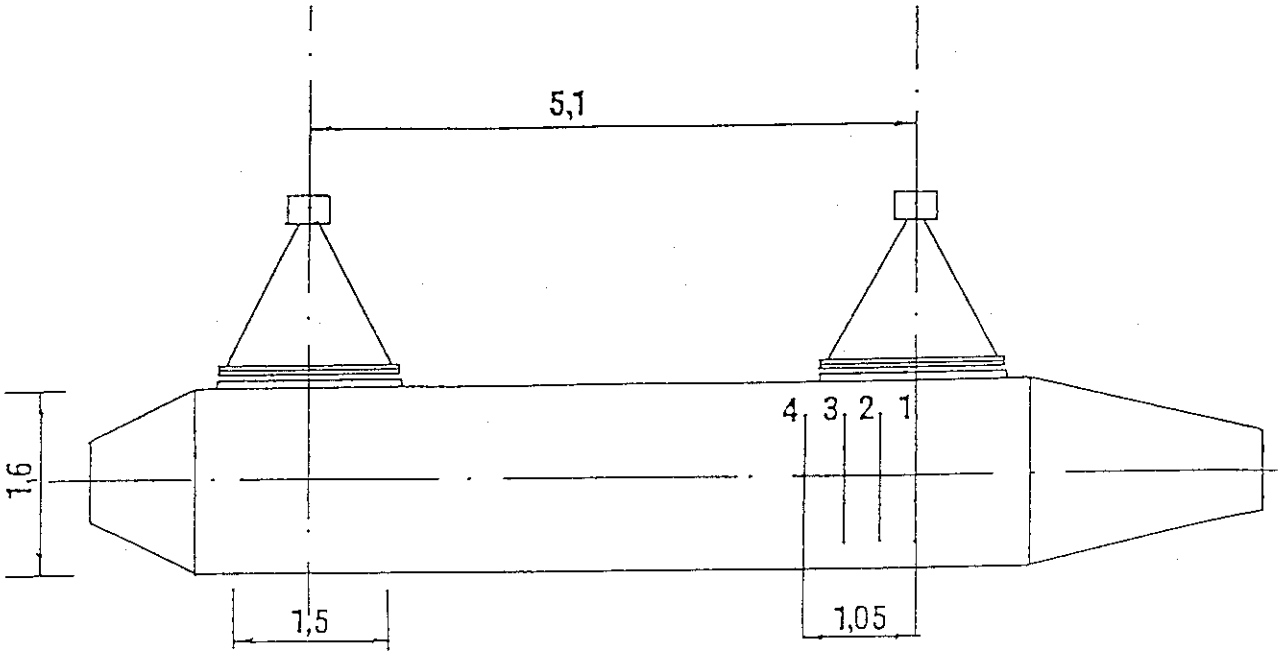

Fig. 3. The configuration of dosimetric foil during dose distribution measurements

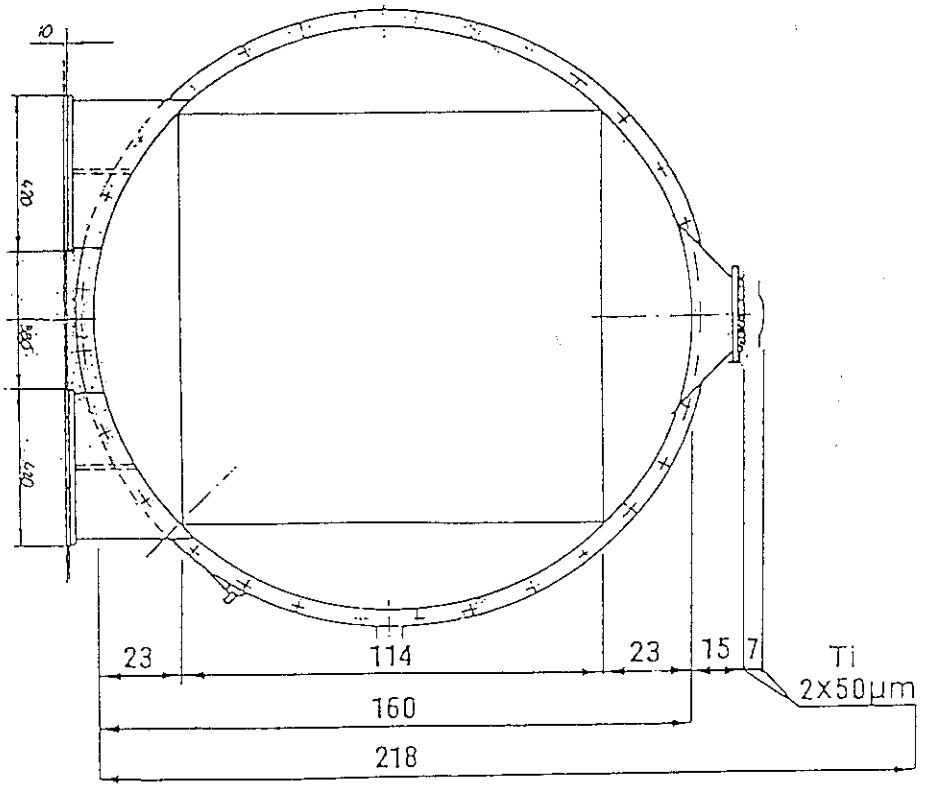

Fig.4. Cross-section of the reaction vessell and its geometrical dimensions

Longitudinal dose distribution was measured by consecutive shifting of frame along the main geometrical axis of process vessel with the step 35 cm. The configuration of dosimetric foil during dose distribution measurements is shown on Fig. 3. Fig.4 shows cross-section of the reaction vessel and its geometrical dimensions. The measurements were performed at 500, 600 and 700 keV of electron energy and 1 mA of electron beam current to keep 500 mAs integral value constant. Radiation induced absorbance of PVC and CTA streapes was spectrophotomertically sampled with the step of 3 cm along each stripe. The reading level from the seventh film stripe of the matrix closest to bottom at the lowest energy (500 keV) was undistinguishable from the unirradiated film absorbance. The results are presented in fig. 5 to 8. The relative distribution of the dose deposited to the gas phase vs the electron penetration depth in reaction vessel is given in Fig. 9.

The mean dose delivered to the flue gas under nominal conditions (20 000 Nm^3/h, 100 kW beam power and initial electron energy 0,7 MeV) is 11,5 kGy at the temperature of the gas phase 80°C during irradiation process in Polish Plant for flue gas treatment.

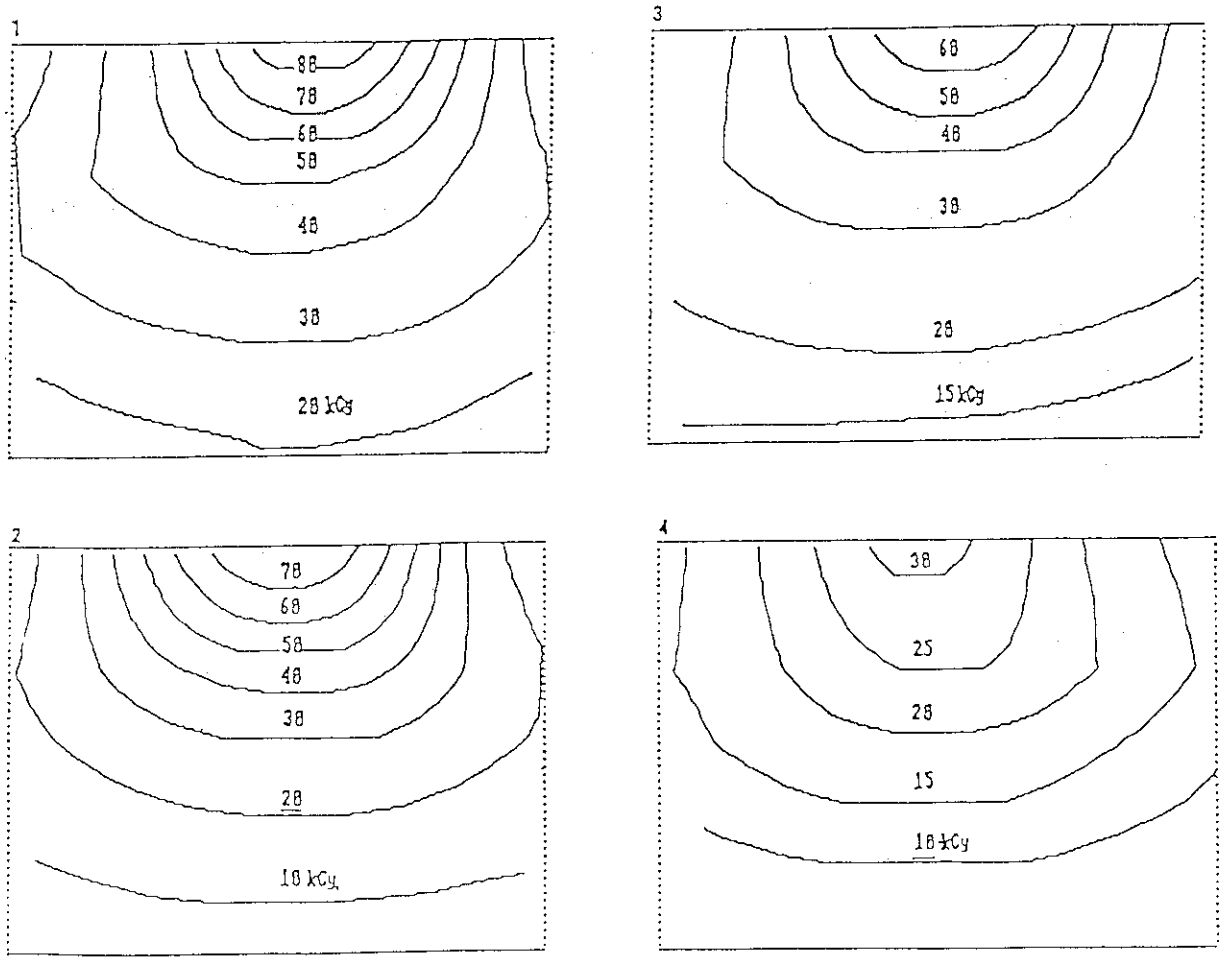

Fig.5. Measured dose distribution for different location of metal frame (position 1 to 4; Fig. 3). Electron energy 600 keV

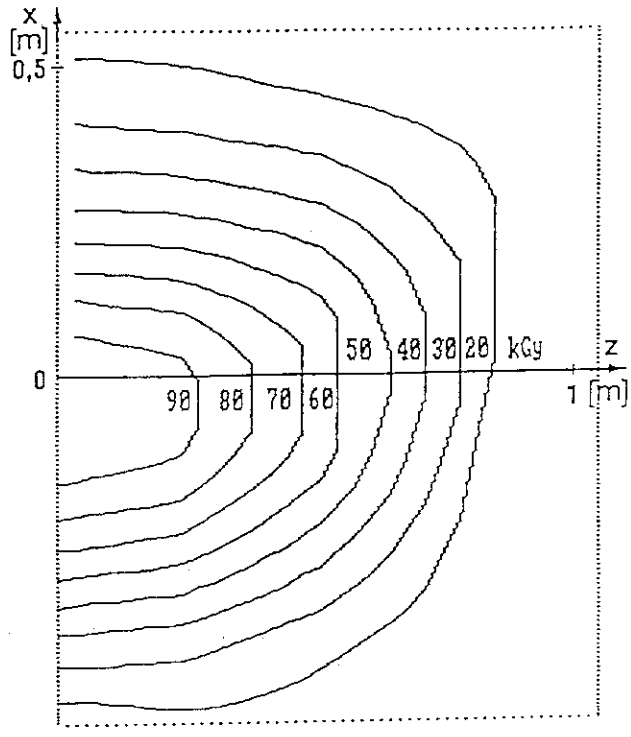

Fig. 6. Calculated dose distribution from the data presented on Fig. 5 along the axis of reaction vessel

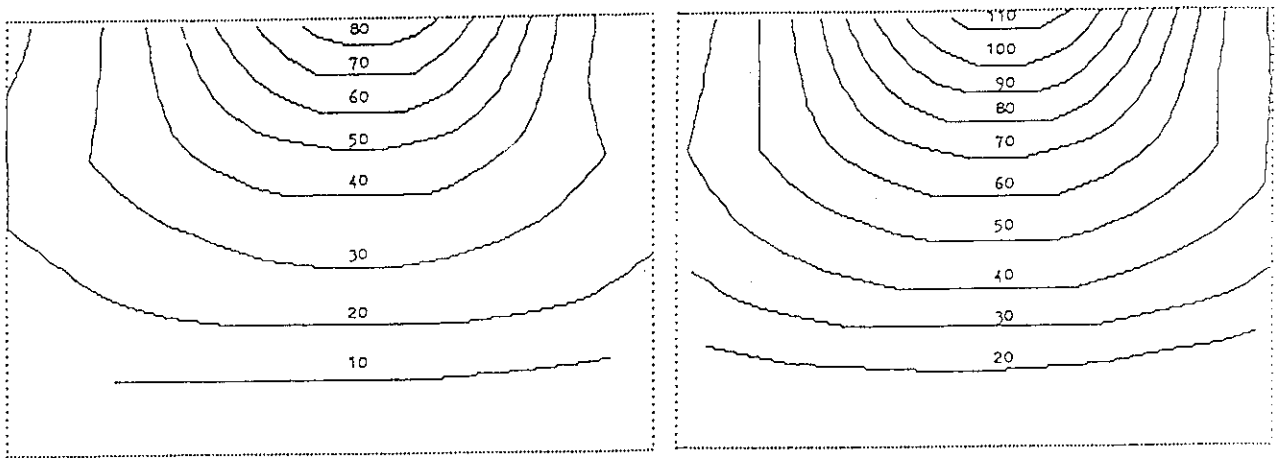

Fig.7. Dose distribution in kGy in reaction vessel for electron energy 500 keV. Total electron beam charge transfered to the system 500 mAs. A - radial distribution, B - axial distribution

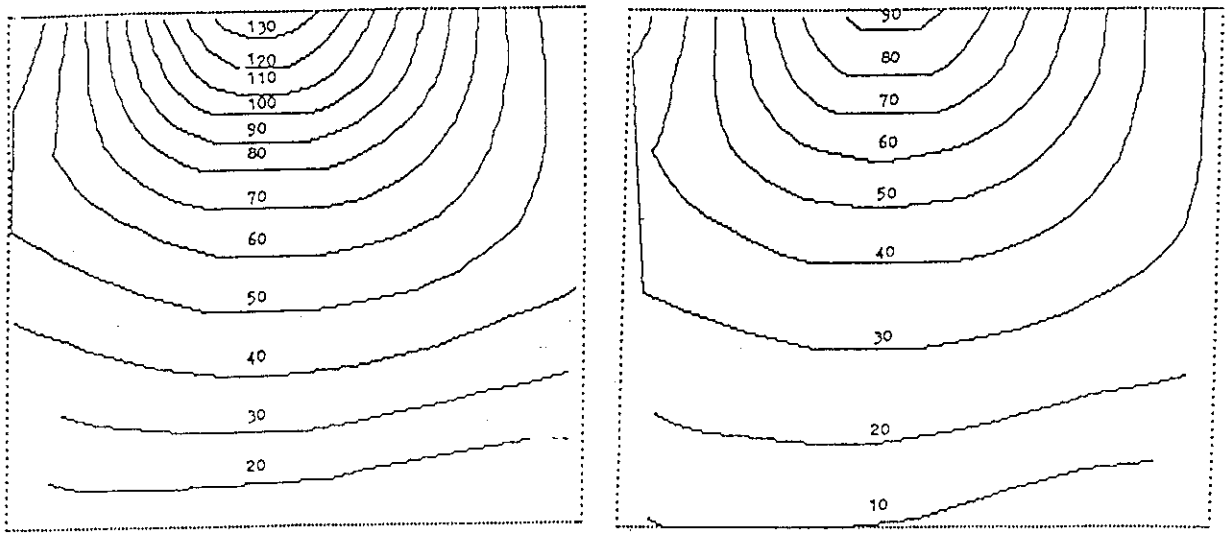

Fig.8. Dose distribution in kGy in reaction vessel for electron energy 700 keV. Total electron beam charge transfered to the system 500 mAs. A - axial distribution, B - radial distribution

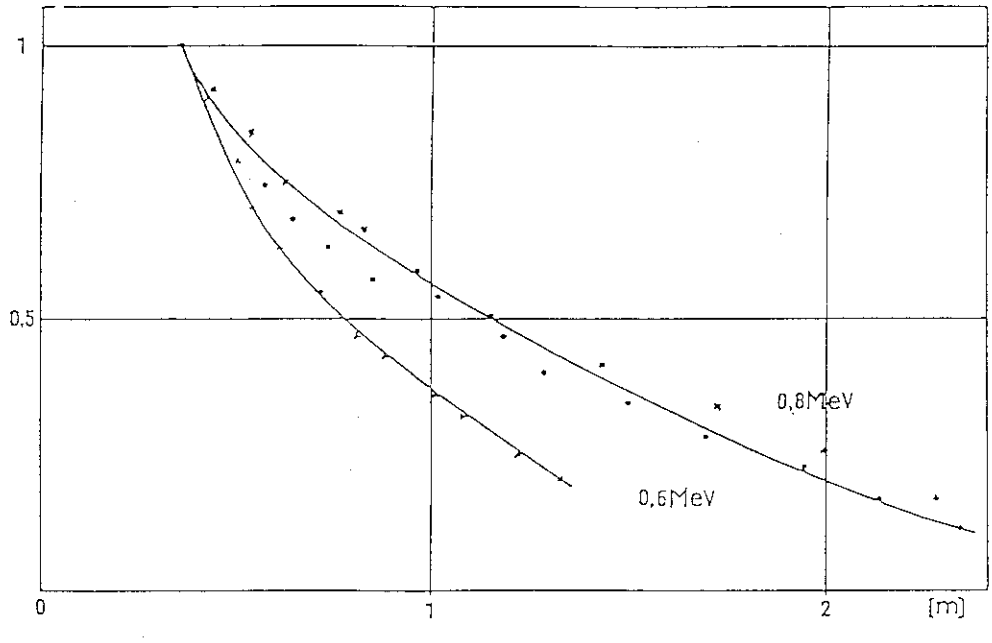

Fig. 9. Deep relative dose distribution in air for electron beam initial energy 0,6 and 0,8 MeV

5.4. The effectiveness of the window system

The dose rate delivered to the flue gas is one of the major parameter of the irradiation process. It has direct relation to the NO_x and SO_2 removal efficiency and required electron beam power engaged to the process (number and size of the accelerators). This means that economy of the process strongly depends upon the effectiveness of the beam power transmission to the flue gas. Electron energy deposited in window system and reaction vessel walls can counted as a energy loss. Electron beam losses in double window system are connected to:

- backscatering of electrons from titanium foils,
- ionization losses in Ti (significant part), simultaneous with electron energy degradation,
- radiation losses (insignificant part)
- partial absorption of some electrons in Ti.

In measurements and utilization of fast electrons, accurate knowledge of backscattering is frequently required. One of the quantities featuring this phenomenon is backscattering coefficient defined as the ratio of the number of backscattered electrons to the number incident electrons. The backscattering is to a considerable degree due to electric field of nucleus (atoms of irradiated material, i.e. Ti in our case) and it increases with Z (atomic number). On the other hand, the backscattering coefficients increase with increasing target thickness until saturation which is reached at a thickness around half the practical range of the incident electrons. It depends also on energy incident electrons. The backscatering coefficient $\check{R}$ at saturation of monoenergetic electrons impinging normally on target has been evaluated by many authors. According to Tabata the relation between the backscattering coefficient $\check{R}$ and energy of incident electrons E may be approximated by the formula:

$$Z = a_1/(1 + a_2 J^{a_3}) \qquad [6]$$

where: $J = E/mc^2$

E - energy of incident electrons, MeV

mc^2 - rest energy of electron, 0,511 MeV

a_1 - constant, 0,221 for Ti

a_2 - constant, 0,134 for Ti

a_3 - constant, 1,36 for Ti

According to Tabata the rms deviation of the experimental data from this equation is expected as about 7%, however Tabata's formula omit the effect of incidence of the total backscattering electrons. Tabata's equation fits 615 experimental points reported in 20 references, but shows slight underestimation according to data of Seltzer and Berger (1987) and our own results.

Experiments performed in INCT with electron beam energy 500 keV and a flat titanium foil of 50 μm showed that reflection was nearly like from thick titanium layers (i.e. for saturation thickness). Similar results were obtained using the computerized coating thickness gauge - GIL-90 PC, which employed beta-rays scattering principle. Sealed source of Tl-204 and Sr-90 were used (mean electron energy 255 to 900 keV). The detailed results are presented in Table 3.

TABLE 3. Flue gas irradiation efficiency at Kaweczyn Pilot Plant

Electron energy	500 keV	600 keV	700 keV
windows (2 x 50 μm), bacscattering	24,9%	17,8%	12,2%
first window absorption	6,7%	5,5%	4,6%
air 70 mm absorption	2,5%	2,9%	1,7%
second window absorption	6,8%	5,5%	4,7%
process vessel, 1600 mm			
side walls losses	7,0%	-	-
bottom losses	-	-	12,5%
total losses	47,9%	30,8%	35,7%
total losses (1)	13,4%	10,8%	9,2%
(2)	24,6%	20,6%	17,9%
(3)	40,9%	30,8%	23,2%
(4)	47,8%	32,2%	36,4%

(1) - calculation with stopping power only (Pages et al., 1970)
when Bethe modified formula was used,
(2) - calculation with stopping power and backscattering according formula [6],
(3) - Cleland et al., 1993 (without side wall and bottom losses)
(4) - Chmielewski, Zimek et al., 1995

The results given in Table 3 was confirmed by temperature measurements of the flue gas before and after irradiation. The thermal balance of adiabatic reactor (process vessel) shows the 69% efficiency of the irradiation process for 0,7 MeV electron energy and 78℃ of the flue gas temperature. It means that 3 1% of total beam power has been lost what is in a good agreement with previous data.

5.5. Conclusions

The mean dose delivered to the flue gas under nominal conditions (20 000 Nm^3/h, 100 kW beam power and initial electron energy 0,7 MeV) is 11,5 kGy at the temperature of the gas phase 80°C during irradiation process in Polish Plant for flue gas treatment. It means that about 64% of total beam power is effectively used for NO_x and SO_2 removal process in certain double window and process vessel configuration. The results of dose measurements are in a good agreement with calculations based on properties of the materials used and construction of the facility and was also confirmed by temperature measurements of the flue gas before and after irradiation. The thermal balance of adiabatic reactor (process vessel) shows that 69% efficiency of the irradiation process for 0,7 MeV electron energy and 78°C of the flue gas temperature. It means that 3 1% of total beam power has been lost what is in a good agreement with presented data.

The optimum electron energy with minimum beam power losses can be found at the certain temperature of the irradiation process. The construction of the double window should be modified by use better quality window material with smaller foils thickness. The higher initial electron energy should be applied with properly bigger size of process vessel to reduce total losses of beam power and increase effectiveness of the flue gas treatment process.

References

Bethe H.A., (1930), Ann. Physic, 5, 325
Bloch F.,(1933), Z. Physic, 81, 363
Bulhak Z., Doctoral Thesis, (1976), INR, Warsaw
Chmielewski A.G., Zimek Z., Panta P. (1991), INCT - 2117/IChTJ
Chmielewski A.G., Iller E., Romanowski M., (1991), INCT Report
Chmielewski A.G., Iller E., Zimek Z., Licki J. (1992), Radiat. Phys. Chem., v 40, No 4, 321
Chmielewski A.G., Tyminski B., Licki J., Iller E., Zimek Z., Dobrowolski A. (1993), Radiat. Phys. Chem. v 42, No 4-6, 663-668
Chmielewski A.G., Zimek Z., Panta P., Drabik W., (1995), Radiat. Phys. Chem., v 45, No 6, 1029-1033
Chmielewski A.G., Licki J., Dobrowolski A., Tyminski B., Iller E., Zimek Z., (1995), Radiat. Phys. Chem., V45, No 6, 1077-1079
Cleland M.R. et all (1993), EPRI Symposium, February 22-24, San Francisco, California
Pages L., Bertel E., Joffre H., Sklavenitis L. (1970), CEA-R-3942,
Panta P. (1992), Radiat. Phys. Chem., v 40, No 4, 327
Popovic J., (1966), Riso Report, No 141
Seltzer S.M., Berger M.J., (1987), Appl. Radiat. Isot., 38, 349
Tabata T., Ito R., Okabe S., (1971), Nucl. Instrum. Meth., 94, 509

6. Experimental studies of the prototype internal beam monitor in Kaweczyn power station installation

E. Kulczycka*, M. Kisieliński*, Z. Moroz*, M. Sowiński, J. Wojtkowska*, A. G. Chmielewski and S. Hashimoto

ABSTRACT

A prototype of the electron beam monitor designated to work inside the irradiation chamber is constructed and experimentally tested in Kawęczyn power station installation. Some results are reported.

6.1. INTRODUCTION

The real-time monitoring of the electron beam during the irradiation process appears to be one of the most important factors if one works in the installation for treatment of the industrial flue gas with low-energy electron beam. A good example of such installation is that in Kawęczyn power station which is dedicated to the removal of the SO_2 and NO_X contaminations. The internal beam monitoring is important both for the control of the irradiation process as well as for further interpretation of the data. Also, estimation of the electron energy deposit in the tank, or dose spatial distribution are of a great value.

The problem is, in fact, a very challenging, because one have to deal with the highly dusty medium of a high humidity, with some contamination of ammonia and/or other aggressive substances. Additionally, in working conditions, the gas medium has quite large temperature, about 100 °C.

For this purpose, a prototype of the internal electron beam monitor was constructed and its performance was tested experimentally in the installation in Kawęczyn power station near Warsaw, Poland. In this report, the construction of this monitor as well as some results of the experimental tests performed by authors in 1994, are described.

* Soltan Institute for Nuclear Studies, Otwock-Świerk

6.2. CONSTRUCTION AND OPERATION PRINCIPLE OF THE DEVICE

Because external conditions in the environment of the monitor are very hard, one certainly cannot use any of known precise electron monitors, like scintillation or semiconductor detectors. So, one must look rather for much simpler device being, however, much more resistive against environmental pollution. On the other hand, working with rather large electron beam currents, one can expect to deal with large electric signals. Therefore, as the charge monitoring sensor was chosen a simple metal plate with the diameter of about one centimetre and thickness of few millimetres, exceeding the full range of the electrons. The electric charge induced by incident electrons is then electronically converted to the train of standard logical pulses with variable charge-dependent frequency. Pulses are later summed out by standard scaler. Thus, an indication of the scaler is proportional to the integrated charge captured by the sensor plate.

The sensor plate itself is closed in a small protecting container with one window only, allowing to detect only electrons from the multiscattering cascade which develops in the entrance window and gas medium. This container, together with additional metal tube, shields also output signal wire against the irradiation and is an electrical screen against electric noise induced by the accelerator.

To protect the sensor plate against dust the entrance window is covered by the phosphor bronze grid. Also, a stream of compressed dry air under pressure of about 2 atmospheres is directed from outside of the tank to the tube and container. Thus, the resulting strong stream of air through the entrance window protects the sensor plate against the dust and corrosion.

The construction of the monitor and its installation in the tank are schematically shown in Fig.1. and Fig. 2., respectively.

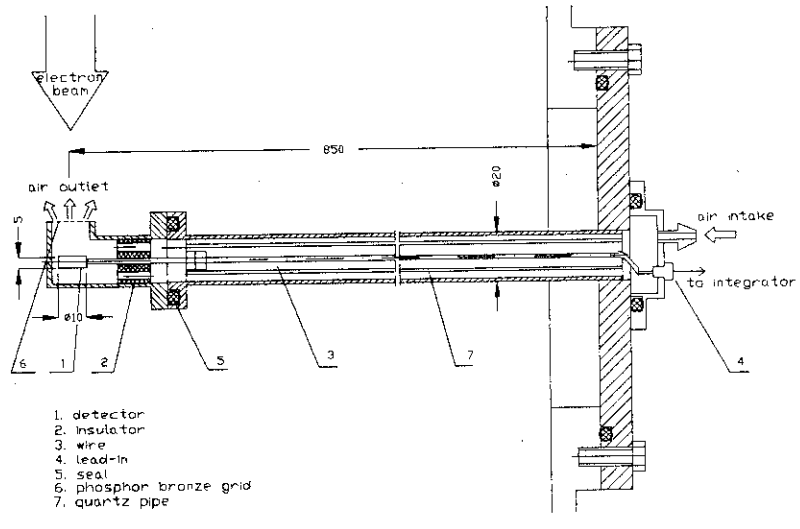

Fig. 1. The construction of the beam monitor.

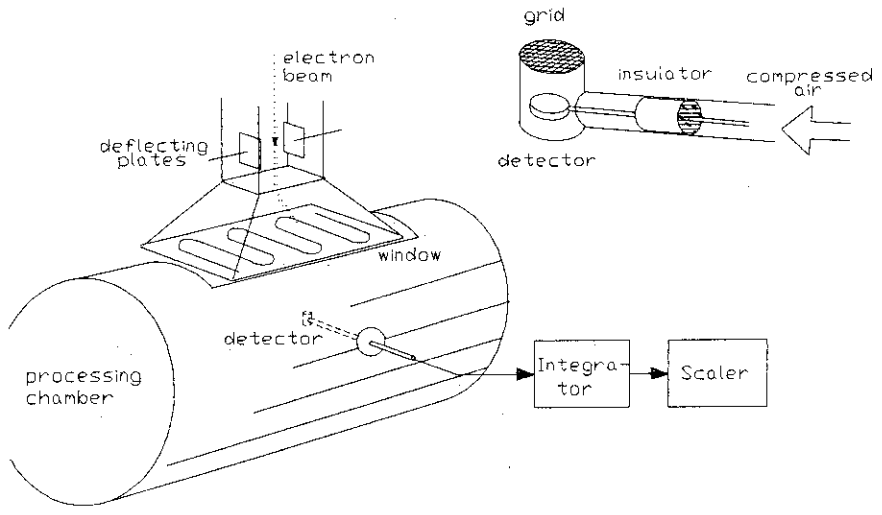

Fig. 2. General view of processing chamber and installation of the monitor.

The block scheme of the electronics is displayed in Fig.3.

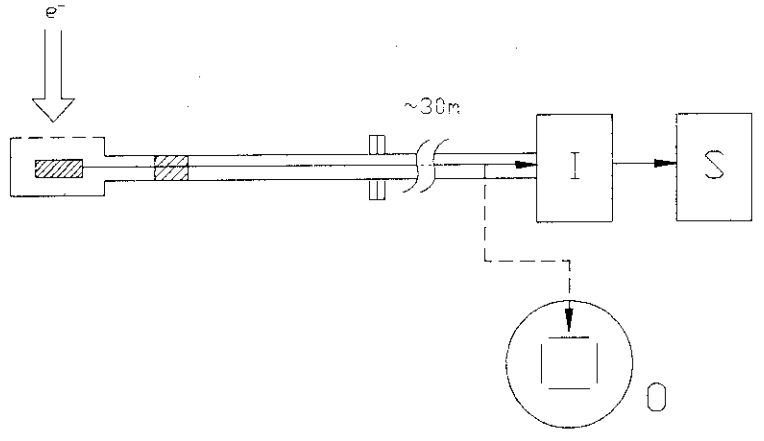

Fig. 3. Block scheme of the electronics.
I - charge integrator (charge-to-frequency converter)
S - scaler
O - oscilloscope.

Using 400 keV electron accelerator in the Institute of Nuclear Studies in Świerk the first oscilloscope observations of the signals from the prototype monitor in the atmospheric air were performed. The accelerator has electron beam of few milliamperes extracted through the titanium window and swept through the air gap with frequency of 50 Hz.

The observed output signal has two components:

(i) AC component with frequency about 50 Hz. The exact shape and position of this signal with respect to the phase of the beam deflecting voltage depends on the position of the sensor plate with respect to the not deflected beam axis and the distance from the entrance window. This signal is due to the direct bombardment of the sensor plate by the electron beam.

(ii) DC component which comes out from the residual charge from previous cycles which is stored in the capacity of the concentric cable joining the monitor and electronics. The level of this signal depends on the effective output time constant of the monitor.

It was found that both signals are proportional to the electron beam current. Thus, each of them can be used for monitoring purpose. It means that simple integration of the total charge induced on the capacity without distinguishing between these two components will satisfactorily do the job, additionally making the response of the monitor almost insensitive to the horizontal position of the device.

During the work of the accelerator extra noise signals were induced by the machine causing some fluctuations of the integrated signal. It was found that a low-pass filter, dumping frequencies higher than 1 kHz satisfactorily cleans out the output signal from this noise, leaving sensitivity of the monitor to the beam signal almost unchanged.

6.3. TESTS PERFORMED IN KAWĘCZYN POWER STATION – SOME RESULTS

The device was installed in Kawęczyn power station and following tests were performed:

6.3.1. Tests with the irradiation tank filled with atmospheric air

TEST 1. Monitor position fixed at the centre of the irradiation tank (Fig. 2.). Linearity of the response v. incident electron beam current has been measured for the energies 500, 600 and 700 keV in the range of the beam currents 5.0 ÷ 100 mA. The results are presented in Fig. 4. The energy dependence of the signal values ratio R(E)/R(500 keV) measured for different beam currents is shown in Fig. 5. Small current dependence of the signal is attributed to some nonlinearity of the signal output visible in Fig. 4. This nonlinearity, however, was removed to a large extent in further models of the monitors. Additionally, the stability of the response was observed. For higher currents, within ranges, which are typical for operating conditions, the observed fluctuations of the scaler counts did not exceed few percent, what is considered as quite satisfactory result.

TEST 2. Monitor position varied vertically. Response of the detector v. its vertical position for different energies is shown in Fig. 6.

TEST 3. An extra model of the monitor was tried, in which metal mesh window was replaced by a metal foil thus enabling the evacuation of the container

surrounding the sensor plate from the air. In this way, no extra charge was induced in the air close to the sensor plate. No significant change of the signal was observed after evacuation of the monitor.

6.3.2. Tests with the irradiation tank filled with flue gas and admixtures of water vapour and ammonia (typical working conditions)

TEST 4. Monitor position fixed at the centre of the tank. Long-term electric signal stability test. During 7 days and nights of continuous work of the installation, the average signal from the monitor was stable within 10 percent.

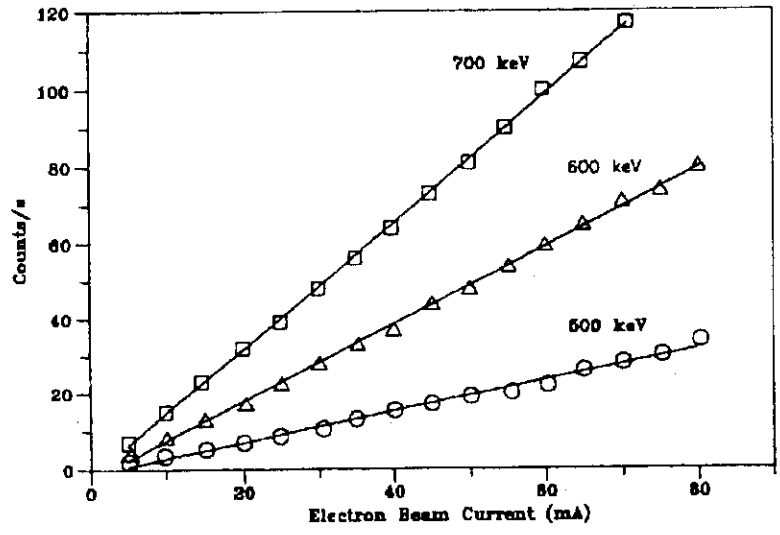

Fig. 4. Linearity of Response v. Beam Current.

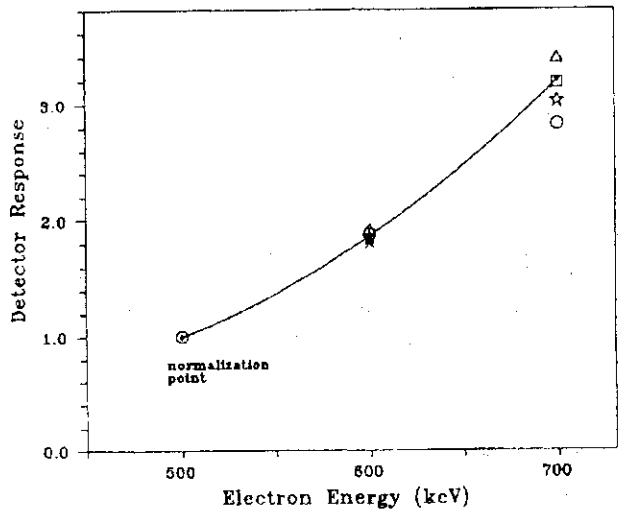

Fig. 5. Response v. Incident Energy.

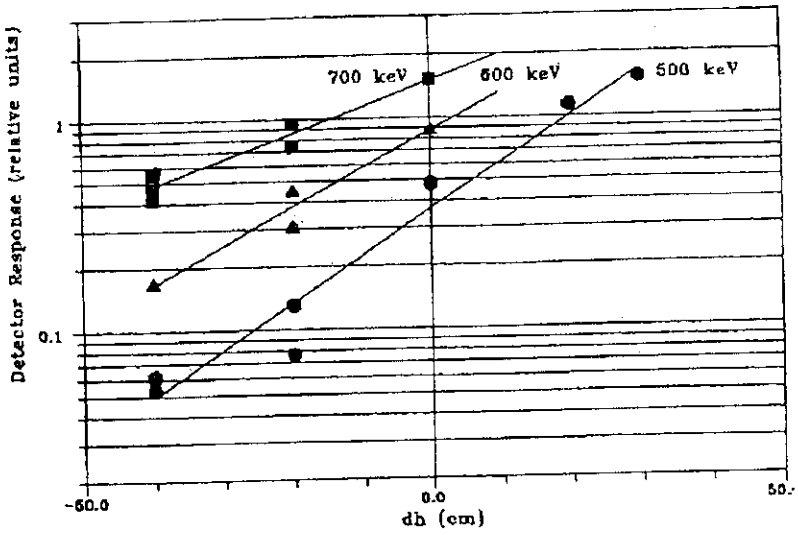

Fig. 6. Response v. Vertical Position of the Detector.

TEST 5. Long-term test of the monitor construction and material against corrosion. During ca 14 days of the installation operation, the monitor was left without dry air protection to see behaviour of the sensor plate and other parts of the device. After this time the sensor plate was found almost unchanged while various outer parts of the construction were corroded to some extent. Those observations were further used to improve mechanical construction of the device.

6.4. CONCLUSIONS AND DISCUSSION

Tests performed with the prototype of the internal beam monitor have shown that one can obtain stable electrical signal proportional to the incident beam current from the accelerator. For given current, the monitor response depend on the incident electron energy as well as vertical position of the monitor in the tank.

Some calculations of the dose distribution in the tank were performed using our Monte Carlo code DSHAPE [1]. It was found that this response of the monitor can be reasonably understood in terms of the model contained in DSHAPE, and that it is strongly correlated with the actual dose absorbed in the corresponding volume element of the irradiation chamber. Some comparisons of the experimental and calculated quantities are presented in our next report [1].

We conclude that the signal from such device can be used for indication of the actual dose deposit in the tank provided that the absolute calibration of the device will be done using one of the standard methods of the dose measurements. Quick response of the monitor makes possible the real time control of the electron beam inside the irradiation chamber during the irradiation process. This feature should make the device very useful to control of the irradiation process.

In the case when accelerator is used to irradiate samples in normal atmospheric environment or other noninvasive gases and free of large dust contaminations, the practical construction of the beam monitor should not differ significantly from that used in the prototype. In many simple cases even the use of the protecting stream of the air is not necessary.

Some other, more complicated and more precise variants of the sensor element are also possible. For example, one can think of extra guard ring surrounding the sensor plate, with a bias voltage, protecting the sensor plate against collecting the charge induced due to ionization of the surrounding gas. Construction of such ring was discussed in [2].

Working in dusty, wet and contaminated with aggressive substances, like ammonia, special measures should be taken to protect important parts of the device against the dust and corrosion. The presence of the protecting dry air stream is very important for long-term stability of the device. Especially, it is not recommended to leave the device unprotected for a long time in the tank when not used for measurements. In this case the most important parts, especially the sensor plate, should be additionally shielded. In some cases, one can think of complete isolation of the sensor plate from the environment, by replacing the mesh window by a metal foil and pumping-out the air from the inside of the monitor.

One can think also of using electrons backscattered from the metal reflector rather than those coming directly from the outside. This geometry may ensure better shielding of the sensor element against environmental dust.

REFERENCES

[1] J. Wojtkowska, Z. Moroz
Calculations of the Spatial Dose Distributions during the Irradiation of a Gas Sample by Low-energy Electrons. Preprint SINS, 1995.
[2] R. Tanaka et al., Nucl. Instr. Meth., Vol. 174, p. 201, 1980.

7. Calculations of the spatial dose distribution during irradiation of a gas sample by low-energy electron beam

J. Wojtkowska*, Z. Moroz* and A.G. Chmielewski

ABSTRACT

Monte-Carlo calculations of the spatial dose distributions during the irradiation of a large gas sample by low-energy (E_el < 1 MeV) electron beam are reported. The calculated results are compared with experimental data of Proksh et al. [1] for E_el = 500 keV. Some predictions at E_el=500, 600 and 700 keV for the conditions existing at the test installation for the treatment of the industrial flue gas in the Kawęczyn power station are reported.

7.1. INTRODUCTION

Studying the processes induced by the bombarding the large volume gas samples by low-energy electrons, like those one can meet in the installation for industrial flue gas treatment dedicated to the removal of the SO_2 and NO_X contaminations, requires some knowledge of the spatial energy deposit, or dose distribution in the irradiation chamber.

In relatively low-energy region (E_el = 100 ÷ 1000 keV), the average range of electrons is often smaller than linear sizes of the irradiation chamber so that a large amount of the incident electrons become absorbed before they reach the walls of the tank. Thus, the spatial energy deposit in the tank is a nonuniform function of the position in the tank. Such distribution is generally energy - dependent and is influenced by details of the applied beam deflection, beam focusing, multiple scattering of electrons in the entrance windows as well as in the gas sample etc. Therefore, it would be nice to have some relatively simple tool to calculate, at least approximately, such dose distributions and various related quantities.

In general, similar problems of the interaction of single electrons of high energy with the environmental matter are solved using Monte-Carlo methods. For example, one of the most general programs of this kind is contained in CERN GEANT-3 package commonly used in various simulations needed in high energy physics. However, for such programs, using rather large computers is required.

* Soltan Institute for Nuclear Studies, Otwock-Świerk

For low-energy but high current irradiations of the gas samples much simpler variants of the Monte Carlo sampling, thus enabling to use a PC computers only, should be of the value. One of such simple programs, named DSHAPE, is written by authors and is reported in the present paper. Results of calculations are compared with some experimental data. Predictions for dose distributions and related quantities are calculated for the conditions typical for the Kawęczyn installation.

7.2. PROGRAM DSHAPE

Program DSHAPE consists of three independent steps which calculate the following:

7.2.1. Simulation of the beam deflector of the accelerator

For this purpose, the suitable geometrical parameters of the deflector are introduced to the program. At some distance z = 0 from the deflector deviations y(t) of the electron trajectory as well as deflection angle $\alpha(t)$ are calculated under deflection voltage V(t). Few different shapes of the deflecting voltage can be used, including linear or sinusoidal ones. The main sweeping frequency is 50 Hz. Additionally, extra sweeping of the beam in the plane (x, y) perpendicular to the main deflecting plane and freely chosen amplitude can be applied. This second deflecting frequency is chosen to be about 400 Hz and its incident phase shift with respect to the main sweeping frequency is random. Thus, in the plane (x, y, z = 0) one gets the overlap of the corresponding Lissajoux figures, which after some time including many sweeping periods fill uniformly the area of desired rectangular shape. Additionally, a beam defocussing in the plane z = 0 is simulated by introducing extra deviation of the beam position in x and y directions chosen at random in the desired beam spot rectangle (bh, bw). Each point in the plane (x, y, z = 0) does not represent a single electron but, rather, some elementary charge q, which is calculated from known average beam current and the time quantization chosen in the calculation.

7.2.2. Beam interaction with entrance windows

Because the beam passes through the two Titanium foil windows placed along the beam trajectory the corresponding energy loss and a part of beam scattered backward are calculated at first. Energy losses are linearly extrapolated from the standard tables and are calculated at each time t for effective foil thickness which depends on the actual angle of incidence $\alpha(t)$. To calculate backscattering of the beam the formulae of Tabata et al. [2] are used. Then, the beam charge which passed through the foils at each time t is further quantized and 100 rays are chosen at random obeying Gaussian multiple scattering law. The average multiple scattering angles are given by standard formula.

7.2.3. Multiple electron scattering in the gas medium

The goal is to calculate 3-dimensional distribution of the deposit of the electron energy in the gas medium, which volume is divided into some number (typically $10\times200\times20$) elementary elements.

Our previous simplified Monte Carlo calculations performed for 400 keV electrons have shown, that one gets quite a good approximation of the measured 2-dimensional dose

distribution at some distance D, if the interaction of the beam with the gas medium is replaced by multiple scattering of the beam by thin "foil" of the corresponding thickness placed at the half-distance between the deflector and measuring plane [3].

In the present calculation, this certainly oversimplified procedure is replaced by another one, where full depth of the tank is divided into 20 layers and each of gas layer is replaced by corresponding "foil" placed at the centre of the layer. Thus, each of the incident trajectories is subjected to utmost 20 subsequent scatterings according to the Gaussian multiple scattering law. Also, the corresponding energy loss is calculated and energy degradation along the trajectory is followed. Thus, the trajectory is approximated by a set of straight line pieces placed between subsequent horizontal layers of the scatterer. It is automatically stopped when the total energy loss exhausts the incident electron energy. For each scattering, deflection values (xn, yn) are calculated for each of zn and the corresponding energy deposit is stored in the suitable volume element. Such calculation is repeated at given time t for each of the above mentioned 100 trajectories and then, the next value of the time t is selected. The block scheme of the sampling procedure is shown in Fig. 1.

The stored values of the energy deposit for each of the volume elements allows to calculate spatial dose distribution, any projection of this distribution as well as some other related quantities. Results can be also plotted using one of standard graphical procedures.

At present, other effects, like e. g. production of delta electrons in the collisions, are neglected. Because of the sequential character of the Monte Carlo sampling procedure, some of them can be relatively easy incorporated into the program, if necessary.

7.3. TESTS OF PROGRAM

At first, program was tested by numerical calculations of some simplified cases which results are easily reproduced by means of the ordinary calculator. Then the special case of 500 eV electrons irradiating the air gap was considered and dose depth profile was calculated. For this case experimental data measured with foil dosimeter were published by Proksh et al. [1]. The characteristic shape of the depth profile is determined by the electron cascade developing in the gas medium. Comparison of the experimental and calculated values are presented in Fig. 2. A good agreement with the experimental data was obtained. Thus, it proves the validity of the approximations used in the DSHAPE code.

7.4. CALCULATIONS OF DOSE DISTRIBUTIONS FOR THE CASE OF KAWECZYN INSTALLATION

The calculations of dose distribution were calculated for the conditions present in Kawęczyn test installation, when the irradiation tank is filled with Air. Three incident electron energies have been chosen, namely 500, 600 and 700 keV. The corresponding (y, z) and (x, z) projections of the distribution for 500 keV are presented in Fig. 3a. and 3b.

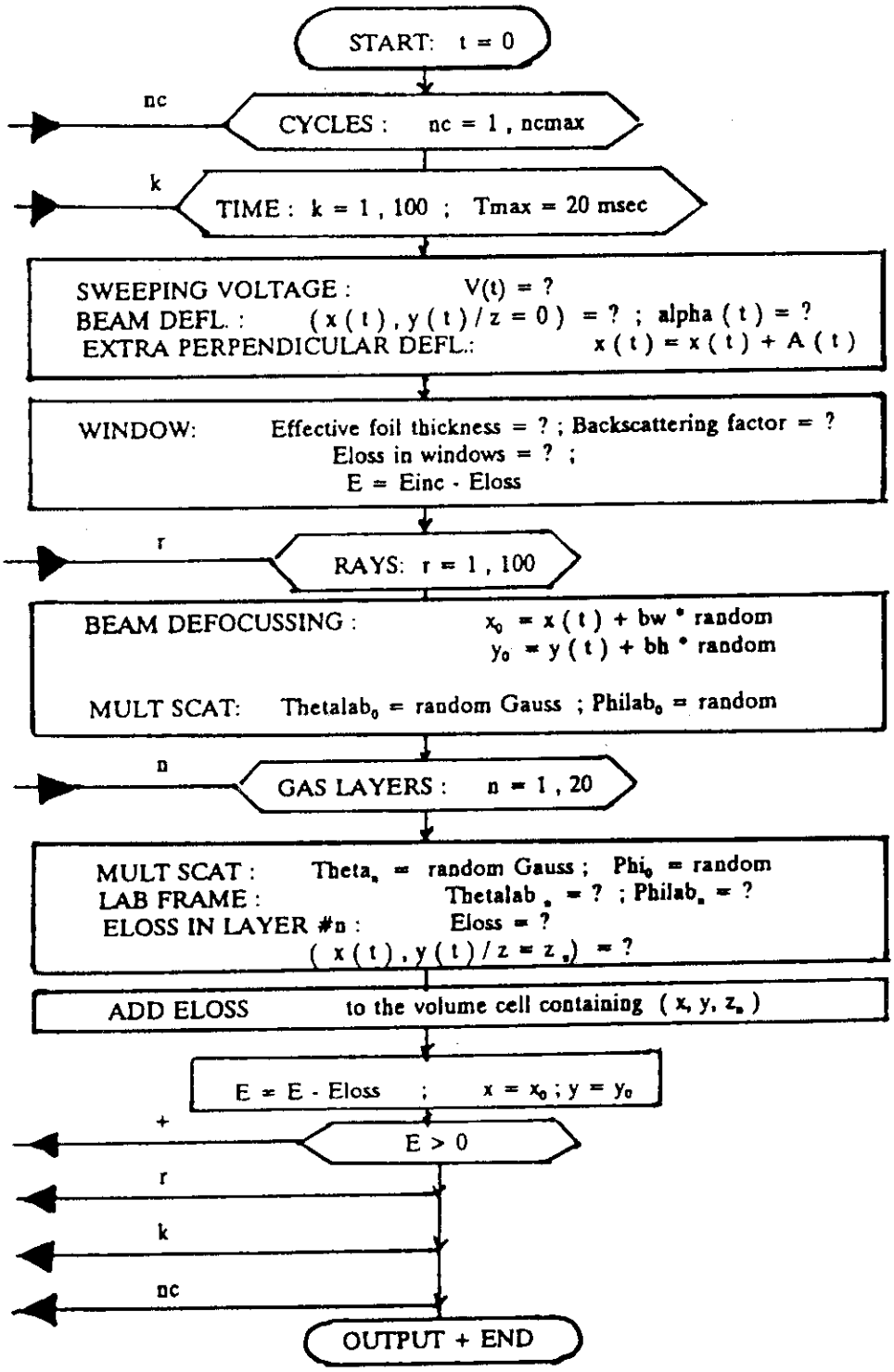

Fig. 1. Flow diagram of the program.

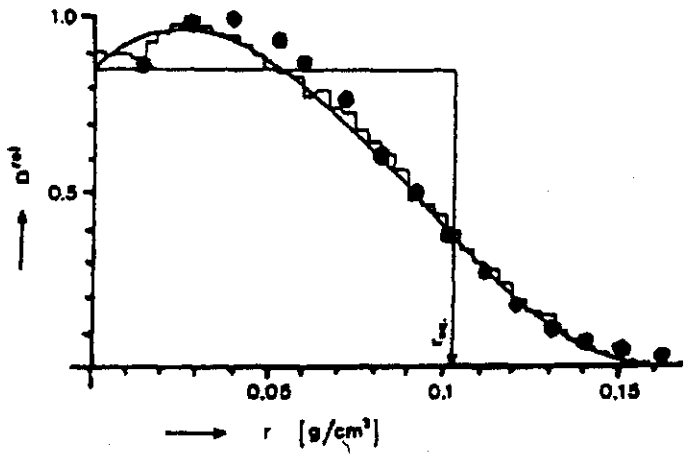

Fig. 2. Depth Profile (relative units).
Histogram: experimental data [1];
Black points: calculated values.

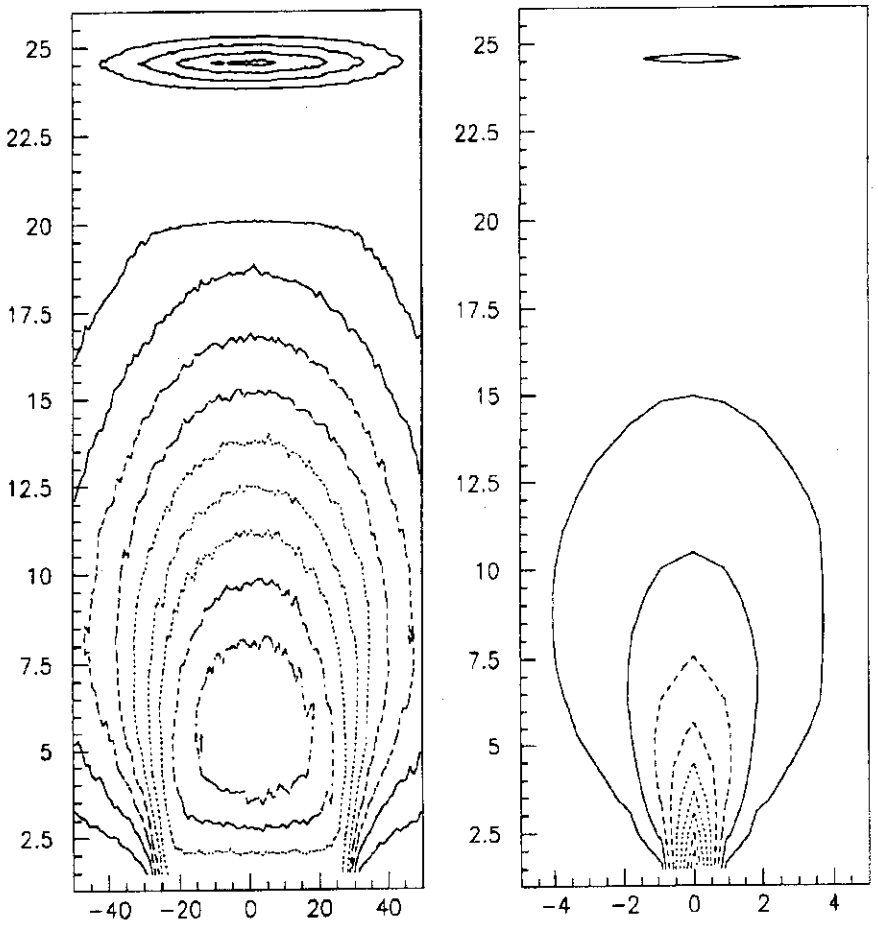

Fig. 3. a) Energy deposit (y, z) [erg]; b) Energy deposit (x, y) [erg].

7.5. CALCULATION OF THE PULSE SHAPE FROM THE INTERNAL BEAM MONITOR

Recently, a prototype internal dose monitor for use inside the irradiation chamber was constructed by us and described in [4]. This monitor was experimentally tested on electron beam in Kawęczyn power station. The tests performed are described in [4]. The first observation was that the output signal from the monitor had two components: the first one was an AC component clearly connected with the interaction of the electron beam with the sensor plate, and the second one, a DC component which origin, at the beginning, was not clear. To elucidate this point, the shape of the resulting charge signal induced by the electron beam passing through the gas medium of proper thickness was calculated. This is shown in Fig. 4. It is seen that the output signal gets a DC component which is increasing with the depth of the gas medium in front of the detector. This is due to development of the electron shower becoming broader and broader because of the multiple scattering of the initially well-collimate beam electrons. In general, the calculated shapes of the output signal reproduce well the pictures observed by us experimentally on the oscilloscope.

7.6. INTERPRETATION OF THE OUTPUT SIGNAL FROM THE PROTOTYPE INTERNAL DOSE MONITOR

The response of the monitor has been measured for different electron energies and different vertical positions of the monitor. The output signal of this monitor was compared with the corresponding values of the electron charge density crossing the central volume element of the tank, calculated with the code DSHAPE.

The calculated values were normalized to experimental ones at the energy 500 keV and central horizontal position of the monitor (dh = 0.0). The results are shown in Fig. 5. In Fig. 5a. raw experimental data are plotted. It is seen that for the electron energies 500 and 600 keV and the detector positions dh = −40 cm and −20 cm the calculated values are significantly higher than the experimental ones, while for dh = +20 cm and +30 cm they are significantly lower. In another words, for lower energies, the slope of the experimental trend of the data is higher than the theoretical.

The reason for such behaviour of the experimental values was further analyzed. Studying the linearity characteristics of the response of the detector v. the beam current it was found that there exist a positive pedestal in the detector characteristic, while the signal from the electron beam is negative. This positive pedestal on the output of the monitor was also observed on the oscilloscope. It was found that it depends on the position of the insulator inside the monitor and was interpreted as an effect of the charging of the insulator by the remnants of the electron beam interacting with the insulator material.

Therefore, it was assumed that the output signal from the detector should be corrected for the presence of this pedestal. For this purpose measured linearity characteristics of the monitor were used. The definition of the new, corrected signal from the detector is schematically shown in Fig. 6.

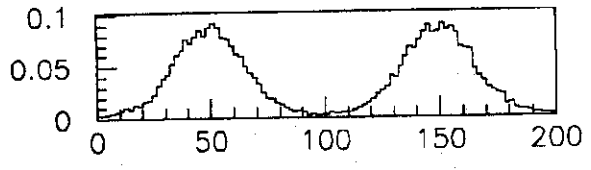

Fig4a. Charge(t)/det1

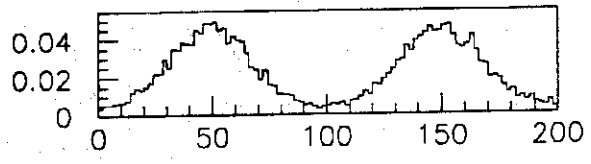

Fig4b. Charge(t)/det2

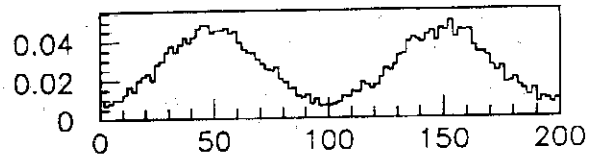

Fig4c. Charge(t)/det3

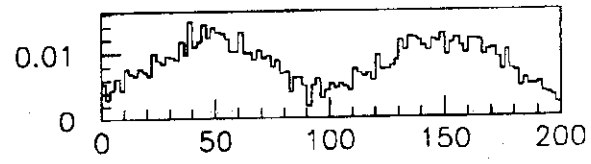

Fig4d. Charge(t)/det4

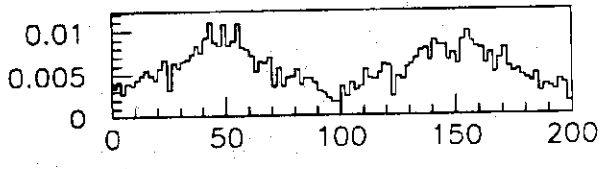

Fig4e. Charge(t)/det5

Fig. 4. Calculated shapes of the resulting charge signal induced by the electron beam passing through the gas medium of proper thickness.

The comparison of these pedestal-corrected signals from the monitor with the previously calculated is shown in Fig. 5b. An improvement in relation with those from Fig. 5a. is clearly evident.

From this we see that our calculated values of the electron charge crossing the elementary volumes of the gas are consistent with the experimental indications of the monitor.

We stress also necessity to take care about the construction of the future models of the monitor, in which the interaction of the electron beam with the insulator should be minimized.

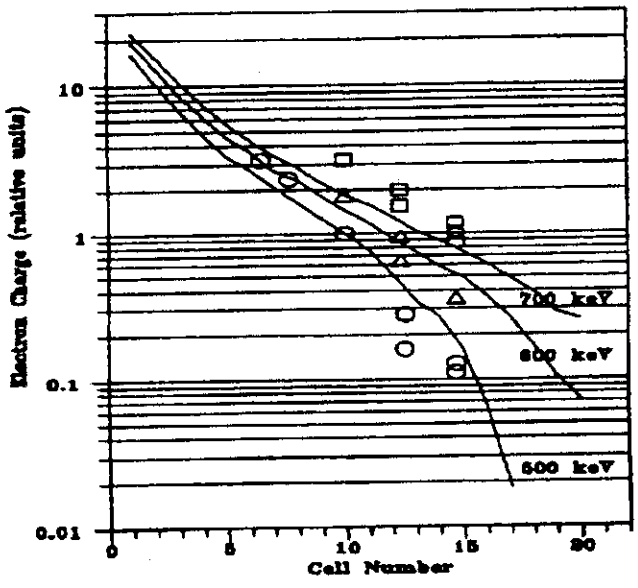

(a)

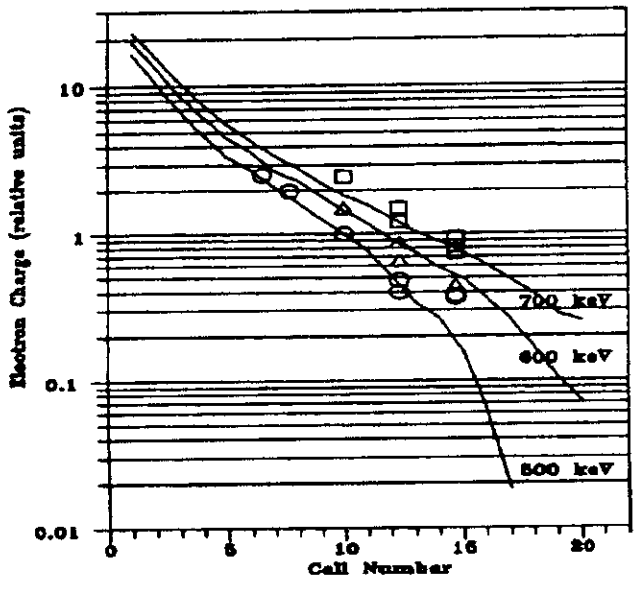

(b)

Fig. 5. Electron charge v. vertical position h of the monitor. Distance $\Delta = (N_{cell} - 10) \times 8.5$ cm measured with respect to the centre of the chamber. Experimental points: a) uncorrected, b) corrected for pedestal.

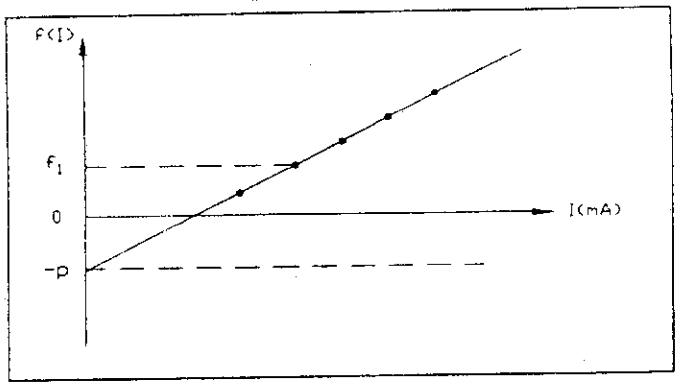

Fig. 6. Principle of the pedestal correction.
Uncorrected signal: $f_1(I)$
Corrected signal: $f(I) = f_1(I) + p$

The output signal from the monitor was reasonably proportional to the electron charge crossing the corresponding element volume, as calculated from DSHAPE program. On the other hand, this charge is in our program unambiguously connected with the radiation dose deposited in the corresponding volume of the gas. Thus, indirectly, the signal from the monitor may serve as a real-time indicator of the dose accumulated in the central volume element of the gas medium. The corresponding spatial dose distribution can be calculated by program DSHAPE and properly normalized to the indication of the monitor. Difficulties in exact calculations of the above mentioned geometrical function cause, that experimental calibration of the monitor is preferred and it can be done by comparison of the output signal from the monitor with some absolute dose measurements made by one of the standard methods, e.g. using a film dosemeter.

7.7. COMPARISON OF CALCULATED AND EXPERIMENTAL DOSE VALUES

Calculated values of the dose absorbed in the centre of the irradiation chamber were compared with values measured in [5] by means of the foil dosemeters. Both measurements and calculations were done for 500, 600 and 700 keV electron beam. Calculated values were normalized to the total electron charge of 500 mA•s of the incident beam, for which all measurements were done. In Table 1. a comparison of experimental and calculated values is shown:

Table 1.

Electron energy [keV]	Measured dose [kGy]	Calculated dose [kGy]
500	33	28
600	37	37
700	38	42

Taking into account that the experimental values were read directly from the 2-dimensional plot of the dose distribution and the calculated were obtained from DSHAPE program for the deflector parameters only approximately describing the real system, an agreement between these quantities must be regarded as satisfactory.

7.6. CONCLUSIONS

We conclude a general consistency of our calculations with the existing experimental data being at present at our disposal. This will be verified in future, when more experimental data become available.

It is shown that measured (and, if necessary, properly corrected) output signal from the internal beam monitor, constructed by us, is within experimental errors, proportional to the electron charge crossing the corresponding volume element of the gas medium which is calculated by our program. Then, from the last quantity, also the corresponding absorbed radiation dose can be deduced by the program.

Thus, our calculations show that, with a reasonably good approximation, a model of the monitor as this implanted in the DSHAPE code can well describe the dose distribution in the tank. To some extent the absolute calibration constant can be also estimated using the code. Of course, better absolute accuracy can be achieved if one use for the calibration purpose experimental values measured e.g. at the centre of the irradiation chamber with a kind of standard film dosemeter. Then, the numerical results of the DSHAPE can be also used to calculate the spatial dose distribution in the entire tank.

REFERENCES

[1] E. Proksh, P. Gehringer, H. Eschweller, Int. Journal of Applied Radiation and Isotopes, Vol. 30, p. 279, 1979.

[2] T. Tabata, R. Ito, S. Okabe, Nucl. Instr. Meth., Vol. 94, p. 509, 1971.

[3] J. Wojtkowska, SINS internal preprint No 0-27/P-II/1988.

[4] E. Kulczycka et al., SINS preprint 1995 (report in preparation).

[5] Inst. Nucl. Chemistry and Technology, Warsaw, Jan. 1995 (report in preparation).

8. Data acquisition and control system

M. Sowiński, M. Kowalski*, E. Iller, R. Kupczak**, J. Licki,
S. Hashimoto and O. Tokunaga

ABSTRACT

In this paper, a system of data acquisition and process control is presented. It is implemented in the pilot installation for flue gas treatment by electron beam irradiation. The main quantities being under control are: the flows of flue gas, water, ammonia and compressed air as well as the absorbed dose of electron beam. The system is installed in the Kawęczyn Electric Power Station.

8.1. INTRODUCTION

The first, simple monitoring system of pilot installation for SO_2 and NO_X removal from flue gas by electron beam treatment method at Kawęczyn power plant was designed and created in 1991. It was based on the apparatus donated by EBARA firm, computer hardware accessible at that time in Poland and conventional automation system, but the organization of the monitoring system and software were original products of the authors of the project. The system played important role in the initial period of exploitation of the pilot installation as the means of practice, promotion and teaching. [1]

The computer system was designed for data monitoring and acquisition of main parameters of the technological part of the Pilot Flue Gas Purification Plant at Kawęczyn Electric Power Station. This system is based on IBM PC 386 computer with analog-to-digital converter cards (analogue signals readout from gas analyzers, thermometers, pressure converters, flowmeters, voltmeters) and digital input cards (readout of range of flue gas analyzers). At the moment, the monitoring system is limited to 18 input analogue parameters: flue gas flow, dust concentration in flue gas at inlet to the installation, ammonia flow rate, gas temperature at five points (at inlet to the installation, at outlet of spray cooler, between accelerators, at outlet of process vessel and at inlet to bag filter), SO_2 and NO_X concentration at inlet to the installation and at outlet of irradiation chamber, energy and current of electron beam of both accelerators, overall pressure drop on the bag filter, and the position finding of damper. Other parameters of pilot installation are manually recorded and then are used during elaboration of new run (are written by keyboard to the computer disk).

---

* Soltan Institute for Nuclear Studies, Otwock-Świerk
** Ellek Co., Warsaw

The investigation program has been enlarged in 1992 - 1993, thanks to IAEA and JAERI support, and the number of measuring and analytical devices has been increased. Consequently, the user qualitative and quantitative demands on monitoring system have grown significantly.

8.2. DATA ACQUISITION AND CONTROL SYSTEM (DACS)

New system of the data acquisition and the process control was worked out taking into attention:

- almost four year experience gained during the work of the pilot installation,
- present and future needs of the users (see Table),
- requirements of the future industrial installation.

The new system consists of two separate subsystems, namely: data acquisition and control subsystems. (Fig. 1.)

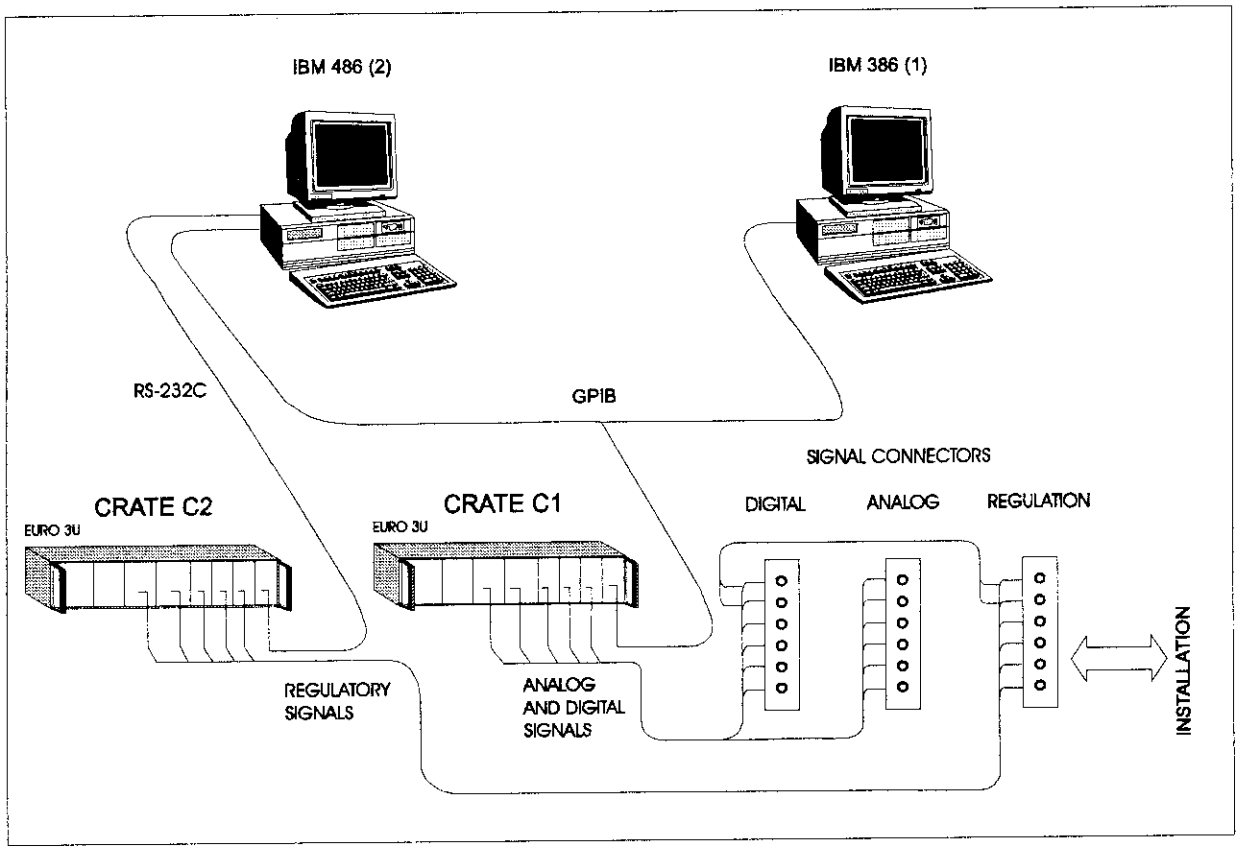

Fig. 1. Scheme of the data acquisition and control system for Pilot Plant at Kawęczyn EPS.

8.2.1. Data acquisition subsystem [2,3]

In principle, it is dedicated to the acquisition, collection and processing of the data which are listed in the Table presented, pos. 1. - 5.

It consists of the following units:

- PC computer IBM-386 together with suitable peripherals,
- VME standard EURO-cassette,
- RS232 and GPIP interfaces.

In this subsystem, an earlier written software was used [1], which was modified and adapted to the requirements of the new hardware. It enables the acquisition, storage, processing and presentation of the following data:

- 56 input analogue signals,
- 72 input digital signals,
- 24 output digital signals.

During the work, values of all parameters are updated with frequency of 1 Hz. These data are stored in hard disks and can be presented on monitors in an arbitrarily chosen time scale (from 1 sec to 168 hours). These data enable the real-time inspection of various subunits of the installation and can be used for automatic or manual correction of the process parameters.

Data presentation:

The data are displayed as functions of time, diagrams and numerical values presented in the form of tables, or graphical synoptic schemes of the installation. The data presentation can be made in real-time (on-line) and can be also retrieved from the disk in the off-line mode.

The data presentation consists of the calibration procedures monitoring for the entire measuring system, various parameters values readout in different scales in various places as needed by the operator. The parameters which are presented in the form of diagrams can be simple (e.g. temperature), as well as complex ones, being calculated from many simple values. Suitable information on the actual value of the amplitude is prescribed to every time diagram. The system automatically signals any excess of any parameter value given limits, and displays on the screen of the monitor its possible reasons.

8.2.2. Control subsystem

It is dedicated to the control and visualization of the locations of various mechanical working elements, which are contained in the installation for flue gas treatment by the electron beam irradiation (see the Table, pos. 6.).

This subsystem enables continuous measurements of the parameters of working elements as: opening degree of the valves of flue gas, ammonia, water and compressed air. Also, it enables measurements of temperature and humidity of flue gas. The system reports also the consumption of ammonia, water, EB (continuous measurement of the absorbed electron dose).

Table. The specification of process parameters

No	Name of the parameter	Measurement range	Param-eter number	Signals		Remarks
				analog	digital	
1.	temperature	0 - 150 °C	7	7		alarms
2.	dP pressure	0 - 5 kPa	3	3		alarms
3.	humidity	0 - 15 %	2	2		JAERI
4.	concentration					
4.1.	inlet					EBARA USA
	SO_2	0 - 5000 ppm	1	4	3*	
	NO_X	0 - 10000 ppm	2			
	O_2	0 - 25 %	1			
4.2.	outlet of the process chamber					SHIMA-DZU JAERI
	SO_2	0 - 5000 ppm	1	5	16	
	NO_X	0 - 5000 ppm	1			
	O_2	0 - 21 %	1			
	CO/CO_2	0 - 1000 ppm / 0 - 15 %	2			
4.3.	outlet of installation					EBARA USA
	SO_2	0 - 5000 ppm	1	5	4*	
	NO_X	0 - 10000 ppm	2			
	O_2	0 - 21 %	1			
	O_3	0 - 1 %	1			
4.4.	supplement					JAERI
	NH_3	0 - 500 ppm	3	4	9	alarm
	N_2O	0 - 300 ppm	1			
4.5	dust	0 - 2 g/Mm^3	1	1		alarm
5.	accelerators					
5.1.	I_0	0 - 100 mA	2	2		alarms
	E_0	500 - 700 keV	2	2		alarms
5.2.	EB scanning control		2	2	8	alarms
5.3.	EB current in process chamber		2	2	12	alarms
6.	measurement and regulation					
6.1.	flow of the flue gas		1	1	18	
6.2.	NH_3	0 - 20 Nm^3/h	1	1		alarm
6.3.	H_2O	0 - 15 Nm^3/h	2	2		alarms
6.4.	pressurized air	0 - 15 Nm^3/h	1	1		alarms
6.5.	dose	0 - 3 Mrad	2	2		alarms
			total	46	79	

*) 9 digital signals for pos. 4.1. and 4.3.

This subsystem works under control of the operating system OS-9. It contains the following units:

- PC computer IBM-486,
- VME standard EURO-cassette,
- RS-232 or RS-485 interface cards.

In Fig. 2. an actual scheme of the measuring, monitoring and control system of the pilot installation for flue gas treatment in Kawęczyn EPS, is presented.

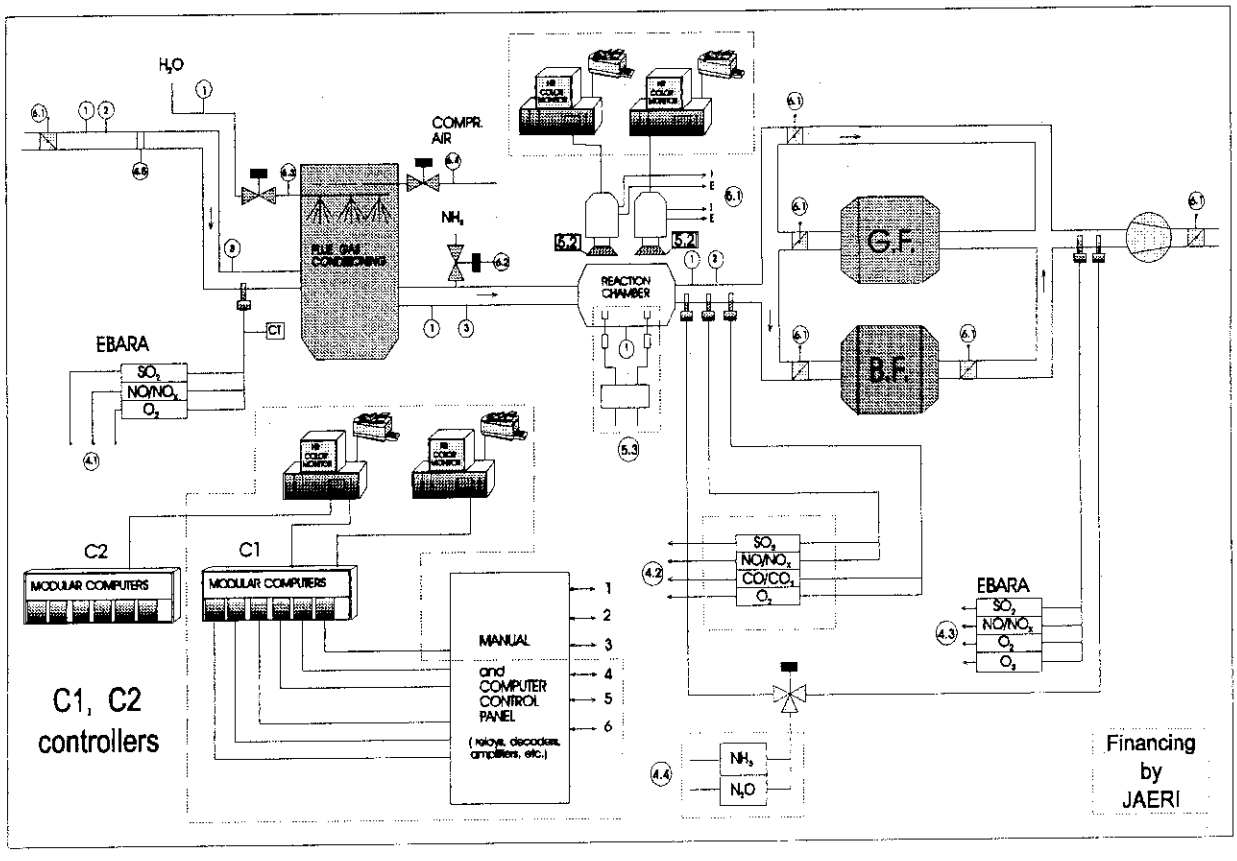

Fig. 2. Measurement, monitoring and control system of Pilot Plant at Kawęczyn EPS.

Features of the microcomputer control system:

- Visualization and continuous measurements of 48 analogue signals.
- Visualization and updating of 32 input binary signals.
- Visualization and control of 32 output binary signals.
- Stepped 3-state program-controlled regulators of PID type with parameters defining (max. 8 regulators).
- Optional configuration of signals presentation in windows.
- History of analogue signals changes.
- Display of measuring points and signals values on the system scheme.
- Data storage and periodical printout in optional sequence and time intervals.
- Reporting media consumption (by hour and month).

- Optional configuration of alarm signals that report overcrossing of the permitted values of any analogue signal.
- Registration of every alarm signal (kind of alarm, time of occurrence, time of disappearance, time of confirmation by operator).
- Scaling of the analogue signals by polynomial of the order of 1, 2 or 3.
- Battery support of the control system (i.e. saving the last results obtained before any drop of the supply power of the system).

Conventional automation systems were modified to make possible either manual or automatic controlling. (Fig. 2.) Control algorithms, using simplified mathematical model and the dependencies experimentally established on pilot installation, are actually tested.

Modified DACS is dedicated to the optimization of the treatment process of flue gas by the electron beam irradiation, taking into attention not only technical, but also economical parameters. In particular DACS can be used for optimization of the following parameters:

- electron beam dose (both, in one- or two-stage regime), using data obtained from external parameters of the beam (I, E) as well as from the data obtained by measurements inside the processing chamber.
- gas temperature and humidity in the processing chamber,
- amount of ammonia (including losses due to not reacting with SO_2 and NO_X),
- time fluctuations of intake gas parameters (such as gas flow, concentration of SO_2, NO_X, temperature, humidity, amount of dust, etc.),
- filtering process of flue gas after electron treatment.

SUMMARY

- Thanks to the support from JAERI and IAEA and also Polish State Committee for Scientific Research the pilot installation was equipped with following devices:
  - modern computer equipment
  - modular computer set
  - system for radiation dose measurement under real conditions (inside the process vessel)
  - control system for electron beam (the board for electron beam control).

REFERENCES

[1] Szlachciak et al. (1992)
Monitoring and control system for an EB flue gas treatment pilot plant - Part II. PC-based data acquisition system. Radiat. Phys. Chem. Vol. 40, No 4, pp. 341 - 346, 1992.

[2] M. Sowiński, R. Kupczak and J. Kołosowski (1994)
Control system for electron beam machines and flue gas irradiation installation (CS). (Not published).

[3] M. Sowiński et al. (1995)
Computer monitoring and control system (CMCS) for electron beam flue gas treatment. Radiat. Phys. Chem. Vol. 45, No 6, pp. 1049 - 1055, 1995.

IV. Conclusion

The results of the research cooperation were evaluated and summarized as follows at the Fifth Coordination Meeting held in Takasaki from 6 to 8 March, 1995.

1) Multi-stage irradiation
The possibility of energy consumption reduction by approximately 20 % by means of double-stage irradiation method has been demonstrated at the pilot-scale test at Kaweczyn. The further energy saving (3-4 %) could be achieved by optimal dose ratio at irradiation stages (first irradiation stage: 60%, second stage: 40 %).

2) Effect of moisture
Some characteristics of the thermal reactions of SO_2 with NH_3 were clarified. The reaction proceed on the surface of reaction vessel, depending on the reaction temperature and humidity in the laboratory experiments in JAERI. To know the effect of moisture, new humidifier has been installed to the pilot plant in Kaweczyn. It allowed to obtain humidity of flue gas up to 11 volume % and to keep the temperature at the outlet of irradiation vessel approximately 65 °C. At these condition removal efficiency of SO_2 increased about 20 % and are over 95 % at the dose of 10 kGy.

3) Product collection and property of the products
New material for bag filter (Moratex) has been tested. It showed better performance in comparison to other materials previously tested.

4) Accelerator control and dose measurement
An accelerator control system will be installed to the pilot plant in Kaweczyn on March, 1995. Dose distribution measurements in the reaction vessel of the pilot plant in Kaweczyn were carried out.

5) Long term performance test
One month operation test at the pilot plant in Kaweczyn has been performed. There was no problem with electron beam machine operation at that mode.

V. Recommendations and future plan

The three years cooperation concerned the subjects; multi-stage irradiation, effect of moisture, effective method for product collection and accelerator control. The following research subject will be investigated in the next phase of the cooperation.

1. Dose measurement and dose control (until Nov. 1995)
   Measurement and control of absorbed dose and dose distribution relating to the design of reaction vessel.

2. Removal of NOx (– Mar. 1996)
   Improvement of NOx removal efficiency by controlling flow patters of gas and dose distributions.

3. Process control (– Mar. 1997)
   Control of accelerator operation and automatic control of NOx and SO2 removal efficiency under various operating conditions of the boiler.

APPENDIX 1 Coordination Meetings and participants

The dates, places and participants of the Coordination Meetings during the First Period of the research cooperation are as follows.

1. First Coordination Meeting

(22–26 March, 1993 at Warsaw)

<IAEA>
S. Machi
V. Markovic
T. Kimoto

<JAERI>
S. Sato
S. Ohno
O. Tokunaga
H. Namba

<INCT>
L. Walis
A. G. Chmielewski
E. Iller
Z. Zimek
B. Tyminski

<Others>

A. Maezawa	(Ebara Corp., Japan)
Y. Hoshi	(NHV America, Inc., Japan)
N. Frank	(Ebara Environmental Corp., USA)
H. Maetzing	(KfK, Germany)
etc.	

2. Second Coordination Meeting

(15–16 November 1993 at Warsaw)

<IAEA>
S. Machi
M. Samiei
V. Markovic

<JAERI>
S. Sato
S. Ohno
O. Tokunaga

<INCT>
L. Walis
A. G. Chmielewski
Z. Zimek
E. Iller
B. Tyminski
S. Bulka
etc.

<Others>

M. Pedzieszczak	(Electro Power Station "Kaweczyn", Poland)
J. Licki	(Inst. of Atomic Energy, Poland)
M. Sowinski	(Inst. for Nuclear Studies, Poland)
M. Romanowski	(Proatom, Poland)
N. Frank	(Ebara Environmental Corporation, USA)

etc.

3. Third Coordination Meeting
(7–9 February 1994 at Takasaki)

<IAEA>
S. Machi
M. Samiei
V. Markovic

<JAERI>
S. Sato
S. Ohno
O. Tokunaga
H. Namba
K. Hirota

<INCT>
A. G. Chmielewski
Z. Zimek
E. Iller

<Others>

M. Pedzieszczak	(Electro Power Station "Kaweczyn", Poland)
Z. Jackowski	("Electrim" SA, Poland)
N. Frank	(Ebara Environmental Corporation, USA)
T. Tanaka	(Chubu Electric Power Company, Japan)
A. Maezawa	(Ebara Corporation, Japan)
T. Sudo	(NKK, Japan)
T. Inamura	(Sumitomo Heavy Industry, Ltd., Japan)
K. Mizusawa	(Nisshin-High Voltage Company, Japan)

etc.

4. Fourth Coordination Meeting

(14–16 November 1994 at Warsaw)

<IAEA>

S. Machi
M. Samiei
V. Markovic

<JAERI>

S. Sato
O. Tokunaga
S. Hashimoto

<INCT>

L. Walis
A. G. Chmielewski
Z. Zimek
E. Iller

<Others>

J. Niewodniczanski	(National Atomic Energy Agency, Poland)
Z. Jackowski	(Electrim S.A., Poland)
Z. Misztal	(Electrim S.A., Poland)
J. Licki	(Inst. of Atomic Energy, Poland)
P. Wilbik	(Energoprojekt, Poland)
M. Pedzieszczak	(Electro Power Station "Kaweczyn", Poland)
N. Frank	(Ebara Environmental Corporation, USA)
Y. Hoshi	(NHV America, Inc., USA)

etc.

5. Fifth Coordination Meeting

(6–8 March 1995 at Takasaki)

<IAEA>
S. Machi
M. Samiei
V. Markovic

<JAERI>
M. Iizumi
S. Sato
O. Tokunaga
S. Hashimoto
H. Namba
Y. Suto
K. Hirota
etc.

<INCT>
A. G. Chmielewski
Z. Zimek
E. Iller

<Others>

J. Niewodniczanski	(National Atomic Energy Agency, Poland)
Z. Jackowski	(Electrim S.A., Poland)
Z. Misztal	(Electrim S.A., Poland)
z. Pawlak	(Zespol Electrownia Dolna Odra, Poland)
P. Wilbik	(Energoprojekt, Poland)
N. Frank	(Consultant Office, USA)
T. Doi	(NKK, Japan)
Y. Doi	(Ebara Corporation, Japan)
H. Ueda	(Nisshin–High Voltage Co., Ltd., Japan)
K. Mizusawa	(Nisshin–High Voltage Co., Ltd., Japan)
T. Tanaka	(Chubu Electric Power Company, Japan)

etc.

APPENDIX 2 Exchange of scientists

1993

From Japan to Poland

Dr. Hideki Namba (Expert mission)
From 17 to 31 March

Mr. Hideo Osono (Inspection of the equipments)
From 23 to 28 March

From Poland to Japan

Mr. Janusz Licki (Expert mission)
From 27 August to 30 September

Mr. Sylwester Bulka (Expert mission)
From 27 August to 30 September

Dr. Bogdan Tyminski (Expert mission)
From 27 August to 30 October

1994

From Japan to Poland

Dr. Hideki Namba (Expert mission)
From 16 to 22 March

Mr. Yoichi Suto (Inspection of the equipments)
From 16 to 22 March

From Poland to Japan

Mr. Janusz Licki (Expert mission)
From 22 August to 4 September

Dr. Edward Iller (Expert mission)
From 24 August to 21 September

Dr. Bogdan Tyminski (Expert mission)
From 24 August to 21 September

Ms. Grazyna Zakrzewska-Trznadel (Expert mission)
From 12 to 25 September

1995

From Japan to Poland

Mr. Koichi Hirota (Expert mission)
From 19 to 31 March

Mr. Takashi Watanuki (Inspection of the equipments)
From 26 to 31 March